CRISPR-based Point-of-Care Detection of Ebola Virus and Lassa Fever

by

Kylene Wupori

A Thesis submitted to the

Faculty of Graduate and Postdoctoral Studies

of The University of Manitoba

in partial fulfilment of the requirements of the degree of

MASTER OF SCIENCE

Department of Medical Microbiology and Infectious Diseases

University of Manitoba

Winnipeg

Table of Contents

Abstract

The currently accepted gold standard for molecular diagnostic testing of high-consequence pathogens (HCPs) such as viral hemorrhagic fevers (VHFs), polymerase chain reaction (PCR), has limited feasibility at the point-of-care (POC) due to its centralized location, high cost, and relatively long turnaround time. POC tests (POCTs) provide rapid results in the field during outbreak response, helping to reduce transmission and time to patient care, and lower the overall impact on the population. POCTs have the potential to be especially useful in rural or remote locations where laboratory testing may have additional logistical constraints, such as in West Africa where VHFs are frequent. Several clustered regularly interspaced short palindromic repeats (CRISPR)-based POCTs have been developed for VHFs such as Lassa fever (LASV) and Ebola virus (EBOV). CRISPR-based POCTs boast quick turnaround times, high sensitivity and specificity, adaptability, and user-friendly designs. Often, CRISPR-based detection is paired with an isothermal amplification method, such as recombinase polymerase amplification (RPA) or loop-mediated isothermal amplification (LAMP). However, many of the CRISPR-based diagnostic tests for LASV and EBOV use RPA paired with the CRISPR-associated (Cas) enzyme Cas13, creating a limited toolbox of potential POCTs. To address this gap, reverse-transcription-coupled LAMP (RT-LAMP) and Cas12b were explored as potential alternatives for LASV and EBOV detection by adapting the STOPCovid.v2 (SHERLOCK testing in one pot) protocol developed by Joung et al. in 2020 to detect severe acute respiratory syndrome coronavirus-2 (SARS-CoV-2). In this thesis, RT-LAMP primers and CRISPR guide RNA (gRNA) were designed to develop an RT-LAMP/Cas12b one-pot assay to detect LASV and EBOV. The RT-LAMP assay was explored on its own and paired with Cas12b in both two-step and one-pot reactions to detect LASV and EBOV, and the STOPCovid.v2 protocol was further optimized for EBOV detection. In

this study, it was found that false positive results were common and could possibly be attributed to the high sensitivity of LAMP to non-specific amplification or contamination. Therefore, it is concluded that while CRISPR-based tests are rapid and user-friendly, the realistic use of RT-LAMP/Cas12b to develop a reliable, sensitive, and specific POCT must be further explored.

Acknowledgements

Thank you to my advisor, Dr. Jim Strong, for guiding this research and always pushing me to strive for excellence. I would also like to thank my committee members Dr. Xiao-Jian Yao, Dr. Shawn Babiuk, and Dr. Alexander Bello for their guidance, to which I would like to extend a special thank you to Dr. Bello for mentoring me through the Co-op program and for encouraging me to pursue graduate studies and continuing to push me out of my comfort zone.

Special thanks to Krisnna Falculan for producing the Cas enzymes used in this study, and Dominic Kielich for your kind words of encouragement and tips on this project.

To all of the ARRRD lab, thank you for being so supportive of my research throughout the Co-op program and graduate studies. Especially Alyssa Stulberg for answering all my questions.

I would also like to extend my gratitude to Jim's lab, including Dr. Lauren Garnett, Kaylie Doan, Anders Leung, and Dr. Zachary Schiffman for your encouraging lab meetings and being ready to help with extractions or removals from CL4. I also appreciate the warm welcome and continuous support the extended Special Pathogens lab provided.

To the CRISPR group, Dr. Brad Pickering, Dr. Ji-Young Kim, Dr, Hongzhao Li, Greg Smith, and Dr. Guodong Liu, for their advice throughout my project.

I would also like to acknowledge this project was funded by the Genomics Research and Development Initiative and the Canadian Safety and Security Program.

Lastly, I would like to thank my family for their support. To my fiancé Nic, thank you for listening to my complaints about graduate school and simultaneous considerations about pursuing further education. I cannot wait to see what our next chapter holds.

List of Abbreviations

AacCas12b ..... *Alicyclobacillus acidoterrestris* Cas12b
AapCas12b ..... *Alicyclobacillus acidiphilus* Cas12b
aM ..... attomolar
amp ..... ampicillin
app ..... application
ATP ..... adenosine triphosphate
BDBV ..... Bundibugyo virus
BIP ..... backward inner primer
BOMV ..... Bombali virus
BOP ..... backward outer primer
bp ..... base pairs
BrCas12b ..... *Brevibacillus* sp Cas12b
Bsu ..... *Bacillus subtilis*
Cas ..... CRISPR-associated
CCHF ..... Crimean-Congo hemorrhagic fever
cDNA ..... complementary deoxyribonucleic acid
CL ..... containment level
CRISPR ..... clustered regularly interspaced short palindromic repeats
CRISPRET ..... CRISPR-based Rapid and Efficient Test
crRNA ..... CRISPR RNA
CT ..... cycle threshold
CV ..... column volume
DENV ..... Dengue virus
DETECTR ..... DNA endonuclease-targeted CRISPR *trans* reporter
DMSO ..... dimethyl sulfoxide
DNA ..... deoxyribonucleic acid
dNTP ..... deoxynucleotide
DPI ..... days post-infection
DTT ..... dithiothreitol
dsDNA ..... double-stranded DNA

EBOV ..... Ebola virus
ELISA ..... enzyme-linked immunosorbent assay
ERASE ..... Easy-readout and sensitive-enhanced
EXPAR ..... exponential amplification reaction
FIP ..... forward inner primer
fM ..... femtomolar
FOP ..... forward outer primer
FPLC ..... fast protein liquid chromatography
GEQ ..... genome equivalents
GP ..... glycoprotein
GPC ..... glycoprotein precursor
gRNA ..... guide RNA
HCP ..... high-consequence pathogen
HAD ..... helicase-dependent amplification
HOLMES ..... one-hour low-cost multipurpose highly efficient system
HPV ..... human papillomavirus
HUDSON ..... Heating Unextracted Diagnostic Samples to Obliterate Nucleases
IDT ..... Integrated DNA Technologies
kb ..... kilobase
L ..... RNA dependent RNA polymerase
LAMP ..... loop-mediated isothermal amplification
LASV ..... Lassa fever
LB ..... loop backward
LF ..... loop forward
Lift-CM ..... lift-heater centrifugal microfluidic platform
LOD ..... limit-of-detection
MARV ..... Marburg virus
MRSA ..... methicillin-resistant *Staphylococcus aureus*
MWCO ..... molecular weight cut-off
NASBA ..... nucleic acid sequence-based amplification
NEB ..... New England Biolabs

NHP ..... non-human primate
NP ..... nucleoprotein
NTC ..... non-template control
NTS ..... non-target strand
PAM ..... protospacer adjacent motif
PCR ..... polymerase chain reaction
POC ..... point-of-care
POCT ..... point-of-care test
RAA ..... recombinase aided amplification
REASSURED .... Real-time connectivity, Ease of specimen collection, Environmentally friendly, Affordable, Sensitive, Specific, User-friendly, Rapid and Robust, Equipment-free and Deliverable to end users
RESTV ..... Reston virus
RFU ..... relative fluorescence unit
RIN ..... RNA integrity number
RNA ..... ribonucleic acid
RNP ..... ribonucleoprotein
RPA ..... recombinase polymerase amplification
RT-LAMP ..... reverse-transcription-coupled LAMP
RT-qPCR ..... quantitative reverse-transcription PCR
RT-RAA ..... reverse-transcription-coupled RAA
RT-RPA ..... reverse-transcription-coupled RPA
RVFV ..... Rift Valley fever virus
SARS-CoV-2 ..... severe acute respiratory syndrome coronavirus-2
SDA ..... strand displacement amplification
SEC ..... size-exclusion chromatography
SHERLOCK ..... Specific High-Sensitivity Enzymatic Reporter UnLOCKing
SNP ..... single-nucleotide polymorphism
SOC ..... Super Optimal broth with Catabolite repression
SSB ..... single-stranded DNA binding proteins
ssDNA ..... single-stranded DNA

STOP ..... SHERLOCK testing in one pot
SUDV ..... Sudan virus
TAFV ..... Taï Forest virus
TB ..... Terrific broth
TCEP-EDTA ..... tris(2-carboxyethyl)phosphine hydrochloride–ethylenediaminetetraacetic acid
tracrRNA ..... *trans*-activating crRNA
Tm ..... melting temperature
TS ..... target strand
USA ..... United States of America
USD ..... United States dollar
UV ..... ultraviolet
VE6 ..... Vero E6
VHF ..... viral hemorrhagic fever
VP ..... virion protein
WHO ..... World Health Organization
Z ..... zinc-binding protein
ZIKV ..... Zika virus

List of Figures

List of Tables

Author Contributions

Wupori, K.; Garnett, L.; Bello, A.; Strong, J.E. CRISPR-Based Detection of Viral Hemorrhagic Fevers at the Point of Care. *Viruses* **2026**, *18*, 218. https://doi.org/10.3390/v18020218

The material from this review article is used in the introduction to this thesis, with additional sections and formatting for the purpose of this thesis.

The author contributions were as follows: Conceptualization, K.W., A.B. and J.E.S.; writing—original draft preparation, K.W.; figures, K.W. created the figures using BioRender; writing—review and editing, L.G., A.B. and J.E.S. All authors have read and agreed to the published version of the manuscript.

1.0 Literature Review

1.1 Introduction

The viral hemorrhagic fever (VHF) disease group consists of many viruses from various families, including *Filoviridae*, *Arenaviridae, Bunyaviridae*, and *Flaviviridae*, which can cause severe diseases with high fatality rates in human populations [1, 2]. The term 'viral hemorrhagic fever' is often used to describe these viruses due to similarities in disease progression and characteristics, including the onset of non-specific "flu-like" symptoms, followed by severe disease progression, as well as increased transmissibility, high fatality rates, and lack of treatment options [1–3]. As the term 'VHF' suggests, hemorrhage is possible, however it occurs infrequently and depends on the pathogen [2].

Notably, certain pathogens within the VHF disease group are categorized as high-consequence pathogens (HCPs) which are a broad group of pathogens characterized by high fatality rates, high transmission, minimal treatment options, and requiring rapid detection and control of outbreaks that can threaten public health and security [4–6]. The term 'VHF' rather than 'HCP' will be used in this introduction to clarify the specific viral families being discussed.

The high transmissibility of VHFs was exemplified during the 2014-2016 West African Ebola virus (EBOV) outbreak, affecting mainly Guinea, Liberia, and Sierra Leone, resulting in over 28,000 cases and 11,000 deaths, with a fatality rate of 39% [7]. The magnitude of this outbreak also led to imported travel-associated cases to other countries, including Europe and North America, reinforcing the broader public health threat these viruses pose [7].

Other VHFs, such as Dengue virus (DENV) and Lassa Fever (LASV), are endemic. DENV, which has the potential to develop into severe dengue and hemorrhaging, is an endemic disease in over 100 countries [8, 9]. Similarly, LASV is endemic in West Africa, with 100,000 to 300,000

cases reported annually, although the true number of cases is likely underreported [10, 11]. Crimean-Congo hemorrhagic fever (CCHF) is another important VHF spreading outside its ecological niche, with contributing factors such as climate change and host migration increasing the risk of cases [12].

In addition to transmissibility, high fatality rates are also of concern for some VHFs. DENV shows a global fatality rate of less than 1%, while LASV demonstrates an overall fatality rate of 1%, which can increase to approximately 15% in severe cases [13, 14]. Other viruses, such as CCHF and EBOV, show fatality rates of up to 40% and 90%, respectively [15, 16].

This thesis focuses on detection of LASV and EBOV. Therefore, this introduction will describe these viruses in more depth.

1.1.1 Ebolavirus

Ebolavirus belongs to the *Filoviridae* family, of which six viral species have been identified [17]. In chronological order, two unrelated outbreaks occurred in 1976 in Zaire (now the Democratic Republic of the Congo) and Sudan, leading to the identification of Ebola virus (EBOV) and Sudan virus (SUDV) [9, 18]. Following this, Reston virus (RESTV) was identified as the cause of an outbreak in cynomolgus monkeys imported from the Philippines to Reston, Virginia, United States of America (USA) in 1989. Since then, RESTV has been responsible for several sporadic outbreaks in monkeys, and in some cases pigs (2008, 2012), with the last recorded outbreak in 2015 [19]. RESTV is not known to be pathogenic in humans, causing only asymptomatic infections [19]. In 1994, Taï Forest virus (TAFV) was identified as the cause of illness in a researcher who conducted an autopsy on a chimpanzee from the Taï National Forest in Cote-d'lvoire [20]. This non-fatal case has been the only recorded case of TAFV [18]. Several years later in 2007, Bundibugyo virus (BDBV) was first identified during an outbreak in the Bundibugyo

district of Uganda [21]. Most recently, Bombali virus (BOMV) was identified in 2018 as the sixth species, named after the Bombali district where the bats which tested positive for BOMV were located. Analysis suggests BOMV can infect humans, but in practice it remains unknown if BOMV causes disease [17].

EBOV is a negative sense, single-stranded ribonucleic acid (ssRNA) virus [22]. Seven genes are included in the approximately 19 kilobase (kb) long genome, in order: nucleoprotein (NP), virion protein (VP) 35, VP40, glycoprotein (GP, including soluble GP and small soluble GP), VP30, VP24, and RNA dependent RNA polymerase (L) [22]. The proteins NP, VP35, VP30, VP24, and L form a filamentous ribonucleoprotein (RNP) that surrounds the viral RNA and is enveloped by a host-derived membrane with GP and VP40 [22]. The main virulence factors include GP, VP35, and VP24 due to their effects on the immune system, including inhibiting the interferon anti-viral response and activating pro-inflammatory mediators [22].

Several hosts of EBOV have been identified; however, the true reservoir has remained elusive [23]. It is thought that the reservoir may have certain characteristics, such as the ability to tolerate infection and support viral replication [23]. Fruit bats have long been suspected of being the reservoir due to the detection of antibodies and partial nucleic acids, as well as occurrence of asymptomatic infections which allow for host survival [23, 24]. However, live virus has not been detected, possibly due to latency or a high rate of viral clearance [23, 24]. To fully identify the reservoir, a list of candidates has been put forward with the recommendation that experts across disciplines work together and sample immune privileged sites during specific reproductive and nutritional periods that support high viral titer [23].

1.1.2 Lassa Fever

Lassa virus belongs to the family *Arenaviridae* and is categorized as an Old World arenavirus [2]. Analysis suggests the origin of LASV occurred over 1,000 years ago in Nigeria [25]. The highly diverse strains of LASV are divided into seven lineages based on their location across Africa [25, 26]. Lineage I was discovered in 1969 in Lassa, northeastern Nigeria, and was named the Pinneo strain after one of the nurses who was helping a LASV patient [25–27]. It is thought that lineage I spread into southern Nigeria creating lineage II, which then diverged into clade IIA in the southeast and clade IIB in south-central Nigeria [25]. Lineage III is also found in Nigeria in the north-central regions, and lineages II and III contain several sub-lineages [25, 27, 28]. Lineage IV expands across West Africa in Seirra Leone, Guinea, and Liberia, and also contains clades IV.A and IV.B [25, 27, 29]. Lineages V, VI, and VII are more recently proposed as new lineages [28]. Lineage V is located in Mali and Cote d'Ivoire, lineage VI was first identified in Kako, and most recently lineage VII was identified in Togo [26, 30–32].

The LASV is a small, enveloped virus that appears sandy due to its ribosomes [9, 26]. The genome is ambisense and encodes a small fragment (S) which contains the GP precursor (GPC) and NP and is approximately 3.4 kb long. The large fragment (L) contains L (RNA dependent RNA polymerase) and a zinc-binding protein gene (Z), and is approximately 7.2 kb long [2, 9, 26].

Unlike EBOV, the reservoir was identified as the rodent *Mastomys natalensis* in 1974, through testing several rodents, bats, and other animals in Seirra Leone for LASV [33]. However, *M. natalensis* is reported to have a smaller geographical range than LASV, prompting research into other species as hosts of LASV, such as *Hylomyscus pamfi* and *Mastomys erythroleucus* [30]. LASV is known to spread from the reservoir to humans via direct contact with an infected rodent or through contaminated food or water, with one report indicating most infections spread from the

reservoir opposed to human-to-human transmission [26, 34]. Identification of the reservoir allows for targeted measures to reduce contact with rodents through trapping or awareness of seasonal rodent behavior such as seeking food, water, or shelter [26, 33].

1.2 Point-of-Care Tests

The presentation of non-specific symptoms and limited treatment and vaccination options available for VHFs add to the public health threat that these viruses pose. During early infection, symptoms often present as general and non-specific, including fever, chills, diarrhea, myalgia, and malaise, making it difficult to clinically differentiate between VHFs and other circulating diseases, such as malaria [1–3]. This difficulty can potentially lead to misdiagnosis, further spread, and delayed patient care [1, 3, 9, 35, 36]. In addition to diagnostic uncertainty, lack of treatment options contributes to the difficulty in developing treatment plans and therefore often relies on supportive care and variably effective antiviral medications to address symptoms [14, 16, 37]. As well, there are no available vaccines for some VHFs, such as CCHF and LASV [14, 16]. Although vaccines have been developed against others, such as DENV and EBOV, they come with specific recommendations and limitations [8, 15]. With the increasing frequency of outbreaks, severity of infections, high fatality rates, and the presentation of non-specific symptoms, national and international efforts to control infections and prevent deaths through improved point-of-care (POC) diagnostic capabilities are of paramount concern.

Early detection and differentiation of circulating viruses support public health by enabling timely testing, accurate diagnosis, appropriate treatment, and rapid isolation of VHF cases to prevent further transmission [1, 38]. The World Health Organization (WHO) originally provided requirements for an ideal POC test (POCT) termed ASSURED (Affordable, Sensitive, Specific, User-friendly, Rapid and Robust, Equipment-free and Deliverable to end-users), which has since

been updated by researchers to REASSURED, adding Real-time connectivity, Ease of specimen collection, and Environmental friendliness to reflect modern technology and current challenges [39]. In essence, the ideal POCT would be connected in real-time using minimal equipment or mobile phones for streamlined data collection and consistent results, have simplified collection methodology, be manufactured using recyclable materials, have a low cost per assay, limit false positives and negatives, be easily used by the layperson, have a quick turnaround time, withstand logistics associated with travel, and be accessible in low resource settings [39, 40].

Serological POCTs that detect antibodies have been developed for VHFs such as DENV (SD Dengue Duo, combined antigen and antibody test) and ebolavirus (antibody test; SUDV, BDBV, and EBOV); however, there are several disadvantages to using antibody-based tests to diagnose acute infections [41, 42]. For example, seroconversion can take days to weeks, with some patients succumbing to VHF infection before producing detectable antibodies, thus severely limiting the use of antibody-based testing at the POC [38, 43, 44]. Other disadvantages of antibody-based testing in the POC setting include difficulty differentiating current or past infection status and the effects of cross-reactivity [1, 45, 46]. However, it is important to note during some infections such as DENV, the virus is rapidly cleared and therefore antibody detection remains an invaluable standard for diagnosis [1, 2].

Recently, the use of clustered regularly interspaced short palindromic repeats (CRISPR) in POC diagnostics has gained traction due to its ability to meet the REASSURED requirements, such as low cost per assay, adaptability, high sensitivity and specificity, and short turnaround time, in addition to deliverability to isolated communities and minimal equipment usage [47, 48]. The goal of CRISPR-based diagnostics is to meet the REASSURED criteria in developing a rapid, field-deployable test for persons with limited laboratory skills to perform the test at the POC.

The introductory section of this thesis will discuss the current molecular-based diagnostic tests for VHFs and outline the CRISPR technology currently being investigated for use in diagnostic testing. In addition, isothermal pre-amplification methodologies, specifically those used in VHF detection, such as recombinase polymerase amplification (RPA), the closely related recombinase aided amplification (RAA), and loop-mediated isothermal amplification (LAMP), will be discussed. Finally, the current development of CRISPR-based diagnostic tests for VHFs that have demonstrated progress toward meeting the POC criteria will be summarized.

1.3 Current Diagnostics

1.3.1 Polymerase Chain Reaction

Current diagnostic tests for VHF's include the "gold standard" for nucleic acid detection of pathogens, polymerase chain reaction (PCR) [1, 2, 49]. Historically, the standard was considered to be viral culture; however, this method is time consuming and while it remains useful in detecting or identifying viruses, the standard has since shifted to PCR [1]. In the context of VHFs, which are all RNA-based, quantitative reverse-transcription PCR (RT-qPCR) uses a reverse transcriptase enzyme, followed by temperature cycling for probe-based detection that tracks the fluorescence produced in real-time, to quantify samples as the complementary deoxyribonucleic acid (cDNA) template is amplified [2, 50]. The use of probes allows for multiplexing, which can detect multiple targets at once [50]. While PCR is highly sensitive and specific, it typically lacks feasibility as a POC option due to the complexity of reactions and machinery [48, 49]. PCR tests offer higher sensitivity than antigen-based rapid tests but are still prone to false negatives in the early stages of infection [3, 51]. For example, it can take 3-10 days post-symptom onset for an RT-PCR test to display a positive EBOV result [3]. A false negative may be encountered if the test is administered

too early during an infection as there may not be enough RNA present to elicit a positive result, necessitating repeat testing at a later time-point [3].

Other disadvantages of using PCR during an outbreak include its lengthy cycling times, reliance on expensive laboratory-based equipment and trained technicians, and the logistical challenges of transporting samples to a laboratory capable of performing diagnostics on risk group 4 pathogens [3, 48, 49, 52, 53]. In resource-limited regions, there may not be adequate or stable power sources to run specialized equipment such as a thermocycler or appropriate cold storage for samples and reagents [48, 54]. As well, PCR can be costly, with a single reaction costing up to 125 US dollars (USD) [55]. These factors highlight the need for improved diagnostic tests and reinforce the importance of developing accurate, reliable, and robust POCTs that can be deployed in the field to provide results in a timely fashion without these special considerations.

1.3.2 Antigen-based Tests

Antigen-based tests, including lateral flow-based tests or enzyme-linked immunosorbent assays (ELISAs), can detect circulating viral proteins in the body to indicate acute infections, a factor which is especially beneficial during outbreaks [53, 56]. The benefits of antigen-based diagnostic tests include their ease of use outside the laboratory with minimal resources and training, affordability, rapid detection capabilities at the POC compared to PCR, and ability to be combined with antibody testing for further sensitivity and specificity [38, 41, 53, 56]. In some cases, such as EBOV, antigen-based tests have been described as preferable to antibody-based tests due to a detectable level of antigen that occurs prior to antibody development [44].

Antigen-based rapid tests have been developed for EBOV, LASV, and DENV [41, 53, 56]. The ReEBOV Antigen Rapid Test detects VP40 in whole blood and plasma with a sensitivity and specificity of 100% and 92.2% when performed at the POC, respectively [53]. The ReLASV Pan-

Lassa Antigen Rapid Test detects NP in whole blood, plasma, and serum with a sensitivity and specificity over 80% and 90%, respectively [56]. Similarly, the Bio-Rad NS1 Ag Strip was shown to detect DENV with 61.6% sensitivity and 100% specificity [41].

However, antigen-based rapid tests do not meet all the qualities desired for a diagnostic tool in the POC setting. The limitations of antigen-based tests include cold storage considerations, long production times, and variable sensitivity and specificity compared to PCR [2, 53, 56–59]. While potentially useful for triage, antigen-based tests may produce false negative results during early infection if the virus is not circulating in levels above the detection threshold, which may necessitate a follow-up test with PCR [53, 58]. In other cases, infections may be cleared too rapidly, rendering antigen-based tests unsuitable, such as during DENV infection [2]. These limitations could result in repetitive testing, potentially leading to further spread of the pathogen and delayed patient care, both of which are of great concern in the case of a VHF infection [43, 59].

Although these tests are unsuitable for POC diagnostics, they remain invaluable when used in specific contexts and in conjunction with other tests and clinical information. An easy-to-use, rapid, and reliable CRISPR-based POCT that can address the limitations of current diagnostic tests could contribute to limiting transmission and increasing effective early patient management for future outbreaks [12, 59].

1.4 CRISPR

1.4.1 CRISPR Background

CRISPR was first identified in *Escherichia coli* in 1987 as a distinctive genetic feature, but its role as a prokaryotic adaptive immune system was not recognized until years later [60]. Since its discovery, researchers have found that the characteristic short repetitive DNA sequences of the CRISPR array and its CRISPR-associated (Cas) enzymes protect prokaryotes against foreign

genetic material that phages and plasmids can introduce [61, 62]. It was soon realized that the unique ability of the CRISPR system to create genetic modifications could be exploited in genetic engineering and therapeutics. The applications of CRISPR range from preventing the transfer of gain-of-function elements such as antibiotic resistance, as a therapy for sickle cell disease, to agricultural benefits, such as increased tolerance of crops to environmental or disease stressors, increased yield, or biofortification [61, 63, 64]. CRISPR technology has expanded into molecular-based detection of infectious diseases and has since gained traction in POC diagnostics for its potential to meet the requirements of an ideal POC assay [47, 48, 65].

Briefly, the CRISPR complex is composed of the CRISPR array, which contains alternating spacer and repeat sequences which transcribe into CRISPR RNA (crRNA), and are adjacent to the *trans*-activating crRNA (tracrRNA) and Cas enzyme sequences [61, 62, 66–68]. The CRISPR response is commonly divided into three stages: adaptation, expression, and interference (figure 1.1) [61, 66–69]. In the adaptation stage, the CRISPR system identifies and stores unique segments of foreign genetic material (spacers) between series of short repetitive host DNA sequences (repeats) in the CRISPR array "library", where it is stored for the next encounter with the same pathogen or gene [67, 68]. To differentiate invading foreign nucleic acid, a short nucleotide sequence on the end of the spacer sequence, termed protospacer adjacent motif (PAM), is often identified to recognize the foreign pathogen and aid in binding [62, 69, 70]. If the same genetic material is reencountered, the expression stage begins, and the unique spacer sequences are then transcribed into crRNA, which pairs with a tracrRNA to form a guide RNA (gRNA) [67, 71]. The gRNA then pairs with the Cas enzyme to form a RNP, which guides the Cas enzyme to the targeted, complementary sequence from the invading pathogen, termed the protospacer [67, 71]. Once the target sequence and PAM site are detected, the Cas nuclease cleaves the target to destroy the

foreign material and prevent infection of the cell, called the interference stage [67]. This property has been applied to POC diagnostic tests where certain Cas enzymes can alert the user of the results of the test using their *trans*-cleavage properties on fluorescent reporters, which will be discussed further below.

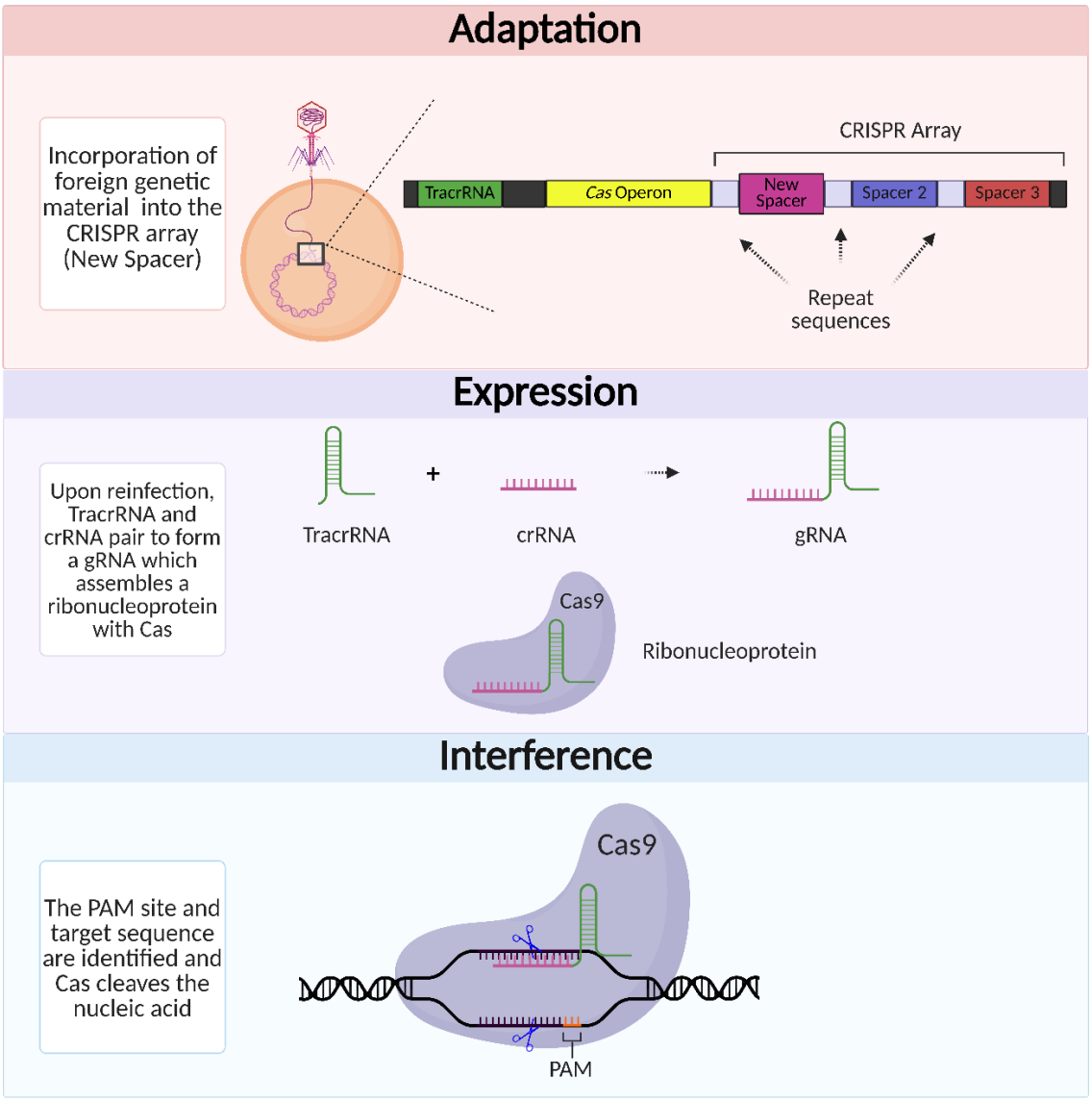

Figure 1.1 Three stages of the CRISPR adaptive response. Adaptation: foreign genetic material is incorporated into the CRISPR array. Expression: RNP is formed following tracrRNA, crRNA, and Cas expression. Interference: foreign genetic material is cleaved. Adapted from [61, 67]. Created in BioRender.com.

1.4.2 Cas Enzymes

CRISPR-Cas enzymes display endonuclease activity responsible for cleaving foreign genetic material, of which several types and subtypes have been identified and formally organized into two classes by Makarova et al. (2015): class I and II [62, 67, 68, 72]. Class I enzymes function as a multi-unit complex and characterize the majority of CRISPR loci, and are further divided into three subtypes: I, III, and IV [62, 67, 68]. Class II enzymes, which are most relevant to this review, function as a single enzyme and are also divided into three subtypes: II, V, and VI [62, 67, 68]. Class II type V CRISPR-Cas enzymes include the DNA-cleaving Cas12 and Cas14, while type VI includes the RNA-cleaving Cas13 enzyme [62, 67, 68, 73]. Certain enzymes within class II, such as Cas12, Cas13, and Cas14, have demonstrated *trans*-effects, also known as off-target, collateral, or indiscriminate cleavage [62, 67]. Once the Cas enzyme becomes activated by target recognition, the enzyme demonstrates *trans*-cleavage activity of surrounding nucleic acids [62, 68]. This property has been exploited by including nucleic acid reporters coupled with a fluorophore and quencher into the diagnostic test, which produces fluorescence once cleaved [62, 68]. Activation of the Cas enzyme by target acquisition and the resulting off-target activity in a CRISPR-based POC diagnostic test can be measured by the increase in fluorescence due to the cleavage of a nearby probe, indicating a positive pathogen detection in the sample [62, 68].

1.4.2.1 Class II Type V-B

The Cas12b enzyme (previously C2c1 (Class 2 candidate 1)) is classified as a type V-B enzyme in class II due to the presence of a single effector molecule and distinct features from other type V-A or V-C enzymes [74]. The Cas12b enzyme uses a dual-guided RNA with a tracrRNA [75]. Cas12b targets both double-stranded DNA (dsDNA) and single-stranded DNA (ssDNA) followed by *trans*-cleavage of ssDNA, with a preference for targeting ssDNA for activation [76,

77]. It was also found that Cas12b shows a preference for the PAM site, 5' – TTN – 3', when targeting dsDNA but can *trans*-cleave ssDNA without a PAM site [75, 76]. Cleavage occurs using a RuvC nuclease 17 base pairs (bp) upstream on the strand containing the PAM site, the non-target strand (NTS), and 23 bp upstream on the complementary target strand (TS), leaving a 5' overhang [75].

1.4.3 Pre-amplification Methods

Amplification is a crucial step in nucleic acid-based detection to reach a clinical level of detection, including during CRISPR-based diagnostics [48, 78]. Several pre-amplification methods can be used to increase the genetic material present for detection. Specifically, isothermal pre-amplification methods are attractive for use in CRISPR-based POCTs because of their minimal equipment requirements [48]. Many isothermal amplification methods have been paired with the CRISPR-Cas system for sensitive and specific pathogen detection, such as LAMP, RPA, the closely related RAA, nucleic acid sequence-based amplification (NASBA), strand displacement amplification (SDA), helicase-dependent amplification (HDA), and exponential amplification reaction (EXPAR) [12, 57, 59, 70, 76, 79–98]. While PCR is often considered the gold standard for molecular-based diagnostics, PCR is not a viable option as a pre-amplification method prior to CRISPR-based detection at the POC due to the limitations previously discussed. This review will focus on the pre-amplification methods commonly used in CRISPR-based POC diagnostics, such as RPA/RAA and LAMP.

1.4.3.1 Recombinase Polymerase Amplification

RPA is one method of isothermal pre-amplification that can exponentially amplify targeted DNA in under 30 min [78]. This amplification method uses phage T4 uvsX recombinase, strand-displacing *Bacillus subtilis* (Bsu) polymerase I, adenosine triphosphate (ATP), and gp32 proteins

for stabilization of ssDNA (figure 1.2) [78]. The isothermal capabilities of RPA allow the reaction to run at 37 °C using only minimal equipment such as a fluorometer or lateral flow strips [78]. Due to the relatively low operating temperature, RPA could potentially run at ambient temperature or utilize body heat alone in locations where a heat block may not be feasible, creating a useful POC option [12]. RPA is highly sensitive, detecting as little as 10 copies of methicillin-resistant *Staphylococcus aureus* (MRSA) using lateral flow strips [78]. RPA also demonstrates multiplexing capabilities, allowing for the amplification and detection of multiple targets at once, as shown with MRSA, Zika virus (ZIKV), and DENV [78, 87]. As well, one study found that most inhibitors of PCR do not affect RPA, even at high concentrations [99]. However, out of the inhibitors tested, whole blood and sodium dodecyl sulfate impeded the reaction [99]. Other limitations include RPA reagent sensitivity diminishing if not stored properly, which can be problematic in resource-limited areas; however, lyophilization is a possibility [48, 94, 100]. In terms of VHFs, RPA pre-amplification has been paired with Cas12 and Cas13 for the detection of DENV, EBOV, LASV, and CCHF, which are discussed in further detail below [12, 57, 59, 98, 101].

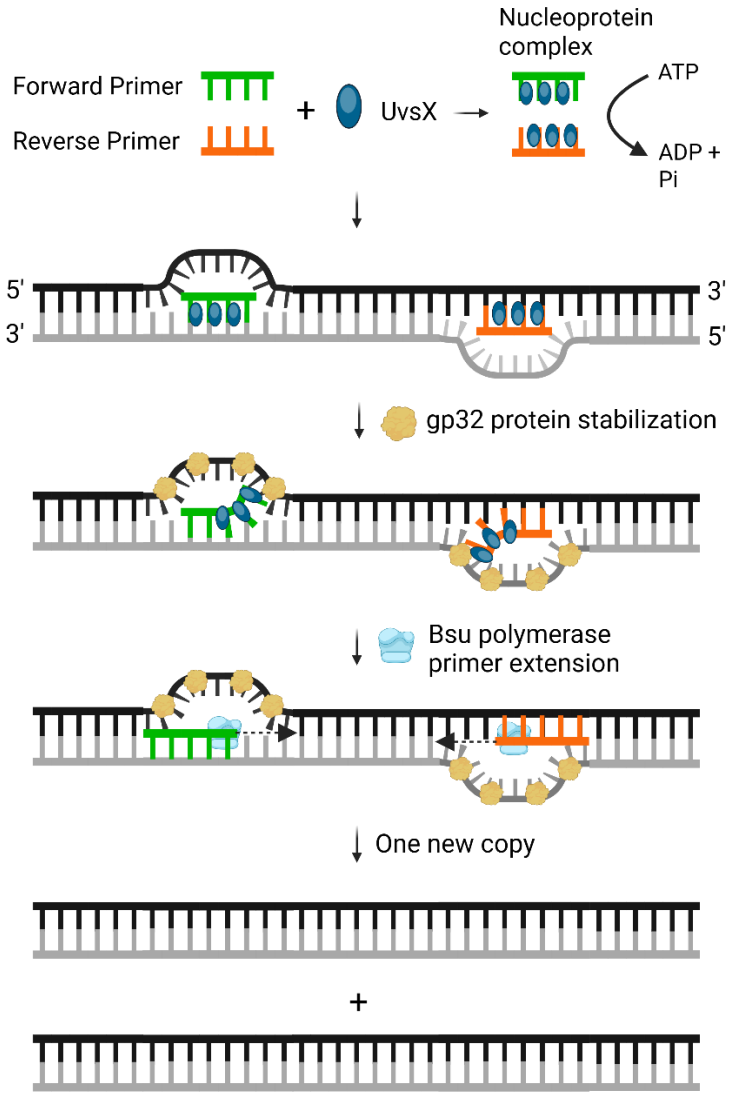

Figure 1.2 RPA-based isothermal amplification. RPA creates one new copy of the template using strand-displacing Bsu polymerase, UvsX recombinase, and stabilizing gp32 proteins. With the addition of ATP, the recombinase displays cooperative binding of the forward and reverse primers and forms a nucleoprotein complex that scans the template for the target site. Once identified, strand invasion occurs**,** and the polymerase extends the DNA from both primer sites, synthesizing one new copy of the template. Adapted from [78]. Created in BioRender.com.

1.4.3.2 Recombinase Aided Amplification

RAA is similar to RPA and has been comprehensively reviewed in ref. [102]. In summary, RPA and RAA share similarities in the reaction temperature, sensitivity, specificity, and rapid diagnostic capabilities at the POC [102]. RAA employs a highly similar mechanism to RPA,

involving recombinase binding of the primers and strand invasion of the target site aided with single-stranded DNA binding proteins (SSB), followed by a strand-displacing polymerase for isothermal amplification [95, 102]. However, RAA has been more widely developed and differs in the origin of the enzymes used, such as bacterial- or fungal-derived recombinase, as opposed to the phage T4-derived proteins found in RPA [95, 97, 102]. RAA and reverse-transcription-coupled RAA (RT-RAA) have been used alone to detect EBOV and paired with Cas12 and Cas13 to detect LASV, DENV, and EBOV [95–97, 103].

1.4.3.3 Loop-Mediated Isothermal Amplification

Similar to RPA, LAMP or reverse-transcription-coupled LAMP (RT-LAMP) is another isothermal method of nucleic acid amplification that can produce billions of copies of DNA in under 1 h [104]. LAMP shows high specificity by using four to six primers that target six to eight regions of the target strand [104]. The primers are termed forward inner primer (FIP), backward inner primer (BIP), forward outer primer (F3 or FOP), and backward outer primer (B3 or BOP) [104]. It was later found that by adding two additional loop primers, loop forward (LF) and loop backward (LB), amplification can occur even more rapidly [105]. Using these primers and a strand-displacing polymerase, LAMP amplifies and elongates the target sequence, creating many stem-loop and cauliflower-like structures of various sizes (figure 1.3) [104].

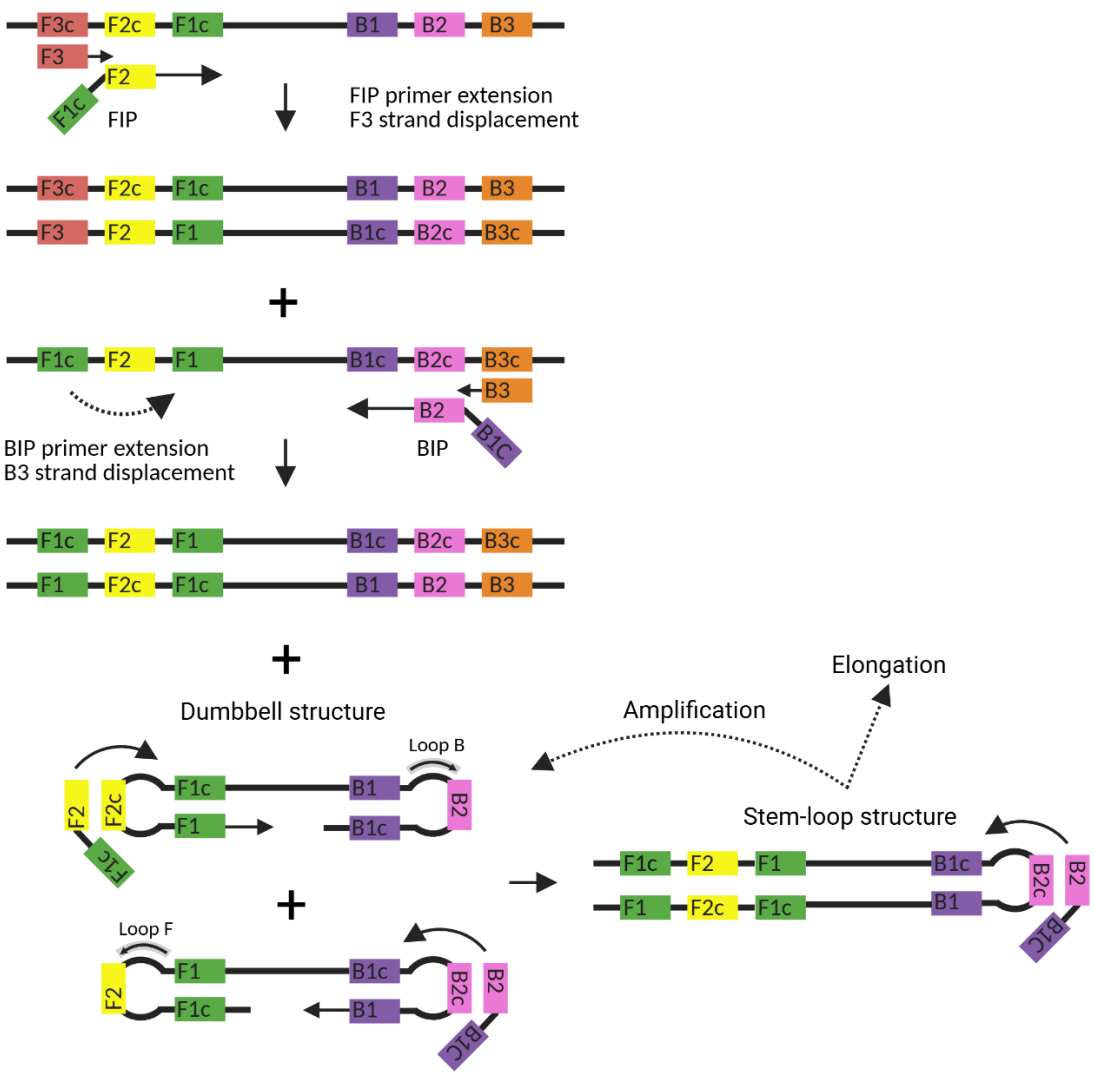

Figure 1.3 LAMP with additional loop primers. Binding of FIP synthesizes a complement to the target strand. F3 performs strand displacement synthesis, releasing a new strand containing the complement to the F1 region. The process is repeated with BIP and B3, forming a strand with complement regions on both ends that fold and form a dumbbell structure. Self-priming initiates the formation of stem-loop structures, followed by the amplification and elongation cycling of LAMP structures [104, 105]. Created in BioRender.com.

The benefits of LAMP include its fast reaction time and minimal equipment requirements, such as a water bath or heating block, to maintain the reaction at approximately 60-65 °C, unlike PCR, which requires the use of a laboratory-based thermocycler [104]. While LAMP runs at a higher temperature than RPA, it can be paired with the thermostable Cas12b for CRISPR-based

diagnostics [76, 83]. LAMP constituents can also be lyophilized, and multiple real-time and end-point readout types have been reviewed, such as turbidity, intercalating dyes, and gel electrophoresis [106]. As well, multiple techniques for multiplexing have also been developed and thoroughly reviewed [106, 107]. In terms of sensitivity, several studies have shown LAMP to outperform conventional PCR or real-time PCR in some contexts, while in other cases, LAMP is comparable to or less sensitive than PCR [11, 106, 108–119]. Similar to RPA, LAMP is inhibited by the same inhibitors as PCR but is more robust and can function at higher concentrations than PCR [120]. For example, urea is a well-known inhibitor of PCR, but LAMP can function at higher concentrations than what would normally be found in a clinical sample, surpassing the capability of PCR [120].

The limitations of LAMP include lack of cloning ability and complicated sequencing due to the stem-loop and cauliflower-like structures LAMP produces, and risk of false positives [106, 109]. Due to its high sensitivity, LAMP is prone to carryover contamination and is susceptible to amplification in non-template controls (NTCs) due to primer hybridizations, potentially contributing to false positives [106]. Care must be taken to reduce aerosol production and prevent contamination by using dedicated spaces with ventilation, sterile techniques, and filtered pipette tips [106, 109]. As well, easily confirming the amplified target by band size through gel electrophoresis is prevented by the "ladder" effect of LAMP, which can be mediated by running a restriction enzyme digest instead [104, 106]. In addition, primer design can be difficult, so primer design tools are available, such as New England Biolabs (NEB) LAMP Primer Design Tool (NEB LAMP) and PrimerExplorer V5 (PrimerExplorer V5), but the primer design may still need to be performed by hand if targeting a very specific area, or redesigned in the case of non-template amplification [106, 121, 122]. In terms of VHFs, and to the best of our knowledge, RT-LAMP has

only been used alone and not paired with CRISPR to detect LASV, Rift Valley fever virus (RVFV), Marburg virus (MARV), and EBOV [11, 108, 111–119, 123–126].

1.4.3.3.1 Current EBOV RT-LAMP Assays

A Pubmed search of "Ebola RT-LAMP" assays yielded 20 results, 11 of which discussed original research on developing an RT-LAMP assay to detect EBOV, which are summarized in table 1. From these 11 results, two primer sets had all six LAMP primers and the space for potential gRNA addition, which have been bolded in table 1. However, the current rVSVΔG-ZEBOV-GP vaccine can create GP RNA, which could lead to false results in vaccinated persons and create uncertainty around diagnosis, therefore the assay targeting the NP gene was selected for further testing instead [59]. The RT-LAMP primers and corresponding gRNA used in this study to detect EBOV are listed in table 3.

Table 1. Summary of EBOV RT-LAMP Publications.

Author	**Target**	**LAMP Primers**
[115]	NP	F3, B3, FIP, BIP, LF, LB
[114]	NP	F3, B3, FIP, BIP, LF, LB (unlisted)
[123]	NP	F3, B3, FIP, BIP, LF, LB
[124]	**GP**	**F3, B3, FIP, BIP, LF, LB**
[108]	NP	F3, B3, FIP, BIP, LF, LB
[116]	L	F3, B3, FIP, BIP
[117]	GP	F3, B3, FIP, BIP, LF, LB
[125]	GP	F3, B3, FIP, BIP, LF, LB

[112]	Trailer region **NP**	F3, B3, FIP, BIP, LF **F3, B3, FIP, BIP, LF, LB**
[118]	NP	F3, B3, FIP, BIP, LF, LB
[126]	Trailer region	F3, B3, FIP, BIP

1.4.3.3.2 Current LASV RT-LAMP Assays

A similar Pubmed search for "Lassa RT-LAMP" yielded five results, three of which described original research on developing an RT-LAMP assay for LASV. Of these sets, two listed all six LAMP primers and could potentially accommodate the addition of a gRNA, which are bolded in table 2. However, phase 2 clinical trials are underway for a similar vaccine, rVSVΔG-LASV-GPC, so the NP target was chosen instead to alleviate potential cross-reactivity in the future (Mutua et al. ID #NCT05868733) [127]. The RT-LAMP primers and gRNA sets used in this study are listed in table 3.

Table 2. Summary of LASV RT-LAMP Publications.

Author	**Target**	**LAMP Primers**
[115]	NP	F3, B3, FIP, BIP, LF, LB
[113]	**GP**	**F3, B3, FIP, BIP, LF, LB** (3 sets)
[11]	**NP**	**F3, B3, FIP, BIP, LF, LB** (2 sets)

1.4.3.4 Amplification-free Methods

Amplification-free CRISPR-based tests have been considered in order to streamline the process by removing the pre-amplification step for targets such as severe acute respiratory

syndrome coronavirus-2 (SARS-CoV-2), human papillomavirus (HPV), and Monkey Pox viral plasmids [128–130]. The use of a pre-amplification method may introduce errors such as non-specific amplification, and extra steps in the workflow may introduce contamination, leading to false results [130, 131]. Logistics such as running temperature of the assay and appropriate cold storage of reagents must also be considered for ease of use at the POC [100, 132]. Additionally, a pre-amplification step may add extra time to the assay when rapid results are desired [130].

To circumvent these challenges, amplification-free tests have been explored, and high sensitivity and quick detection times can still be achieved at the POC. One method pairs Cas13 with the Csm6 enzyme for increased signal amplification [87, 132]. The Csm6 enzyme is classified as a type III nuclease and is activated by cyclic oligoadenylate molecules [87, 132]. In this method, Cas13 is first activated by target recognition, which then cleaves the Csm6 oligoadenylate activator, enabling the activation of the Csm6 enzyme and subsequent amplified reporter cleavage, followed by fluorescence [132]. Using this method, with Cas13 and Csm6 working in tandem, 31 copies/μL of RNA could be detected in under 1 h, highlighting its potential usefulness during an outbreak [132]. Removing the pre-amplification reagents could potentially lower the cost of the test as well [132].

In some contexts, removing the pre-amplification step may not be beneficial and may require more research into the feasibility of amplification-free methods on testing clinical samples [94, 100]. For example, one study showed the combination of RPA and Cas13a could detect a concentration of 2 attomolar (aM) of viral RNA, while running the assay without the pre-amplification step showed a sensitivity in the 50 femtomolar (fM) range, demonstrating that combining the reaction with RPA resulted in a significant increase in sensitivity [94]. Similar results were found with Cas12a, where the combination with RPA provided aM sensitivity, but

not with Cas12a alone [86]. The ability to detect a lower concentration of viral RNA when combined with RPA shows that a pre-amplification step may continue to be a valuable addition to POC testing, especially during infections when the viral titer may be in the low aM range [94].

Amplification-free methods for VHFs such as EBOV and DENV are discussed in more detail in their respective sections below [100, 133].

1.4.4 CRISPR-based Detection Methods

As discussed, CRISPR-based diagnostic tests endeavor to meet the ASSURED/REASSURED criteria, as they are easily adaptable to circulating strains or pathogens, provide faster results than PCR at the POC, and demonstrate similar sensitivity and specificity as PCR in some contexts [48, 57, 59, 86]. Furthermore, CRISPR-based tests demonstrate low cost, with two studies quoting less than 1 USD per test, and another quoting 6 USD per test [59, 94, 100]. CRISPR-based POCTs may also use minimal equipment and non-invasive sampling methods, such as saliva [59]. Even though PCR testing is at a disadvantage at the POC compared to other methodologies such as CRISPR or antigen-based assays, it remains the gold standard for diagnostic sensitivity and specificity to which new diagnostic assays are compared.

Several CRISPR-based tests that use different variations of pre-amplification methods and Cas enzymes have been developed, most notably DETECTR (DNA endonuclease-targeted CRISPR *trans* reporter), SHERLOCK (Specific High-Sensitivity Enzymatic Reporter UnLOCKing), HOLMES (one-hour low-cost multipurpose highly efficient system), and STOP (SHERLOCK Testing in One-Pot, version 2) [76, 86, 87, 94, 134, 135]. These methods will be briefly described in this section.

The DETECTR method combines Cas12a and RPA in a one-pot format to detect DNA targets within 1 h [86]. It was discovered that Cas12a targets dsDNA and *trans*-cleaves ssDNA, and this

method was applied to rapidly detect two types of cancer-associated HPV, HPV16 and HPV18, from patient anal swabs with high concordance with PCR [86].

Similar to DETECTR, the SHERLOCK method combines RPA or reverse-transcription-coupled RPA (RT-RPA) and Cas13a coupled with T7 transcription to cleave RNA [94]. Using this method, ZIKV was detected in clinical serum and urine samples at aM concentrations [94]. As well, two different strains with single-nucleotide polymorphisms (SNPs) could be differentiated for both ZIKV and DENV [94]. The SHERLOCK method is inexpensive, sensitive, and maintains performance when lyophilized and reconstituted, showing promise for POC diagnostics [94].

In SHERLOCKv2, the multiplexing and signal amplification capabilities of SHERLOCK were further developed [87]. Multiplexing was achieved by combining four different Cas enzymes with their respective reporters containing their preferred motifs in the same reaction [87]. By using multiple fluorescent channels, different targets were detected, which can be applied to identify co-circulating viruses such as influenza or SARS-CoV-2 at the POC [87]. As well, quantitation and lateral flow readout were explored [87]. The combination of RPA, Cas13, and Csm6 was applied to lateral flow strips, which allowed for rapid, sensitive, and mobile detection [87].

Another method that was developed using the Cas12a enzyme is known as HOLMES [134]. Similar to SHERLOCK, HOLMES could detect SNPs to differentiate between virus and vaccine strains and could also detect DNA and RNA viruses with aM sensitivity [134]. However, PCR was used as the pre-amplification method, which is unsatisfactory for POC diagnostics as previously discussed [134].

HOLMESv2 overcame the limitation of HOLMES by combining the thermophilic Cas12b enzyme with LAMP/RT-LAMP and further explored a one-pot system and quantitation [76]. Cas12b is thermostable and demonstrates nuclease activity at higher temperatures, with the optimal

temperature determined to be 55 °C for *Alicyclobacillus acidoterrestris* Cas12b (AacCas12b) in a one-pot reaction with LAMP, and up to 64 °C for *Brevibacillus* sp. Cas12b (BrCas12b) [76, 83]. Therefore, Cas12b pairs well with LAMP, which functions optimally at 60-65 °C [76, 83, 104]. HOLMESv2 demonstrates the practicality of LAMP in a fast, one-step CRISPR-based format for ease of use at the POC [76].

Lastly, the STOPCovid.v2 method also combines LAMP with Cas12b for rapid, sensitive, and specific detection [135]. The one-pot test uses magnetic bead-based extraction, which increased the sample input and resulted in the detection of concentrations as low as 33 copies/mL, much lower than the RT-qPCR test the assay was compared to [135]. The STOPCovid.v2 assay detected SARS-CoV-2 in less than 45 min with 93.1% sensitivity and 98.5% specificity [135].

1.5 CRISPR-based Diagnostic Tests for VHFs at the POC

To the best of our knowledge, CRISPR-based diagnostic tests for VHFs that address use in the POC setting have been developed for DENV, EBOV, LASV, and CCHF, which are outlined below. This section will focus on those that employ the isothermal amplification methods RPA or RAA, and LAMP.

1.5.1 Dengue Virus

A field-deployable diagnostic test for ZIKV and DENV was developed using the SHERLOCK method combining RPA and Cas13 [57]. In this study, a new technique was developed to bring viral nucleic acid extraction outside the laboratory environment, termed HUDSON (Heating Unextracted Diagnostic Samples to Obliterate Nucleases) [57]. HUDSON uses a mix of tris(2-carboxyethyl)phosphine hydrochloride–ethylenediaminetetraacetic acid (TCEP-EDTA) followed by a two-part heating procedure to extract viral nucleic acid and inactivate ribonucleases and virus straight from a clinical sample [57]. Using SHERLOCK, DENV

was detected in 24 RT-PCR-positive samples of extracted RNA, while the combination of SHERLOCK and HUDSON detected DENV in eight clinical serum samples and three clinical saliva samples in under 1 h [57]. Out of the different sample types, saliva demonstrated a lower viral load but also potential for a rapid and non-invasive sample type, which meets one of the REASSURED POCT characteristics discussed above [57]. The assay was further developed to detect a positive sample out of a panel of flaviviruses (ZIKV, DENV, West Nile virus, and Yellow Fever), as well as any combination to detect a possible co-infection [57]. Similarly, the assay can detect which serotype (or multiple) of DENV is present [57]. The ability to differentiate between multiple viruses or serotypes that may be co-circulating with indistinguishable symptoms would be greatly beneficial in a readily deployable POCT. Lastly, to highlight the adaptability of SHERLOCK and its ability to detect SNPs, a successful new test was created within one week of identifying a new ZIKV mutation, demonstrating the usefulness of CRISPR-based POC diagnostic tests in future outbreaks [57].

In another study, Cas13a and Cas12a were combined to develop a field-deployable lateral flow test to detect DENV [133]. The assay did not use pre-amplification of the DENV RNA, rather it was found that using both Cas13a and Cas12a increased the sensitivity to 190 fM versus 741 fM when Cas13a was used alone, not quite reaching aM concentrations that other assays described here have demonstrated [94, 133, 134]. The assay was also highly specific to DENV-1, detecting serotype 1 and not serotypes 2, 3, or 4 [133]. While the *trans*-cleavage activity of the Cas enzymes is still taken advantage of, this test works differently in that fluorescence is observed when the pathogen is not present [133]. When DENV RNA is present, Cas13a is activated and the Cas12a gRNA is consequently degraded, leaving the DNA-based reporter intact to display the test line of

the flow strip [133]. When DENV RNA is not present, Cas12a degrades the reporter, illuminating only the control line [133].

Recently, a unique one-pot system was developed to detect all four serotypes of DENV (serotypes 1–4) using RT-RPA and Cas12a [101]. In this reaction, RT-RPA was run at its optimal temperature (38 °C) in the reaction tube, while the Cas12a components were stored in the lid of the closed tube [101]. The tube was then centrifuged and the temperature increased (48 °C) for the Cas12a detection of the amplified targets [101]. The test detected plasmids containing DENV 1–4 in under 1 h in both tube-based and lateral-flow formats [101]. In this study, no cross-reactivity was observed, and the detection limit was assessed to be lower for the tube-based format at approximately 91.7 copies/test (95% probability), while the lateral-flow test was found to be reliable above 250 copies/test [101].

Another one-pot test was recently developed, combining RAA with Cas13a, termed CRISPR-based Rapid and Efficient Test (CRISPRET) [97]. The one-pot test achieved high sensitivity and specificity when tested on plasma samples of all four serotypes, with an average of 95.8% and 96.6% when compared to qPCR, respectively [97]. As well, each assay was specific to only the serotype tested for [97]. It was noted that while the one-pot system is rapid and reduces the possibility of contamination, combining amplification and detection may result in lower sensitivity and specificity than if these reactions were performed separately [97].

1.5.2 Ebola and Lassa Virus

The SHERLOCK method was again employed to develop an inexpensive and easy-to-use POCT to successfully detect EBOV and clades II and IV of LASV from clinical samples in West Africa (figure 1.4) [59]. The assay used both fluorescence and lateral flow readouts and showed that fluorescence-based tests were 10 times more sensitive than lateral flow strips for the detection

of LASV, similar to the DENV test described above [59, 101]. Fluorescent readout detected LASV clades II and IV to 10 copies/uL and 100 copies/uL, respectively, and EBOV to 10 copies/uL [59]. The assays were also tested on 16 EBOV and 10 LASV clinical samples and found to agree 100% with RT-qPCR, with the LASV clade IV assay outperforming RT-qPCR [59]. Aside from sensitivity, both LASV and EBOV assays were highly specific and showed no cross-reactivity with other VHFs [59]. As well, the safety and practicality of HUDSON as a POC extraction/inactivation technique was further assessed [59]. It was found that using either 70 °C for 30 min or 95 °C for 10 min worked to inactivate viruses in whole blood, urine, and saliva [59]. Among these sample types, saliva again showed the highest sensitivity [59]. Lastly, a smartphone application (app) was developed to ensure bias-free, consistent readings of the lateral test strips [59]. The HandLens app maintains high accuracy and demonstrates progress towards real-time connectivity, one of the REASSURED characteristics [59].

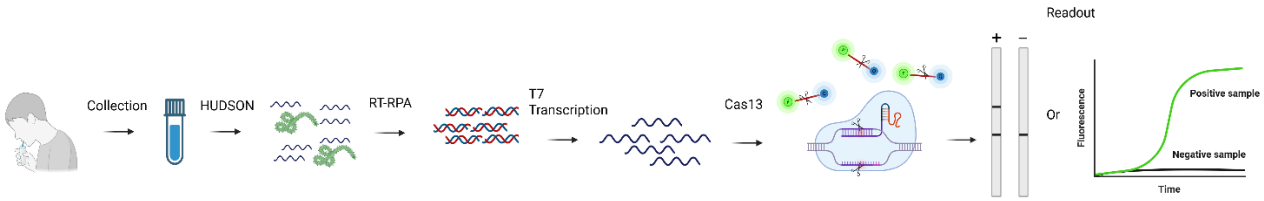

Figure 1.4 SHERLOCK and HUDSON workflow. Patient samples (such as saliva) are collected, and the HUDSON technique is employed to inactivate and extract viral RNA. Reverse-transcription and isothermal amplification of DNA occur, followed by transcription back into RNA. Recognition and cleavage by RNA-based enzyme Cas13 can be read through lateral flow strips or real-time fluorescent readout. Adapted from [59]. Created in BioRender.com.

Due to drawbacks of RPA, such as the complexity and stability of reagents, an amplification-free method was chosen in another study, where a small microfluidic device was developed for Cas13a POC detection of EBOV [100]. Compared to PCR, the assay is quick and inexpensive, with the ability to run 24 samples in 30 min and low cost of approximately 6 USD/assay [100]. Furthermore, the assay does not require complicated sampling procedures, as it

is compatible with finger prick tests, making it attractive for use in the POC setting [100]. The assay works by first extracting viral RNA from blood prior to running the sample on the microfluidic chip system, which is also capable of multiplexing and quantitation [100]. The Cas13a gRNA is first added to the detection reservoir, followed by extracted EBOV RNA, and the resulting fluorescence is measured using a small benchtop fluorometer aligned with the microfluidic chip [100]. Without target amplification, the assay has a limit-of-detection (LOD) of $5.45x10^7$ copies/mL [100]. This can be compared to the mean viral load found in initial blood draw samples from patients who presented to the Liberian Ebola Treatment Unit and later succumbed to infection of $1.55x10^7$ copies/mL [136]. Due to the amplification-free nature, it is possible that not all infections will be detected, and the application of the device on clinical samples during the early stages of infection, as well as incorporation of RNA extraction into the system, should be further studied [100].

Recently, a so-called "tube-sleeve-tube" one-pot assay was developed to detect a conserved region of the EBOV *VP40* gene using RT-RAA paired with Cas12a [96]. In this assay, the RT-RAA reaction is run in the bottom of the tube, while a smaller, uncapped tube containing the CRISPR reaction is placed into the larger tube upside down [96]. Centrifugation allows the reactions to mix, and the resulting fluorescence can be measured [96]. The test is rapid, detecting 3.6 copies/uL of linearized plasmid in under 1 h [96]. As well, the assay did not detect other viruses of concern, and when tested with extracted EBOV RNA, it showed high concordance with RT-qPCR [96].

RT-RAA has also been paired with Cas13a to detect LASV [95]. In this study, lateral flow strips termed easy-readout and sensitive-enhanced (ERASE) strips were developed and used to detect plasmids containing the targeted NP region [95]. The detection limit was determined to be

100 copies/uL, which was less sensitive than the 10 copies/uL that fluorescence-based readout and qPCR achieved, a trend seen in other assays described here [59, 95, 101]. The test is also rapid, uses portable equipment for the POC, and does not detect other viruses such as DENV or ZIKV [95].

1.5.3 Crimean-Congo Hemorrhagic Fever Virus

In this proof-of-concept study, RPA and Cas13a were combined to target all clades of CCHF [12]. The high sequence diversity between the multiple CCHF clades creates difficulty in targeting a conserved region [12]. However, it was found that using degenerate nucleotides in the gRNA allowed the test to overcome the diversity between clades while maintaining high specificity, as the test did not detect other related viruses, including RVFV [12]. The two-step assay showed high sensitivity with a detection limit of 1 copy/μL and a fast turnaround time of under 40 min, making the assay a strong candidate for further development as a one-pot POCT [12]. It was also noted that the degenerate gRNA demonstrated similar efficacy as other non-degenerate-based gRNAs, while maintaining a greater ability to detect CCHF despite mutations [12]. Although the study did not include testing clinical samples, it successfully detected samples contaminated with DNA, a known contributor to false positives that could be found in clinical samples [12].

Due to the competitive nature and temperature difference of the components involved in designing a one-pot test, a microfluidic device with separate chambers for isothermal amplification and CRISPR–Cas detection was developed, termed the lift-heater centrifugal microfluidic platform (Lift-CM) [98]. The device is potentially suited for the POC, as it is quick, portable, compatible with lyophilization, and low cost [98]. As well, the device is linked with a smartphone app to set up and monitor the activity of the assay such as the temperature and fluorescence

produced in real-time [98]. The Lift-CM platform uses a spatially encoded centrifugal disc (termed SEC-disc) containing eight channels where the extracted samples are added, and dual-heating and centrifugation elements allow for pre-amplification and Cas detection to be carried out separately [98]. Plasmids containing the target such as CCHF and EBOV (10^4 copies/uL) were detected using RPA combined with Cas12a [98]. The microfluidic device was also compatible with LAMP/Cas12a, highlighting its adaptability for the POC [98].

1.6 Discussion

The diagnostic landscape for VHFs has historically relied on established modalities such as PCR, antigen detection assays, and antibody-based tests [1, 2]. While these platforms have proven indispensable in outbreak settings, each carries inherent limitations, including requirements for specialized infrastructure, time-intensive workflows, or reduced sensitivity during early infection [1]. In recent years, CRISPR technology has emerged as a promising alternative, offering rapid, highly specific, and potentially field-deployable POCTs [48, 65]. By leveraging isothermal amplification strategies and Cas-mediated nucleic acid recognition, CRISPR-based assays present a paradigm shift in POC testing [48]. A critical comparison of these approaches highlights not only the strengths and shortcomings of conventional diagnostics for VHFs but also the potential of CRISPR-based platforms to expand capacity for timely and decentralized detection in future outbreak responses.

1.6.1 Strengths and Limitations

CRISPR-based diagnostics show promise in meeting the REASSURED criteria, as they boast low cost and minimal equipment requirements, as well as demonstrate rapid detection times, characteristics that are of great importance when developing a POCT for areas with limited infrastructure [39, 48, 59]. As well, the CRISPR-based tests described here have demonstrated

high sensitivity and specificity. The SHERLOCK test developed to detect DENV demonstrated 100% agreement with RT-PCR when tested on 24 DENV-positive samples [57]. When applied to 10 clinical samples of LASV, SHERLOCK again achieved 100% agreement with sequencing and RT-qPCR [59]. Specifically for LASV clade IV, this level of sensitivity outperformed two different PCR assays, a Nikisin RT-qPCR assay (40% sensitivity) and an in-house RT-qPCR assay (50% sensitivity), which was attributed to differences in primer design [59]. The same results were found when tested on 16 clinical samples of EBOV, with SHERLOCK in 100% agreement with sequencing [59]. Furthermore, detection of concentrations as low as 1 copy/uL were achieved [12, 57]. Each test was also shown to be highly specific to their respective target of DENV, LASV, EBOV, or CCHF after testing for cross-reactivity with other viruses [12, 57, 59, 95–97, 101, 133]. Lastly, most of the assays showed rapid detection times under 1 h [12, 57, 95–98, 100, 101, 133]. While these tests show high sensitivity and specificity, the number of clinical samples tested is low and could benefit from greater sampling to better showcase the accuracy and reliability of CRISPR-based diagnostic tests.

It is important to note the conversion between the different concentrations described in these CRISPR-based diagnostic tests, such as molarity versus copy number. Many of these articles report the LOD of the CRISPR assay in molarity, often seen so far in this introduction to be in the aM or fM range, while others report the LOD in copies/volume. The concentration in copies/μL can be converted to molarity using Avogadro's number (6.022×10^{23} molecules/mol) and converting the volume. For example, the LOD of 1 copy/μL is approximately equal to 1.66 aM, demonstrating that CRISPR-based assays reporting LODs in the low aM range are comparable to single copy numbers [12, 57].

There are other VHF's that were not addressed in this review, including those that the WHO previously described as high-priority pathogens such as MARV or RVFV, for which no CRISPR-based POC diagnostic assays have been developed [137]. Furthermore, the assays described here for DENV, EBOV, LASV, and CCHF commonly use the RPA/RAA pre-amplification method paired with the Cas13a enzyme, with some variations including Cas12a [12, 57, 59, 95–98, 101]. Evidently, on top of the limited number of CRISPR-based POCTs for VHFs, there is also an absence of variety in these assays. To circumvent this, other pre-amplification methods and Cas enzymes could be further explored as potential POCTs. For example, LAMP and Cas12 enzymes have unique features that may advance CRISPR-based POCTs for VHFs by adding more options to the CRISPR-based toolbox. The successful combination of LAMP and Cas12 has been previously demonstrated with several pathogens, which can be leveraged to contribute to a wide variety of CRISPR-based POCTs for future outbreaks of VHFs [76, 83, 85, 135, 138].

1.7 Conclusion

CRISPR-based assays are a valuable tool for the development of POC diagnostics tests due to their ability to be easily adapted to the current circulating strain of the pathogen and their feasibility for use in the field due to minimal, low-demand equipment, low cost per assay, and high sensitivity and specificity. CRISPR-based assays provide faster results than traditional molecular-based tests like RT-qPCR, enabling more rapid responses, which is especially critical in resource-limited settings where timely diagnosis can significantly improve outbreak control and patient management. VHFs such as DENV, EBOV, LASV, and CCHF have successfully been detected using CRISPR-based diagnostics [12, 57, 59, 95–98, 100, 101, 133]. However, more development of CRISPR-based POCTs is needed to explore different combinations of pre-amplification methods and Cas enzymes to ensure public health safety in the event of future VHF outbreaks.

1.8 Aim and Hypothesis

Aim: This study aims to expand the CRISPR-based toolbox by adapting and optimizing the STOPCovid.v2 protocol by Joung et al. (2020) to develop a rapid and user-friendly RT-LAMP/Cas12b one-pot test to separately detect two VHFs, LASV and EBOV. The assay aims to use minimal, field-deployable equipment to provide quick and accurate diagnosis at the POC in low-resource and outbreak prone settings, helping to reduce transmission.

Hypothesis: It is hypothesized that RT-LAMP and Cas12b can be combined to develop a one-pot assay to successfully detect LASV and EBOV in a sensitive and specific manner.

1.9 Objectives

Objective 1: Optimize the current CRISPR-based diagnostic assays in the literature, such as the STOPCovid.v2 method, for application to LASV and EBOV using RT-LAMP and Cas12b for successful one-pot detection.

a) Design RT-LAMP primers and gRNA to amplify and detect LASV and EBOV.
b) Optimize the assay for successful amplification and detection in a one-pot format.

Objective 2: Optimize the sensitivity of the RT-LAMP CRISPR-Cas12b assay by measuring the LOD and limiting the number of false positives and negatives.

a) Apply and test these parameters on infected containment level 4 (CL4) animal samples.
b) Apply and test these parameters on spiked matrices.

2.0 Materials and Methods

2.1 In-house AapCas12b Production and Purification

The *Alicyclobacillus acidiphilus* Cas12b (AapCas12b) enzyme was produced in-house following a modified version of the Kellner et al. (2019) and Yang et al. (2023) protocols [131, 139]. First, 100 µL of bacterial BL21 (DE3) competent cells were transformed with 50 ng of pAG001 His6-TwinStrep-SUMO-AapCas12b (Addgene #153162). The cells were incubated for 5 min on ice, heat shocked at 42 °C for 45 s and then returned to ice for 2 min. Next, 400 µL of pre-warmed (37 °C) Super Optimal broth with Catabolite repression (SOC) medium was added to the cells, and the cell suspension was spread on pre-warmed (37 °C) Luria broth agar plates containing 100 µg/mL ampicillin (amp) and incubated at 37 °C overnight. A single colony was inoculated into 10 mL of Terrific broth (TB) supplemented with 100 µg/mL of amp and incubated overnight at 37 °C and 300 revolutions per min (rpm). The following morning, four 2 L flasks were prepared with 2 mL starter culture and 400 mL TB with amp and were incubated at 37 °C and 220 rpm. The suspension was monitored every 30 min until the optical density at 600 nm reached 0.4-0.6 (no unit). Protein expression was induced using 250 µM isopropyl ß-D-1-thiogalactopyranoside after cooling the suspension on ice for 30 min. The cells were then incubated for 20 h at 16 °C and 160 rpm. The pellet was collected by centrifuging at 3,000 relative centrifugal force (RCF, or g) for 30 min at 4 °C and stored at -80 °C until purification.

Protein purification was performed using a gravity flow column and fast protein liquid chromatography (FPLC) with the proteins stored at 4 °C in between steps to avoid repetitive freezing and thawing. If required, the proteins were stored in storage buffer at -80 °C. Cell lysis was performed using 4X (w/v) supplemented lysis buffer (lysis buffer supplemented with 1 cOmplete tablet/10 mL, 0.5 mg/mL lysozyme, and 1 µL/100 mL benzonase) and mixed at 4 °C for

30 min until homogeneous. The cells were lysed using sonication set up on ice with an amplitude setting of 75% for 10 s on and 60 s off for a total of 4 min of sonication time. Care was taken to avoid heat denaturation or foam production. Cell lysate was collected after centrifugation at 13,000 g for 30 min at 4 °C. The Strep-Tactin resin was prepared and mixed with the cell lysate for 2 h at 4 °C with gentle shaking. A 50 mL Bio-Rad Glass Econo-Column was washed twice with cold lysis buffer (20 mM Tris-HCl, 0.5 M NaCl, 1 mM dithiothreitol (DTT), pH 8) and equilibrated with 20 mL of cold lysis buffer. The lysis buffer was drained, and the resin was washed eight times with 5 mL of lysis buffer. The resin was resuspended with 15 mL of SUMO cleavage buffer and incubated overnight at 4 °C with gentle shaking. The protein was collected by draining the column and rinsing with 5 mL of lysis buffer three times.

Further purification was performed using ion-exchange and size exclusion FPLC (AKTA system) to ensure removal of any contaminating proteases or nucleases. The buffers were filtered, and the protein was prepared by centrifugation (3,000 g, 10 min) or filtration (0.45 μm) and diluted with binding buffer (10 mM sodium phosphate, pH 7) to lower the NaCl concentration for efficient binding. Ion-exchange chromatography was performed using a HiTrap Heparin HP column with the following program set at 5 mL/min: 10 column volumes (CV) binding buffer wash, load sample, 10 CV binding buffer wash, 10 CV elution buffer gradient (0% to 100%; 10 mM sodium phosphate, 2 M NaCl, pH 7; 0.25 mL fractions), 10 CV 100% binding buffer wash, 5 CV milliQ water wash, followed by 5 CV 20% ethanol for column storage. The fractions containing the protein were identified and pooled. If size exclusion chromatography was performed next, the buffer was exchanged with the size exclusion buffer (10 mM HEPES buffer (pH 7), 5 mM $MgCl_2$, 1 M NaCl, 2 mM DTT) and concentrated to < 2 mL using a 20 mL 50 kDa MWCO (molecular weight cut-

off) concentrator and spun at 3,000 g for 5-15 min intervals at 4 °C and then stored at 4 °C. Otherwise, the buffer was exchanged with storage buffer and stored at -80 °C.

To prepare for size-exclusion chromatography (SEC), the protein was centrifuged (10,000 g, 10 min) or filtered (0.22 µm), buffer exchanged with the size exclusion buffer, and concentrated. SEC was performed using a Superdex 200 Increase 10/300 GL column with the following program set at 0.75 mL/min: 2 CV milliQ water equilibration, 2 CV exclusion buffer equilibration, load sample, 1.2 CV size exclusion buffer elution (0.25 mL fractions), 1 CV milliQ water wash, 1 CV NaOH wash, 2 CV milliQ water wash, followed by 2 CV 20% ethanol for column storage. The fractions containing the protein were identified and pooled. The buffer was exchanged with storage buffer (50 mM Tris-HCl (pH 7.5), 0.6 M NaCl, 5% glycerol, 2 mM DTT) and concentrated using a 50 kDa MWCO concentrator and spun at 3,000 g for 5-15 min intervals at 4 °C until the protein volume was 0.5-1 mL and then stored at 4 °C.

The total protein yield was determined to be 665.25 µg, and aliquots were stored at -80 °C until use.

2.2 RT-LAMP Primer and CRISPR gRNA Design

2.2.1 RT-LAMP Primer Design

The LAMP primers were designed by using the online tools NEB LAMP or PrimerExplorer V5 and following the guidelines and considerations outlined below by Lucigen Corporation and Eiken [121, 122, 140, 141]. The LAMP primers were synthesized by Integrated DNA Technologies (IDT) and ordered as “LabReady” in 100 µM IDTE buffer (10 mM Tris, 0.1 mM EDTA, pH 8.0) or lyophilized. Lyophilized primers were preferred to avoid introducing additional buffers to the RT-LAMP or one-pot reactions.

Stability:

Gibbs free energy $\Delta G \leq -4.0$ kcal/mol, calculated using the 6 bp on the 3' and 5' ends of the following primer regions:

3' – F2, B2, F3, B3

5' – F1c, B1c

Primer length:

F3/B3 = 15 - 25 bp

F2/B2 = 15 - 25 bp

F1c/B1c = 15 - 25 bp

LF/LB = 15 - 22 bp

Melting Temperature (Tm):

ΔTm = 5 °C

F3/B3 = 55 - 63 °C

F2/B2 = 55 - 63 °C

F1c/B1c = 60 - 68 °C

LF/LB = 64 - 66 °C

Distance between bases:

F2 - F3/B2 - B3 = 0 - 60 bp

F2 - B2 = 120 - 180 bp

F1c - B1c = 0 - 100 bp*

Loops (F1 - F2/B1 - B2) = 40 - 60 bp

*It was found during this project that a bigger space, closer to 100 bp, leaves room for a gRNA to be designed without overlapping with a primer, which can contribute to background noise [139].

GC content:

40 - 60%

If GC rich: 50 - 60%

If AT rich: 40 - 50%

Amplicon size:

≤ 300 bp for optimal efficiency [104]

Dimers:

$\Delta G \geq -3.5$ kcal/mol

Avoid:

Runs of ≥ 3 of the same type of nucleotide, especially GGG, or dinucleotide repeats

Secondary structures

AT rich regions at the 3' end

Complementary sequences at the 3' end

2.2.2 CRISPR gRNA Design

CRISPR gRNAs were designed by following the previous findings for Cas12b, outlined below, and were synthesized by IDT:

Constant region (scaffold) [85, 135]:

5'–GUCUAGAGGACAGAAUUUUUCAACGGGUGUGCCAAUGGCCACUUUC

CAGGUGGCAAAGCCCGUUGAGCUUCUCAAAUCUGAGAAGUGGCAC – 3'

Length of target region (spacer) [75, 76]:

17 – 24 bp

PAM site:

5' – TTN – 3', located immediately upstream of the spacer on the NTS, opposite of the TS that the spacer binds to [75].

2.3 List of RT-LAMP Primers, gRNAs, and Reporters Used in This Study

Table 3. Summary of LASV and EBOV RT-LAMP primers, gRNA candidates, and reporters used for this study.

Set Name and Author	**RT-LAMP Primers**	**AapCas12b gRNA**
Kurosaki_2016_NP [112] Target: Makona strain, NP Accession No. KJ660348.2	**F3:** TGAAGTCAAGAAGCGTGATGG **B3:** AGTCCTTGCTCTGCATGTACT	**Kurosaki2016_gRNA** (designed for this study) GCUUCAGUCGUCUC CUCUUC

	FIP: CATGGCAGCAAGTGTTCTCTTTTT AGTGAAGCGCCTTGAGGAA **BIP:** CAGTTTCTCTCCTTTGCAAGTCTT TTTGAACCTTCTCAAGGCAAGCC **LF:** TGTTTTTTCCACTAGATACTGCTG G **LB:** TCCTTCCGAAATTGGTAGTAGGA	
Ebo_TTT_L2 (designed for this study) Target: Makona strain, L Accession No. MG572234.1	**F3:** ATCAGGAATGACTACTCCTAG **B3:** TTCGTACAATTTCGATCTGTT **FIP:** TGGCTTGCTGAGTTGTTAAGAATA AGATGCTTCTACCTGTTATGTCA **BIP:** TACTTGGTTTAAAGACCAAAGAG CAGTCGTCTCTGCATCCATG **LB:** GGCTACCTAGGCAAGTCGAGG	**Zaire_TTT_L2 (gRNA)** (designed for this study) AAAGACCAAAGAGC AAGGCU **Ebo_TTT_L2_gRNA2** (designed for this study) TGCTCTTTGGTCTTT AAACCA

Ebo_TTC_L2 (designed for this study) Target: Makona strain, L Accession No. MG572234.1	**F3:** CGACAGCAATATTATTTTCCAGAA **B3:** TTCATTTTCTCGGTATCTTGTT **FIP:** TGGATATCTGTAGCCTCAGTGTATAAATTATGCAGTTGCACTGTT **BIP:** TCGTGCTCACCTTCATCTAACTAAGATCTAAATCCAATGTAGATGTGT **LB:** GGGAGGTACCAGCTCAGTACTTAA	**Zaire_TTC_L2** (designed for this study) AUCUAACUAAGUGUUGCACC **Ebo_TTC_L2_gRNA2** (designed for this study) GAUGAAGGUGAGCACGAUUAU **Ebo_TTC_L2_gRNA3** (designed for this study) GUUAGAUGAAGGUGAGCACGA
Fukuma [11] Target: Josiah strain, NP Accession No. J04324	**F3:** ATTCTCAGCTGATGACCCTC **B3:** GTCTGTGACATCAATCCCATGT **FIP:** TCCACTGGATCTTCAGGTCTTCCTTTTTAAGGATGCAATGCTGCAAC	**Fukuma_KWgRNA** (designed for this study) GGGUCAAGUUGCAGCAUUGC

	BIP: GCCCTCTATCAACCAAGTTCAGG CTTTTGCATCCTGCTTGAACTGCT **LF:** AATGTCCATCCAGGTCTTAGC **LB:** TGCTACATACACTTCTTCCGTG	
Jos_NP2 (designed for this study) Target: Josiah strain, NP Accession No. JN650517.1	**F3:** CTGGAATCAGATGGGAAGCC **B3:** GCAGCCTGAACTTGGTTGAT **FIP:** TAAGCCCAGCGGTAAACCCTGAC AGAAAGCTGACAGCAACA **BIP:** GCAATGCTGCAACTTGACCCAAG GGCAATTTCCACTGGATCT **LF:** CTGGAATTGTTGCTGTCAGC **LB:** AAGACCTGGATGGACATTGAAGG	**Jos_NP2_gRNA** (designed for this study) CAGCAUUGCAUCCU UGAGGG
FAM_6T_BHQ1 [82]	TTTTTT	---

HEX_N12_BHQ1 [76]	NNNNNNNNNNN	---
FAMTTTTT3IABkFQ [135]	TTTTT	---

Note: RT-LAMP primers and gRNA are listed in 5' – 3'. Only the spacer of the gRNA is listed.

2.4 RNA Inactivation and Extraction

The viral stocks were stored in CL4, with EBOV grown in Vero cells and LASV grown in Vero E6 (VE6) cells. Standard operating procedures were followed to inactivate the samples by CL4 trained biologists. The samples were then brought to CL2 for purification. The QIAamp® Viral RNA Mini Kit (Cat. #52906) was used to inactivate the majority of the samples with viral lysis buffer (AVL buffer) throughout this project. Briefly, 140 µL of sample was added to 560 µL of AVL buffer with carrier RNA, unless linear acrylamide was substituted as a potentially better alternative for downstream application. The mixture was incubated for 10 min and mixed with 560 µL of 100% ethanol. The protocol for spin column purification of viral RNA was followed. As an alternative to column-based purification, the bead-based MagMAX Viral/Pathogen II (MVP II) Nucleic Acid Isolation Kit (Cat. #A48383) was thought to provide a gentler method of extraction with the KingFisher System following AVL inactivation. In this method, 1 deep-well block was set up with binding beads and solution, sample, and proteinase K. The washes were set up as 1 mL wash buffer, 1 mL 80% ethanol, 0.5 mL 80% ethanol, and 60 µL elution buffer.

It was later thought that another method might provide a purer RNA product for application to the one-pot assay. Therefore, the Direct-zol RNA Mini Prep Plus Kit (Cat. #R2072) was used as

an alternative to inactivate samples in CL4 with TRIzol instead. Samples were then purified in CL2 using the kit protocol.

Extracted RNA was aliquoted and stored in the freezer until further use.

2.5 RNA Quantification

2.5.1 EBOV Quantification

To quantify the EBOV RNA, plasmids containing the EBOV *L* gene, and associated equations outlined below, were prepared prior to this study by the Special Pathogens group. The insert size was 6639 bp, and the plasmids were serially diluted from $6.3x10^{1}$ to $6.3x10^{-10}$ ng/µL. These plasmids were used to create a standard curve on the QuantStudio 5 of CT (cycle threshold) values versus $\log_{10}$ (Genome Equivalents (GEQ)/5 µL) to which the unknown concentration of extracted EBOV RNA was compared. To create the standard curve, the concentration of plasmid DNA in ng/µL was converted to $\log_{10}$ (GEQ/5 µL) using equation 1. The standard curve produced a CT value of the extracted EBOV RNA, 14.45, which was used in equation 2 to calculate the unknown concentration. The dilution factor from the AVL inactivation was accounted for by using equation 3 to calculate the GEQ/µL of the extracted RNA, which was found to be $2.69x10^{8}$ GEQ/µL.

Equation 1: $\log_{10}(\frac{GEQ}{5\ uL}) = \log_{10}\left(\frac{5\ uL \times \boldsymbol{X}\frac{ng}{uL} \times 6.022{\times}10^{23}\frac{molecules}{mol}}{6639\ bp \times 660\frac{g}{mol} \times 10^{9}\frac{ng}{g}}\right), \mathbf{X} = [plasmid]$

Equation 2: $\log_{10}(\frac{GEQ}{5\ uL}) = \frac{CT-b}{m}, b = intercept;\ m = slope$

Equation 3: $\frac{GEQ}{uL} = 10^{\left[\mathbf{X} + \log_{10}\left(\frac{\frac{Elution\ volume\ 60\ uL}{PCR\ volume\ 5\ uL}}{Extracted\ volume\ 140\ uL}\right)\right]}, \mathbf{X} = \mathrm{X}\log_{10}(\frac{GEQ}{5\ uL})$

2.5.2 LASV Quantification

There was no plasmid standard available for LASV, therefore the Nanodrop spectrophotometer provided an estimate of RNA concentration. The Nanodrop was cleaned, and a blank solution was run prior to loading 1 µL of sample to measure the concentration of RNA in ng/µL.

2.6 RNA Integrity

As RNA is susceptible to ribonuclease degradation, and the quality of RNA may affect the performance of the assays, the Agilent Bioanalyzer was used to assess the integrity of the RNA for optimal one-pot performance. The Bioanalyzer is a microfluidic electrophoretic device which produces an electropherogram, a laser-induced fluorescence-based measurement of RNA molecules separated by molecular weight over time. Also produced is the gel image, and an algorithm calculated RNA Integrity number (RIN) ranging from 1 (completely degraded) to 10 (intact) [142].

The Agilent RNA 6000 Pico Kit (Cat. #5067-1513) was used which measures a range of 50 – 5000 pg/µL of RNA (in water), and the assay protocol was followed. Briefly, the instrument electrodes were cleaned, and the gel-dye mix was prepared by adding 1 µL of intercalating dye to 65 µL of filtered gel and centrifuged at 13,000 g for 10 min. The microfluidic chip was prepared by adding the gel-dye mix, pressurizing the system, and then adding the rest of the gel-dye mix, conditioning solution, prepared ladder, and 1 µL of heat denatured RNA samples to the appropriate wells. The chip was then run on the instrument and the RIN, electropherogram, and gel image were collected. The RNA samples for each virus were run in duplicates, one of which is shown for LASV and EBOV in figure 3.5 and figure 3.15, respectively.

2.7 RT-LAMP Reactions

The RT-LAMP reactions were performed using reagents and protocols from NEB. Reagents included *Bst* 2.0 WarmStart® DNA Polymerase (Cat. #M0538L), 10X Isothermal Amplification Buffer (Cat. #B0537S), WarmStart® RTx Reverse Transcriptase (Cat. #M0380L), 10 mM Deoxynucleotide (dNTP) Solution Mix (Cat. #N0447L), 100 mM Magnesium Sulfate ($MgSO_4$) Solution (Cat. #B1003S), LAMP Fluorescent Dye (Cat. #B1700S), Control LAMP Primer Mix (rActin) (Cat. #S0164S), WarmStart® LAMP Kit (DNA & RNA) (Cat. #E1700L), WarmStart® Colorimetric LAMP 2X Master Mix (DNA & RNA) (Cat. #M1800S), as well as nuclease-free water from Invitrogen (Cat. #AM9939/10977015).

A 10X LAMP primer pool was prepared by mixing 16 µM of FIP/BIP, 4 µM LF/LB, and 2 µM of F3/B3. If primers were lyophilized, they were reconstituted in nuclease-free water to a concentration of 100 µM to avoid introducing buffers to the reaction, as per NEB (protocol #M1800). The 10X primer pool was prepared by adding 16 µL of 100 µM FIP/BIP, 4 µL of 100 µM LF/LB, 2 µL of 100 µM F3/B3 and bringing the volume to 100 µL with nuclease-free water [135].

The reactions were run following the appropriate NEB RT-LAMP protocols. Reactions were run for 30 min or 1 h, at 60 °C or 65 °C, and assessed for amplification using the LAMP Fluorescent Dye, turbidity, 1-3% agarose gel electrophoresis, or the WarmStart® Colorimetric assay. The reactions were run using the Dialunox ESEQuant TS2.4, Thermo Fisher Scientific QuantStudio 3/5 Real-Time PCR Systems, conventional ProFlex PCR System, or Bio-Rad CFX96 Real-Time System.

2.7.1 Melting Curve Analysis

Melting curve analysis, a technique used to differentiate LAMP amplicons, was run on the QuantStudio 3/5 system to assess potential non-specific amplification or contamination [107, 120]. RT-LAMP reactions were run using the intercalating LAMP Fluorescent Dye for 30 min at 65 °C, with a ramp rate of 1.6 °C/s, followed by a melting curve analysis of 95 °C for 15 s, 1.6 °C/s; 60 °C for 30 s or 1 min, 1.6 °C/s; 95 °C for 15 s, 0.1 °C/s. A melting curve analysis was run for both LASV and EBOV, shown in figure 3.9 and figure 3.30, respectively.

2.7.2 Sanger Sequencing

To confirm the false positives results in some reactions were caused by contamination in the LASV (Josiah) reactions, Sanger sequencing was performed by the National Microbiology Laboratory Genomics Core. First, new reagents were opened and used to run 50 µL RT-LAMP reactions containing 2 µL template or water (NTC) for 30 min at 65 °C, followed by an inactivation period of 10 min at 85 °C. After the RT-LAMP reaction, 1 µL from the template-containing reaction and NTC reaction was used as a template in PCR, using the Invitrogen IV One-step RT-PCR kit (Cat. #12595010). The kit protocol was followed and the RT-LAMP F3 and B3 primers were used as the forward and reverse primers. After PCR, a 3% agarose gel was run to confirm the expected band size, and the DNA was extracted from the gel using the NucleoSpin® Gel and PCR Clean-up kit (Cat. #740609.50). The product was then sent for sequencing and the DNASTAR Lasergene SeqMan Ultra and MegAlign Pro program (version 18.1.1) was used to analyze the results.

2.8 Cas Enzyme and gRNA Activity

After the AapCas12b enzyme was produced in-house, the activity was assessed to ensure the enzyme was working properly and its activity was compared to the activity of the SignalChem (Cat. #C12B1-E311U) enzyme (figure 3.1 and figure 3.2). The Cas enzyme activity was assessed by following a modified protocol from the HOLMESv2 method containing 250 nM AapCas12b, 250 nM gRNA, 1 µL DNA template or water (NTC), 500 nM HEX_N12_BHQ1 reporter, and 10X Isothermal Amplification Buffer [76]. The total volume was brought to 25 µL with nuclease-free water and the assay was run on the Dialunox ESEQuant TS2.4 reader for 60 min at 60 °C. For this reaction, DNA templates were made from the LASV and EBOV RNA by using the One-Step Ahead RT-PCR kit (Cat. #220213) and the LAMP F3 and B3 primers. The DNA was then extracted from a 1% agarose gel and purified using the NucleoSpin® Gel and PCR Clean-up kit (Cat. #740609.50) and used as template for the reaction described above.

2.9 RT-LAMP/Cas12b Two-step Reactions

While LAMP has been used on its own as a POCT, it is theorized that CRISPR may provide a level of specificity to overcome any non-specific amplification that may occur in the LAMP reaction [48, 81, 82]. So-called two-step reactions have been discussed in the literature, however true one-pot reactions are desired for the POC for a few reasons, such as reducing the number of steps and time, decreasing the risk of carryover contamination, and increasing user-friendliness [82, 83, 135]. However, combining reactions may come at the cost of sensitivity, as the one-pot requires coordination of two reactions [82]. Nevertheless, running a two-step reaction ensures that the CRISPR-part of the reaction, including the Cas enzyme, gRNA, and associated buffers can detect the RT-LAMP amplicon amid other enzymes, salts and buffers.

A modified version of the STOPCovid.v2 one-pot method was used to run the two-step reaction. First, the RT-LAMP reaction was run for 30-60 min at 60-65 °C. Aliquots of the RT-LAMP reaction, typically 1-3 µL, were then added to the CRISPR part of the reaction, typically containing 31.25 nM AapCas12b, 31.25 nM gRNA, 250 nM reporter, 10X Isothermal Amplification Buffer and nuclease-free water to a total volume of 50 µL. Reactions were run for 1 h at 60-65 °C on a device that measures fluorescence such as the Dialunox ESEQuant TS2.4 or Thermo Fisher Scientific QuantStudio 3/5 Real-Time PCR System.

Detection of the RT-LAMP reaction containing the amplified target and no detection of the RT-LAMP NTC reaction shows that the Cas-gRNA complex can identify and cleave the correctly amplified target, which is reflected in figure 3.31.

2.10 RT-LAMP/Cas12b One-pot Reactions

The RT-LAMP/Cas12b one-pot reactions were typically run at 60-65 °C for 30-60 min on the Dialunox ESEQuant TS2.4, Thermo Fisher Scientific QuantStudio 3/5 Real-Time PCR Systems, or Bio-Rad CFX96 Real-Time System. Reagents followed the STOPCovid.v2 protocol, including 1 M Tris-HCl, pH 8 (ThermoFisher Scientific, Cat. #AM9855G), 2 M Ammonium sulfate (Millipore Sigma, Cat. #76399), 1 M $MgSO_4$ solution (Millipore Sigma, Cat. #M3409), Tween 20 (Millipore Sigma, Cat. #P9416), Taurine (Millipore Sigma, Cat. #86329), Proteinase K inhibitor (Millipore Sigma Cat. #539470), Dimethyl sulfoxide (DMSO) (Millipore Sigma Cat. #D2650), 100 mM $MgSO_4$ Solution (NEB, Cat. #B1003S), NEB *Bst* 2.0 WarmStart® DNA Polymerase, NEB WarmStart® RTx Reverse Transcriptase, NEB 10 mM dNTP Solution Mix, nuclease-free water (Invitrogen, Cat. #AM9939/10977015), as well as the LAMP primer pool, AapCas12b, gRNA, and reporter [135]. Most reactions were run using the AapCas12b enzyme produced in-

house, otherwise the Cas12b enzyme was ordered from NEB (special order) or SignalChem (Cat. #C12B1-E311U).

The one-pot reactions followed the STOPCovid.v2 method, or a modified version [135]. The modified version included the optimizations made in section 3.4.3.2.1, such as 8 mM $MgSO_4$, 240 units/mL *Bst* 2.0 WarmStart® DNA Polymerase, 0.5X LAMP primer pool, and 500 nM reporter. Other changes included removal of proteinase K inhibitor and Tween 20, and addition of 2 mM DTT and 1% Brij-35.

2.11 Statistical Analysis and Equipment

The results were graphed using GraphPad Prism 10.6.1 for Windows, GraphPad Software, Boston, Massachusetts USA, www.graphpad.com. For the context of this study and purpose of optimization, the assay was assessed via the presence or absence of fluorescence in the template-containing reactions compared to the NTCs. Otherwise, a positive result was considered as 3x greater than the read-out value (Relative fluorescence units (RFU), fluorescence, or mV) of the NTC, with the mean ± 2 or 3 standard deviations or 3x the mean also considered if technical replicates were run.

It is important to note the different machines used to run the RT-LAMP or RT-LAMP/Cas12b assays measured the resulting fluorescence in different units, such as mV when using the Dialunox ESEQuant TS2.4 reader, fluorescence when using Thermo Fisher Scientific QuantStudio 3/5 Real-Time PCR Systems, and RFUs when using the Bio-Rad CFX96 Real-Time System, which are displayed in their corresponding graphs below.

3.0 Results

3.1 Cas12b Enzyme Activity

The Cas12b enzyme activity was assessed after it was produced in-house to ensure it was working correctly and was compared to the purchased SignalChem enzyme. It was found that the Cas12b enzyme produced in-house demonstrated a faster signal in figure 3.1 than the SignalChem enzyme in figure 3.2. It is unknown why this was the case and could be attributed to differences in the enzyme insert or production and purification methods, as well as the in-house produced enzyme may have been produced more recently than the purchased enzyme was. Therefore, the in-house produced enzyme was used for the majority of this study.

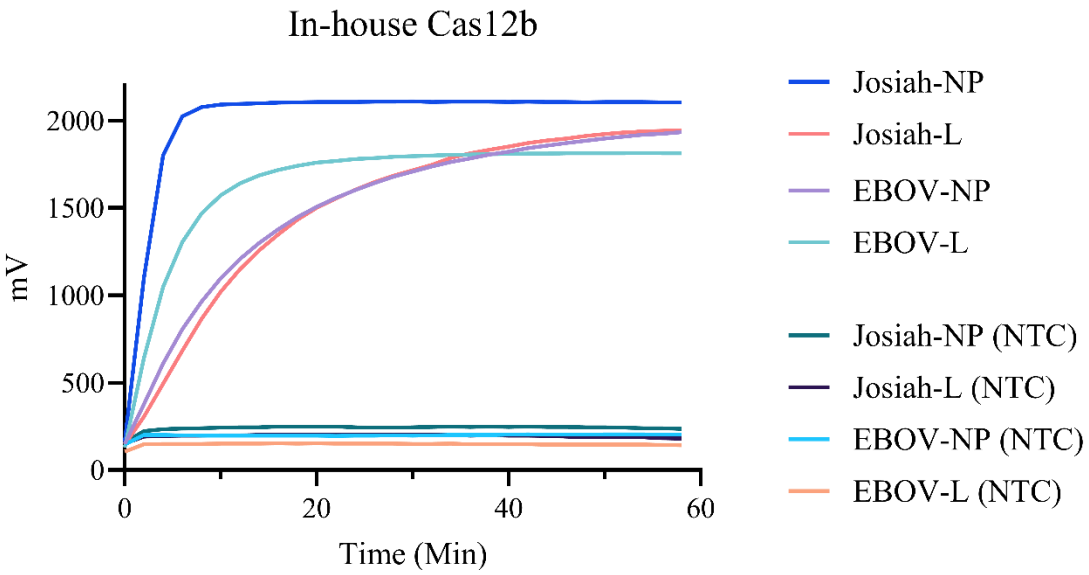

Figure 3.1 AapCas12b produced in-house and associated gRNA can detect PCR pre-amplified LASV and EBOV DNA templates. Primer sets targeting LASV or EBOV NP or L and associated NTC, primer sets are not shown. Reaction run at 60 °C on TS2 reader.

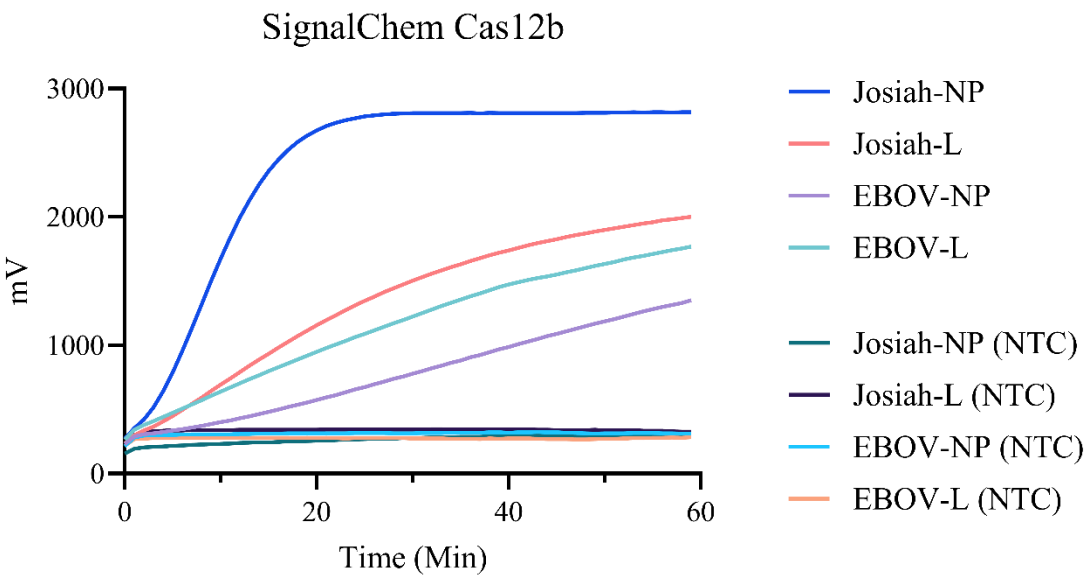

Figure 3.2 SignalChem AapCas12b and associated gRNA can detect PCR pre-amplified LASV and EBOV DNA templates, although slower than in-house produced enzyme. Primer sets are not shown. Reaction run at 60 °C on TS2 reader.

3.2 Current LASV and EBOV Assays

The published LASV and EBOV RT-LAMP assays that had potential for gRNA addition for one-pot testing chosen in table 1 and table 2 (and listed in table 3) were tested. These primer sets were ordered and a gRNA was designed. It was found that these sets had less desirable activity, and other RT-LAMP/gRNA sets were chosen for further testing instead. The LASV one-pot using the RT-LAMP primers designed by Fukuma et al. (2011) is shown in figure 3.3 [11]. In this reaction the fluorescence occurs late, the intended target is not detected, and high variability is seen between reactions. The EBOV one-pot using RT-LAMP primers designed by Kurosaki et al. (2016) is shown in figure 3.4 [112]. In this reaction, the activity is slow with low distinction between template-containing reactions and the NTC.

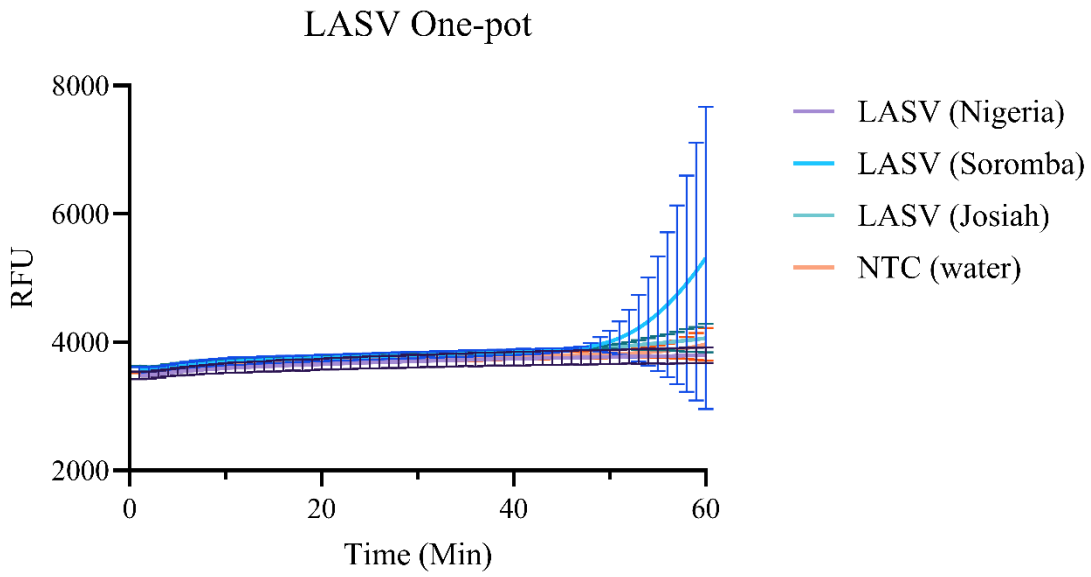

Figure 3.3 LASV one-pot run in triplicate using primers by Fukuma et al. (2011). Reaction run at 60 °C on CFX96 system.

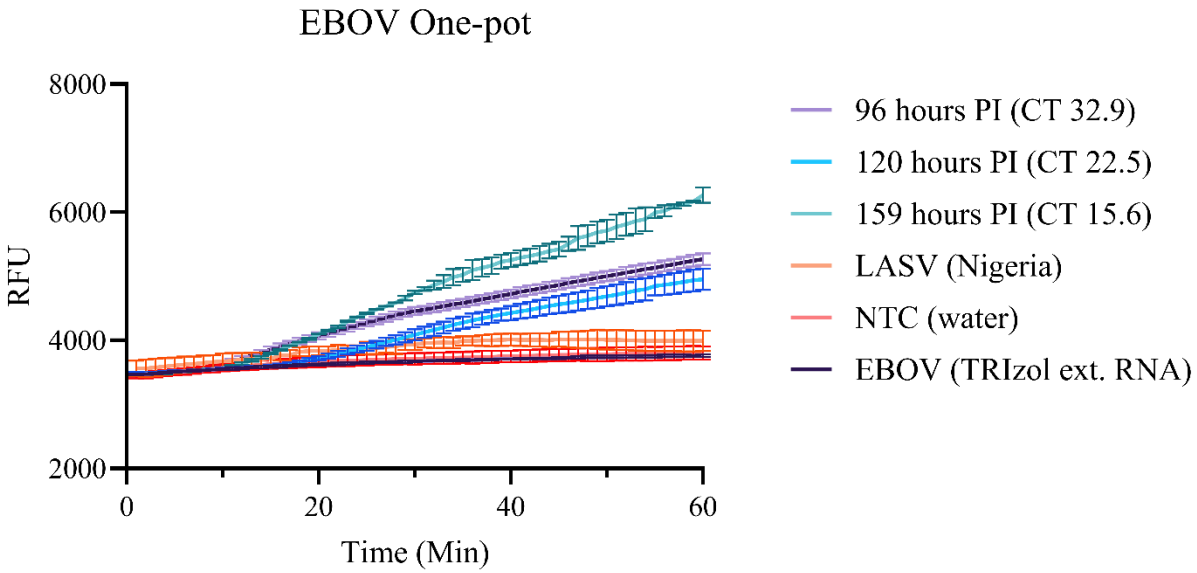

Figure 3.4 EBOV one-pot run in triplicate using primers by Kurosaki et al. (2016). Reaction run at 60 °C on CFX96 system.

3.3 Lassa Fever

The reactions in this section detect LASV using the primer set "Jos_NP2" listed in table 3.

3.3.1 LASV Quantification

The LASV RNA concentration was measured using the Nanodrop spectrophotometer and the results are listed below.

Table 4. LASV Quantification.

Template	**Concentration (ng/µL)**
LASV (Josiah)	14.5
LASV (Soromba)	3.3
LASV (Nigeria)	16.8

3.3.2 LASV RNA Integrity

Several tests on the TS2 reader showed results in the low mV range when running EBOV titrations in section 3.4.3.2.1. To assess the RNA quality as a possible reason for the low mV output, the Bioanalyzer was used to generate a RIN. The LASV RNA was found to be of low quality, as the RIN was determined to be 2, indicating a high level of degradation [142].

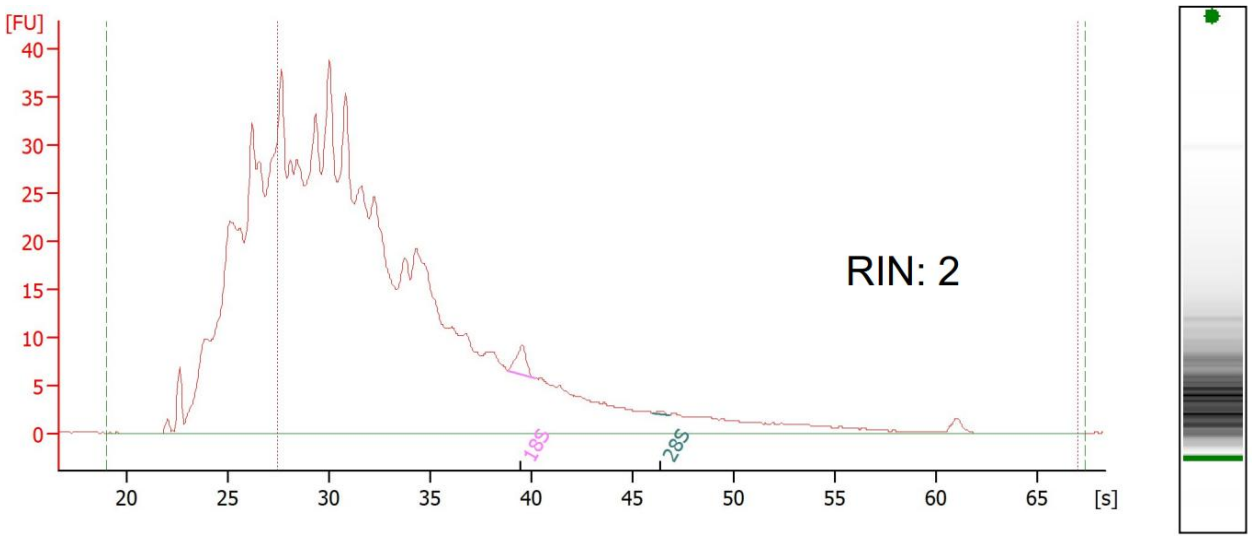

Figure 3.5 RNA Integrity and RIN of LASV (Josiah). The RIN was determined to be 2.

3.3.3 RT-LAMP Assay

RT-LAMP assays were run separately from the one-pot reaction to ensure the RT-LAMP primers were suitable to amplify and detect the intended target without side effects, as described in section 2.7. The figures below demonstrate the RT-LAMP detection of LASV compared to the NTC, using fluorescence (figure 3.6) and gel electrophoresis (figure 3.7). The gel electrophoresis demonstrates the LAMP "ladder" effect seen in lane 2 (template-containing) compared to lane 3 (NTC). Note that the marker in lane 1 is unlabeled as LAMP amplicons are not measured by a specific banding size.

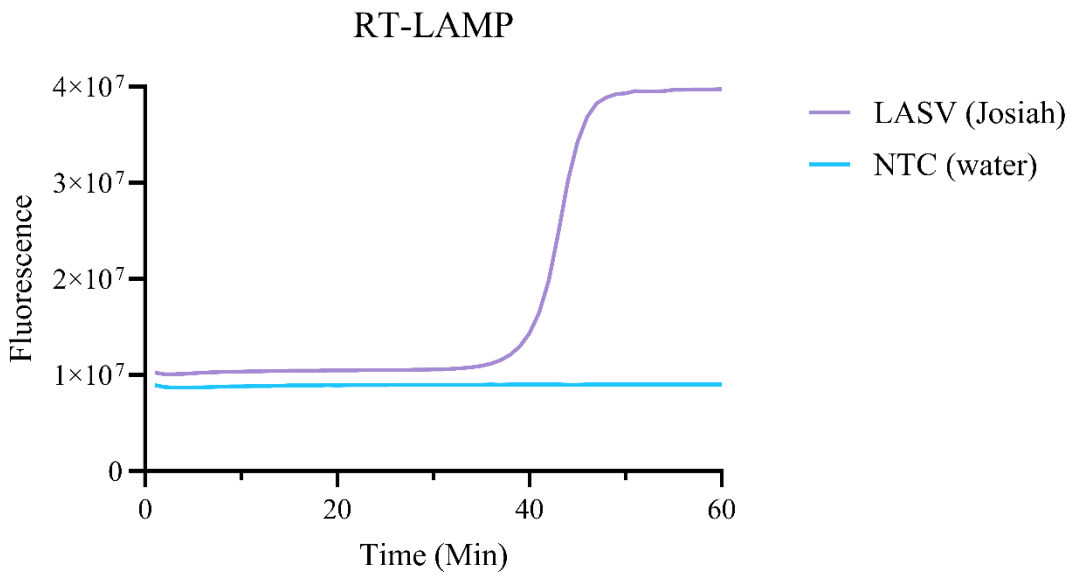

Figure 3.6 RT-LAMP assay of LASV (Josiah). Reaction run at 65 °C on QuantStudio system.

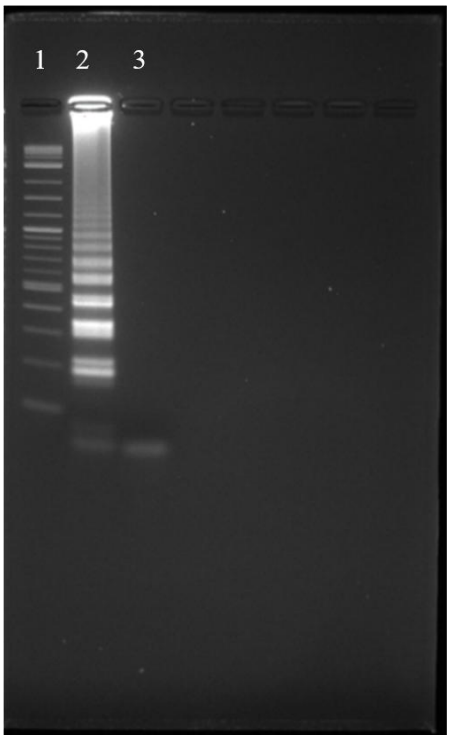

Figure 3.7 LASV RT-LAMP gel electrophoresis. Lane 1: marker, lane 2: LASV (Josiah) template, lane 3: NTC. Reaction run at 65 °C, 30 min, 2% agarose gel electrophoresis.

3.3.3.1 DMSO

After seeing false positive results in the one-pot reactions (section 3.3.4), it was tested if adding DMSO or increasing the temperature would resolve the false positives, as 7.5% of DMSO has been shown to inhibit non-specific amplification in LAMP reactions [143]. Two temperatures, 65 °C and 67 °C, were tested with 7.5% DMSO. Lanes 1 (template-containing) and 2 (NTC) show the RT-LAMP reaction at 67 °C, lanes 3 (template-containing) and 4 (NTC) show the reaction with 7.5% DMSO at 65 °C, while lanes 5 (template-containing) and 6 (NTC) show the reaction with 7.5% DMSO at 67 °C. It was found that the combination of 67 °C and DMSO affected the reaction as these are dimmer than the others; however, the template-containing reaction in lane 5 is dimmer than the NTC in lane 6.

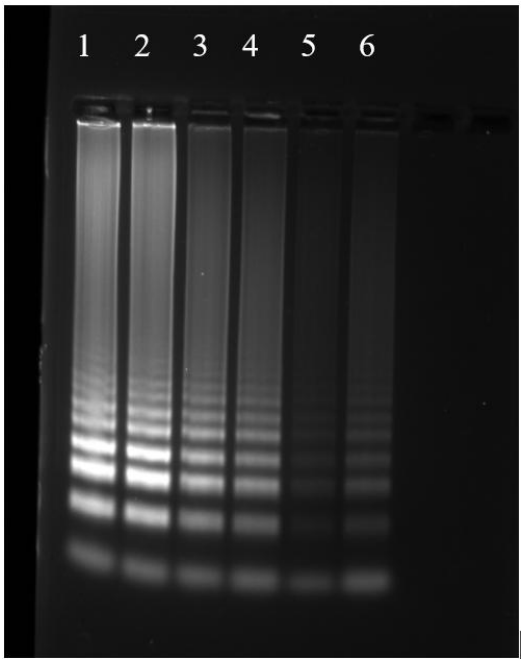

Figure 3.8 LASV RT-LAMP assay with DMSO. Lane 1 and 2: 67 °C template-containing and NTC, Lane 3 and 4: 65 °C + 7.5% DMSO template-containing and NTC, Lane 5 and 6: 67 °C + 7.5% DMSO template-containing and NTC.

3.3.3.2 Melting Curve Analysis

A melting curve analysis was also run to address the cause of the false positives. The RT-LAMP reaction was run in duplicate with both the template and water (NTC). Theoretically, if the melting temperatures are similar this indicates contamination from the template, as the RT-LAMP reaction is producing the same amplicon. If the melting profiles are different, this indicates non-specific amplification [107, 120]. The melting curve analysis below indicates that the template-containing reactions had similar melting temperatures at approximately 85 °C, while the NTCs showed temperatures of 86.49 °C and 87.30 °C. As well, one of the NTCs showed activity at approximately 80 °C, which could potentially be due to primer dimer interactions [120].

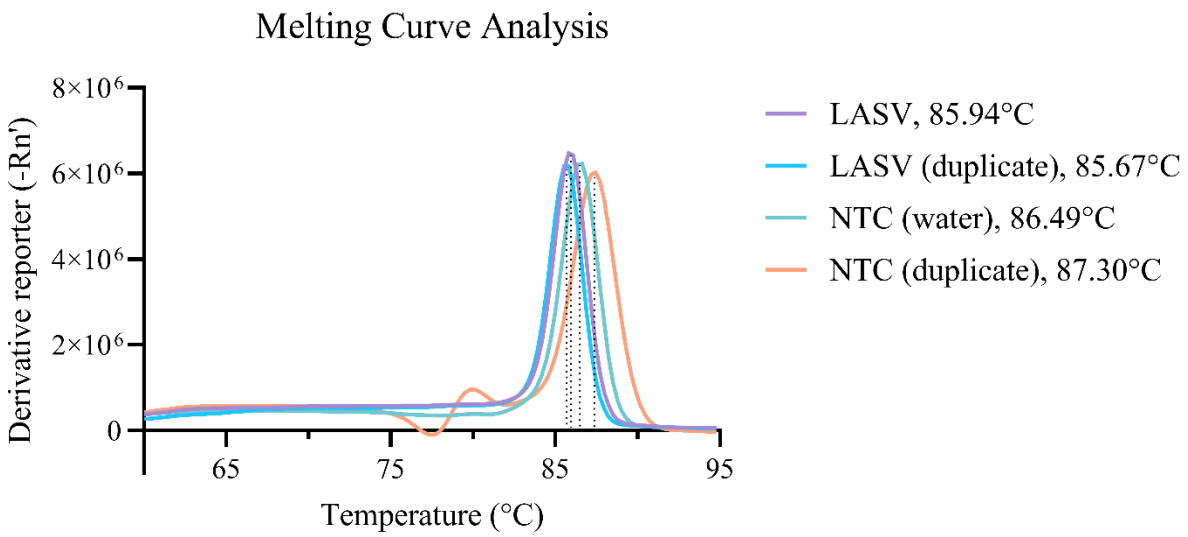

Figure 3.9 Melting curve analysis of LASV (Josiah). Reaction run on QuantStudio system.

3.3.3.3 Sequencing

While the melting curve analysis in figure 3.9 provided insight into potential non-specific amplification due to the difference in melting temperatures and occurrence of primer artifacts, it could not be confidently confirmed to be either non-specific amplification or contamination as the cause of false positives. Consequently, the false positive results shown in the LASV RT-LAMP and one-pot reactions were confirmed to be contamination by Sanger sequencing, as it was found that the NTC was 98.3% similar to the template-containing reaction, indicating contamination in the LASV reaction (data not shown).

3.3.4 RT-LAMP/Cas12b One-pot

The CRISPR-based one-pot reactions were successful until false positive results occurred, which were confirmed to be contamination. Figure 3.10 demonstrates a successful one-pot reaction with detection of LASV occurring rapidly.

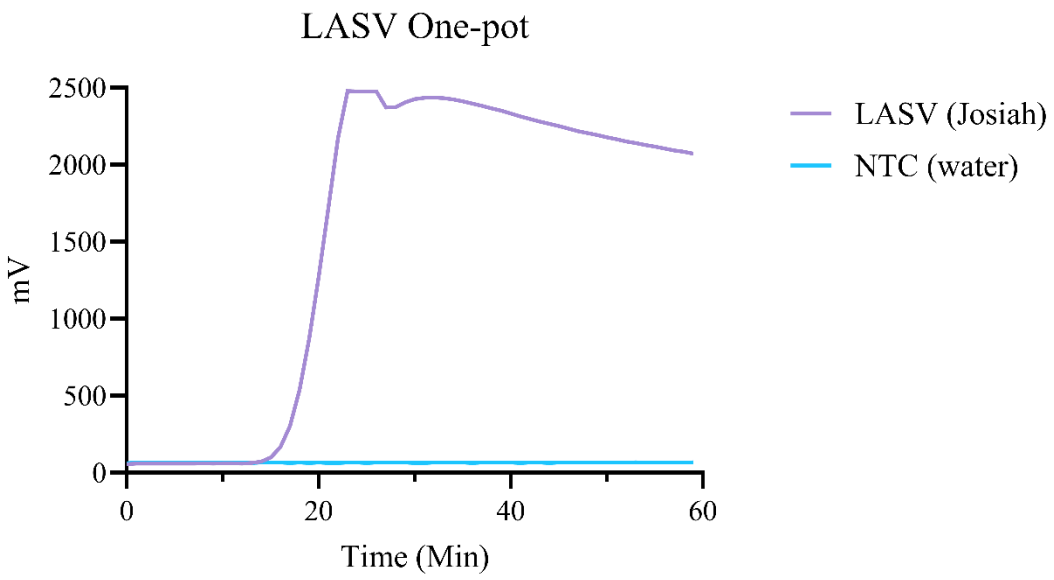

Figure 3.10 LASV (Josiah) one-pot run in singlicate. Reaction run at 65 °C on TS2 reader.

3.3.4.1 Cross-Reactivity

The cross-reactivity of the LASV one-pot assay was assessed by running the assay with other LASV and EBOV targets, as well as VE6 cell lysate and supernatant, as the LASV was grown in VE6 cells. The reaction in figure 3.11 did not detect other targets; however, several NTC's with water were run (x6), one of which showed activity after 40 min.

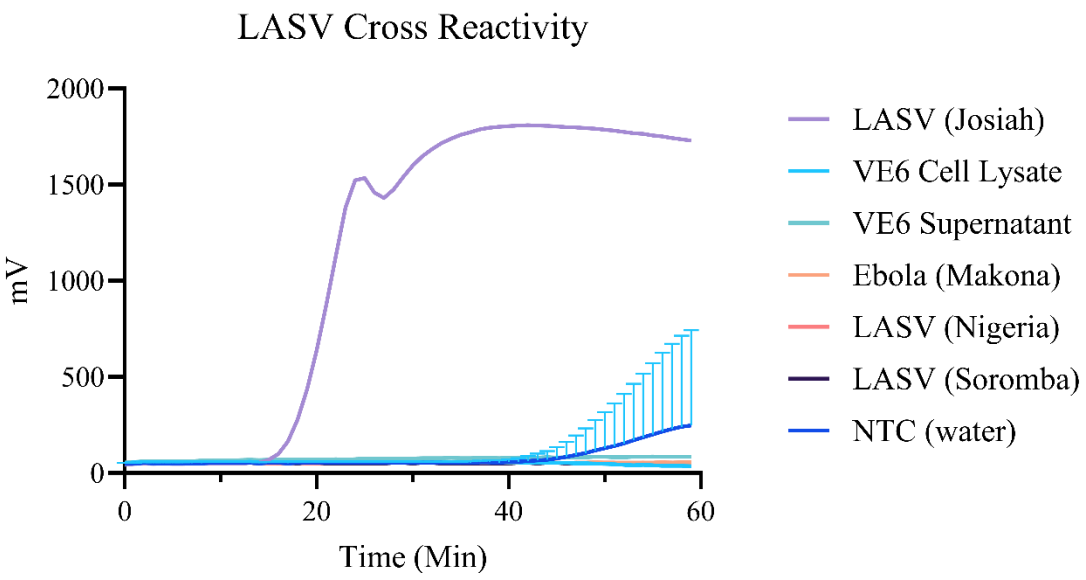

Figure 3.11 Cross-reactivity of LASV one-pot assay. LASV assay does not detect VE6 cell lysate or supernatant, EBOV, or other LASV targets. NTC was run six times with one replicate detected. Reaction run at 65 °C on TS2 reader.

3.3.4.2 NHP Samples

To test the one-pot assay on animal samples, non-human primate (NHP) blood samples were obtained from a previous LASV study in the Special Pathogens laboratory. The extracted blood RNA samples ranged from 1 day prior to infection to 14 days post-infection (DPI), which are listed with their corresponding CT values from 14.09 to > 40 in figure 3.12. The one-pot showed false positive results, as the assay detected both the NTC and the sample with the CT >40, which was 1 day prior to infection, and is therefore not expected to contain the targeted RNA.

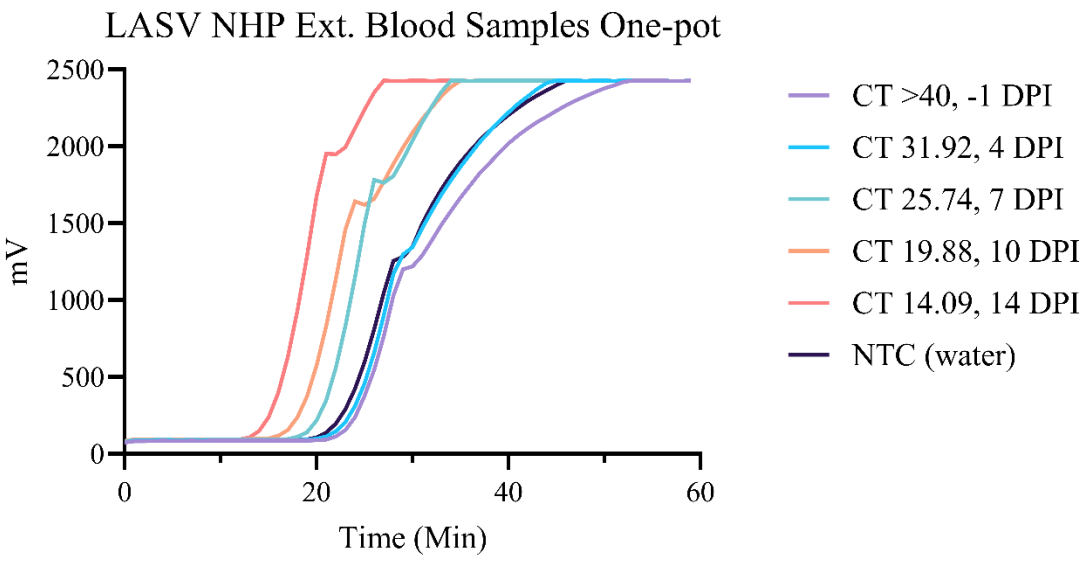

Figure 3.12 LASV one-pot with NHP extracted blood samples. Reaction run at 65 °C on TS2 reader.

3.3.4.3 One-pot Without Cas12b and gRNA

As another way to assess the false positive results, the one-pot was run with and without template, as well as without the Cas12b and gRNA (-cas12b, -gRNA). Unsurprisingly, it was found that Cas12b and gRNA are necessary to produce a false positive result.

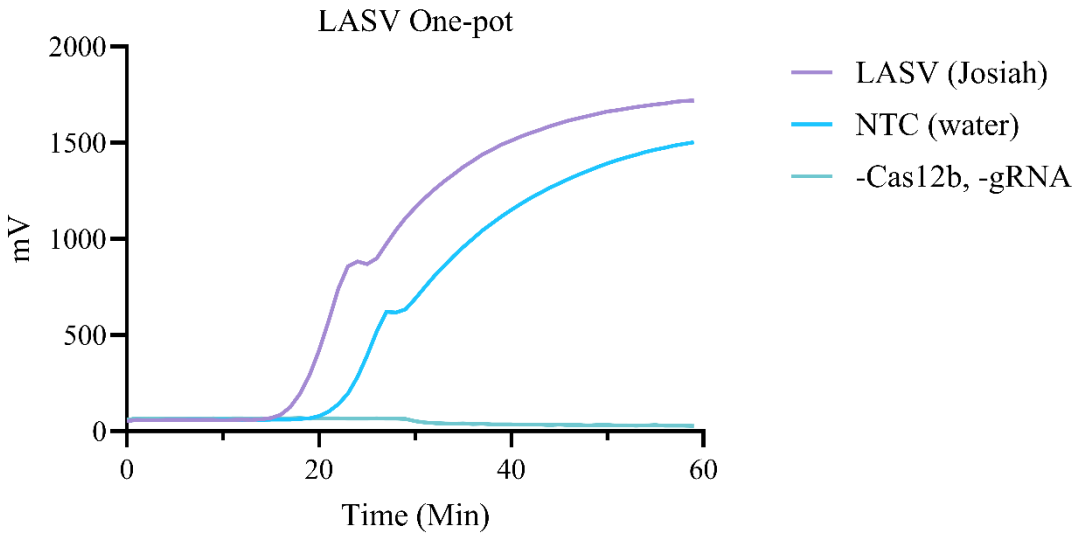

Figure 3.13 LASV one-pot without Cas12b and gRNA does not produce false positive. Reaction run at 65 °C on TS2 reader.

3.3.4.4 Primer-gRNA Interaction

To assess the primer-primer interactions and primer-gRNA interactions as a possible reason for the false positive results, the primers and gRNA were assessed with the Multiple Primer Analyser, ThermoFisher Scientific. Interestingly, there was a theoretical interaction between the BIP and two gRNAs, with an overlap of 9 bp and 20 bp. This theory was tested by inserting each LAMP primer (F3, B3, FIP, BIP, LF, and LB) as the "template" into the CRISPR reaction containing the gRNA with the 20 bp complement. However, this was not the gRNA used in the one-pot assays, and the BIP concentration was increased by 6.25X before the interaction below in figure 3.14 was seen in the one-pot reaction. Therefore, while it is possible that the gRNA can detect the primer, this is not likely the cause of the false positives.

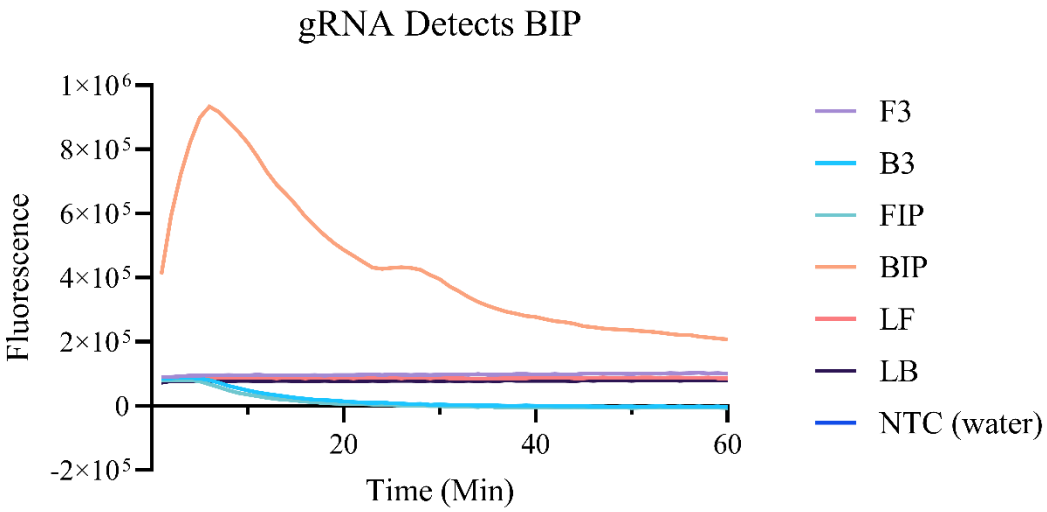

Figure 3.14 LASV one-pot detects LAMP primer BIP. Reaction run at 65 °C on QuantStudio system.

3.4 Ebola Virus

3.4.1 EBOV Quantification

The LAMP primer and gRNA sets outlined for EBOV titled "Ebo_TTT_L2" and "Ebo_TTC_L2" in table 3 are designed to detect the *L* gene. Therefore, the concentration of the *L* gene was calculated to be 2.69x10^8 GEQ/µL, by using the previously designed plasmid standards and the equations outlined in section 2.5.1.

3.4.2 EBOV RNA Integrity

The EBOV RNA integrity was assessed at the same time as the LASV RNA and also found to be of low quality. The RIN was calculated to be 2.2, which corresponds to a high level of degradation [142].

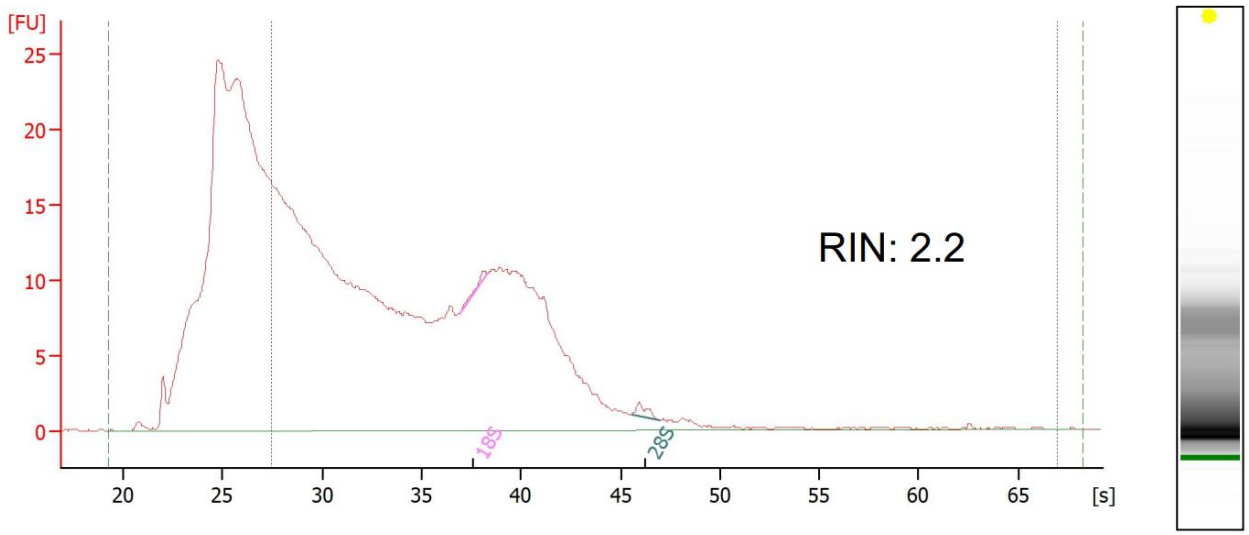

Figure 3.15 RNA integrity and RIN of EBOV. The RIN was determined to be 2.2.

3.4.3 EBOV Set 1

The EBOV reactions displayed in this section refer to the set labeled "Ebo_TTC_L2" in table 3.

3.4.3.1 RT-LAMP Assay

Similar to the LASV reactions, the EBOV RT-LAMP assays were run separately from the one-pot reaction to ensure the LAMP primers were suitable to amplify and detect the intended target without side effects, as described in section 2.7. The figure below demonstrates the RT-LAMP detection of EBOV compared to the NTC run in duplicate, using fluorescence. In this reaction, the NTC also shows activity shortly after 20 min, and there is high variability between the replicates.

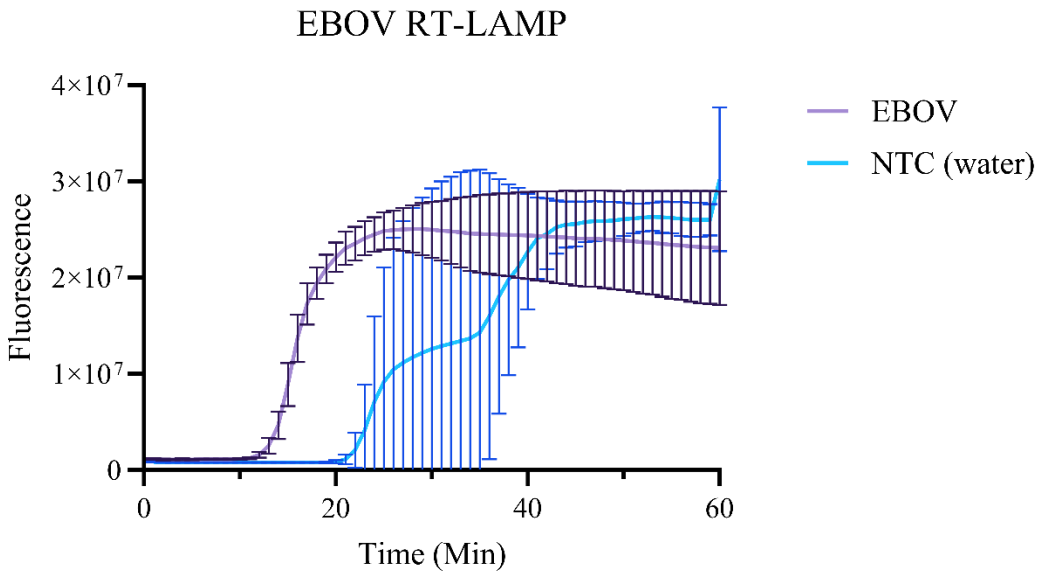

Figure 3.16 EBOV RT-LAMP assay run in duplicate. Reaction run at 65 °C on QuantStudio.

3.4.3.2 RT-LAMP/Cas12b One-pot

This section demonstrates the optimization of the STOPCovid.v2 one-pot protocol by assessing a range of concentrations of various reagents, such as enzymes, primers, and reporters in section 3.4.3.2.1, followed by a comparison of the post-optimized protocol to the original STOPCovid.v2 protocol in section 3.4.3.2.2, and finally an assessment of the cross-reactivity in section 3.4.3.2.3.

3.4.3.2.1 Titrations

Here, various concentrations of $MgSO_4$, dNTPs, LAMP primers, *Bst* 2.0 polymerase, RTx reverse transcriptase, and the reporter are assessed to determine the fastest or strongest signal on the Dialunox ESEQuant TS2.4 reader in an effort to optimize the STOPCovid.v2 one-pot protocol for EBOV detection.

3.4.3.2.1.1 $MgSO_4$

The concentration of $MgSO_4$ was assessed from 0 mM to 11 mM. The optimal concentration was determined to be the original 8 mM, as it had the best combination between the strongest and earliest signal.

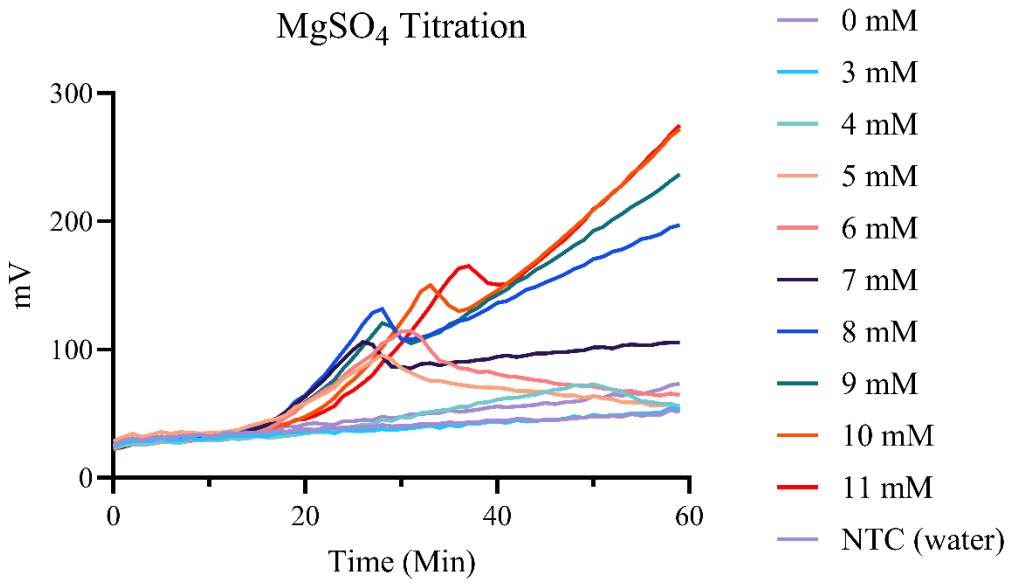

Figure 3.17 $MgSO_4$ titration. Reaction run at 60 °C on TS2 reader.

3.4.3.2.1.2 dNTP

The concentration of dNTP was assessed from 0 mM to 2.8 mM. The optimal concentration was determined to be the original 1.4 mM, as it had the strongest signal.

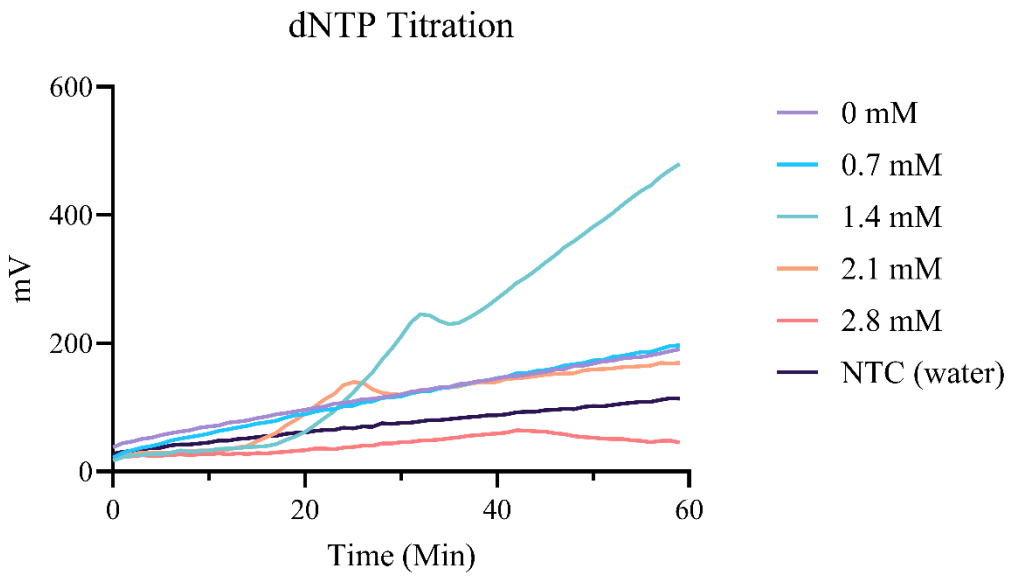

Figure 3.18 dNTP titration. Reaction run at 60 °C on TS2 reader.

3.4.3.2.1.3 LAMP Primers

The LAMP primer pool was assessed from 0.0X to 2.0X. The optimal concentration was determined to be 0.5X, instead of the original 1X, as it had the strongest signal.

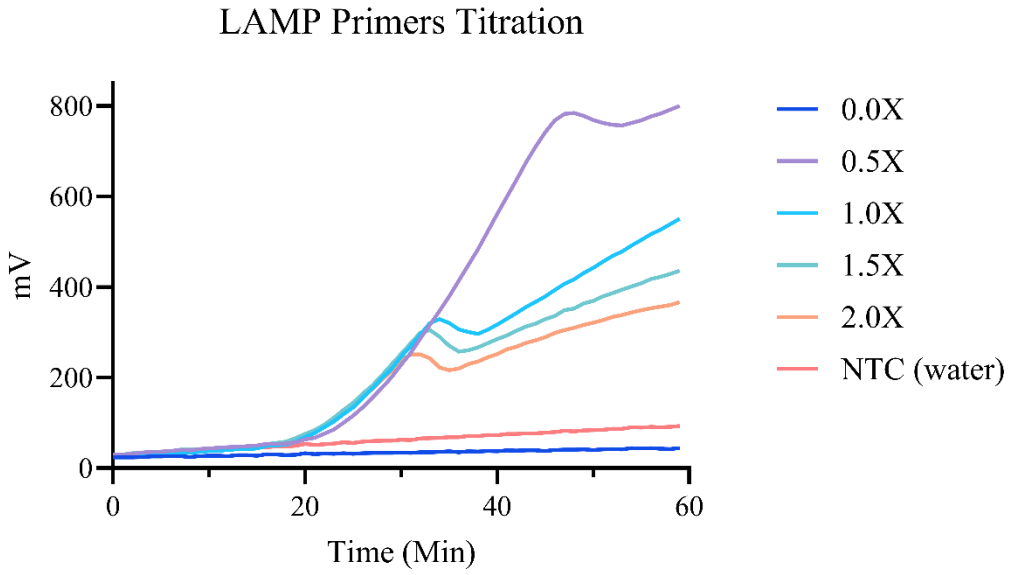

Figure 3.19 RT-LAMP primer titration. Reaction run at 60 °C on TS2 reader.

3.4.3.2.1.4 RTx Reverse Transcriptase

The concentration of RTx reverse transcriptase was assessed from 0 units/mL to 600 units/mL. The optimal concentration was determined to be the original 300 units/mL, as it had the best combination between the strongest and earliest signal.

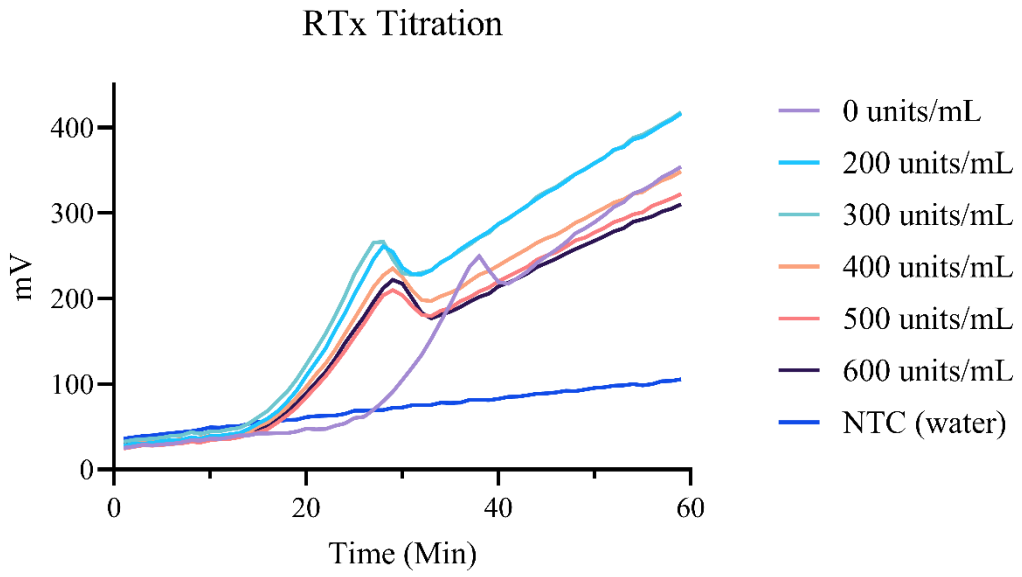

Figure 3.20 RTx reverse transcriptase titration. Reaction run at 60 °C on TS2 reader.

3.4.3.2.1.5 *Bst* 2.0 Polymerase

The concentration of *Bst* 2.0 polymerase was assessed from 0 units/mL to 640 units/mL. The optimal concentration was determined to be 240 units/mL, instead of the original 320 units/mL, as it had the strongest signal.

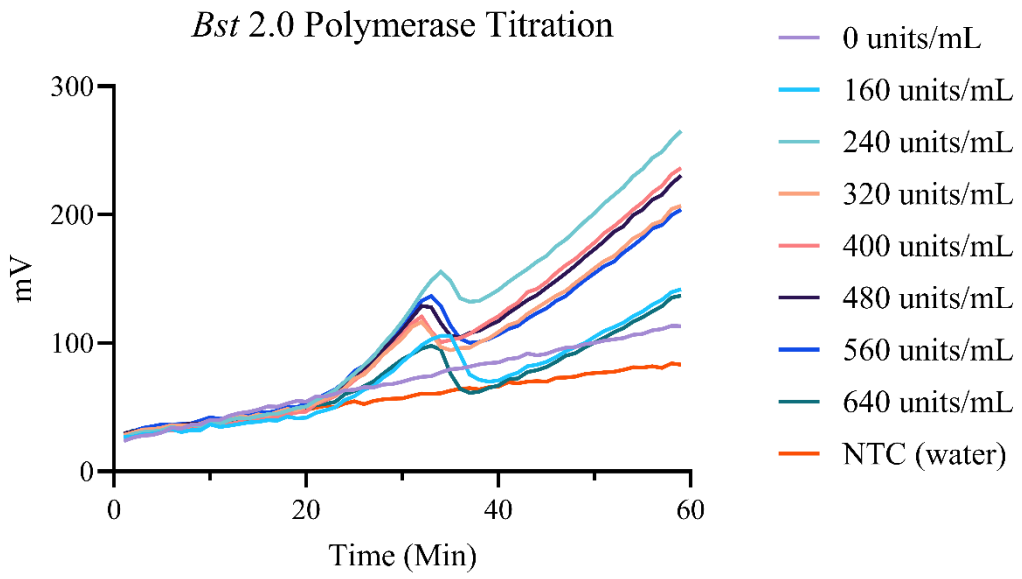

Figure 3.21 *Bst* 2.0 polymerase titration. Reaction run at 60 °C on TS2 reader.

3.4.3.2.1.6 Reporter

The concentration of the FAM-6T-BHQ1 reporter listed in table 3 was assessed from 0 nM to 500 nM. The optimal concentration was determined to be 500 nM, instead of the original 250 nM, as it had the strongest signal. However, it was noted as a risk that doubling the concentration of reporters could affect the background signal in the NTC.

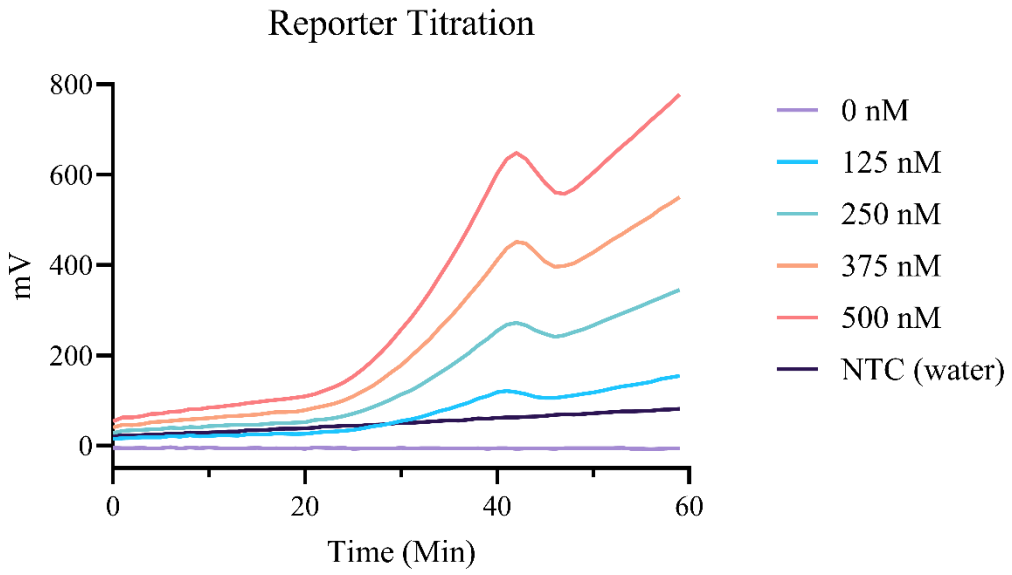

Figure 3.22 Reporter titration. Reaction run at 60 °C on TS2 reader.

3.4.3.2.2 STOPCovid.v2 Protocol Versus Post-Optimized Protocol

After the one-pot protocol had been optimized, it was compared to the original STOPCovid.v2 protocol by Joung et al. (2020) [135]. It was found that optimization of the selected reagents resulted in a stronger signal in both the template-containing and NTC reactions.

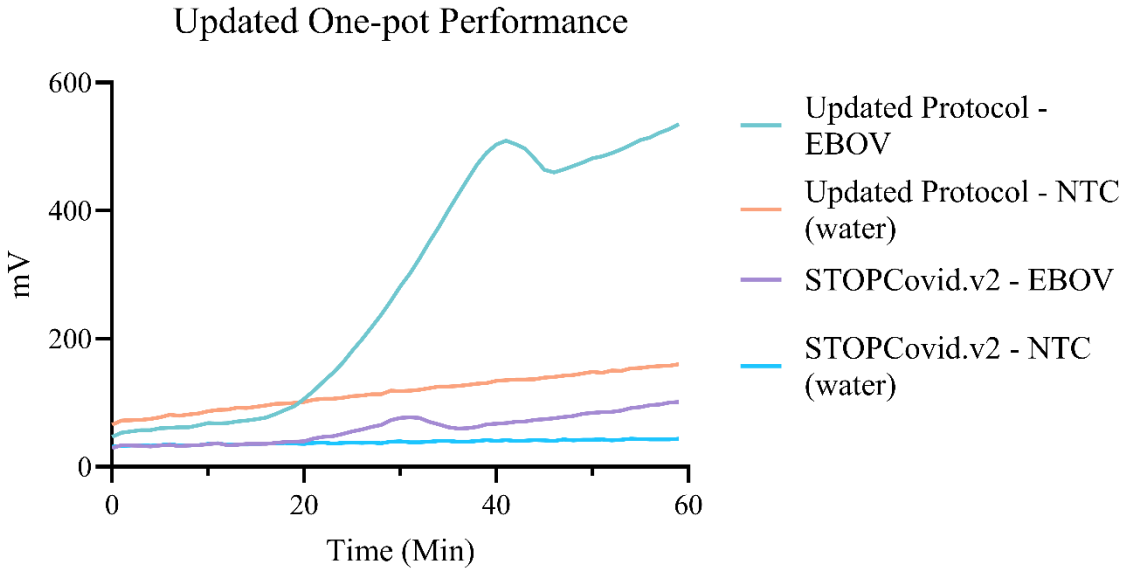

Figure 3.23 Post-optimized one-pot protocol compared to STOPCovid.v2 protocol. Reaction run at 60 °C on TS2 reader.

3.4.3.2.3 Cross-Reactivity

The cross-reactivity of the EBOV one-pot reaction was assessed with LASV targets, SARS-CoV-2, and other potentially relevant viruses such as DENV and MARV. The one-pot assay was found to specifically detect EBOV, as shown below.

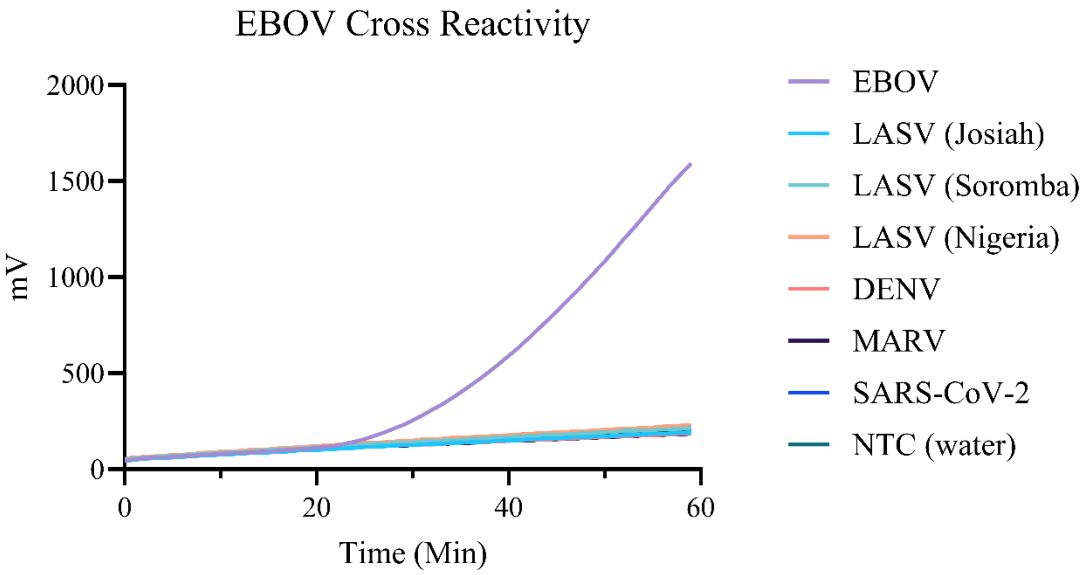

Figure 3.24 Cross-reactivity of EBOV one-pot assay. Reaction run at 60 °C on TS2 reader.

3.4.4 EBOV Set 2

The EBOV reactions displayed in this section refer to the set labeled “Ebo_TTT_L2” in table 3.

3.4.4.1 RT-LAMP Assay

As described before, the EBOV RT-LAMP assays were run separately to assess the LAMP primer suitability according to section 2.7. The RT-LAMP assays in this section are shown using different readout methods, such as fluorescence, color change, or gel-based. The RT-LAMP detection of EBOV compared to the NTC in triplicate, using fluorescence, is shown in figure 3.25.

In figure 3.26, the NEB colorimetric assay is used to show the successful detection of EBOV, followed by gel electrophoresis in figure 3.27.

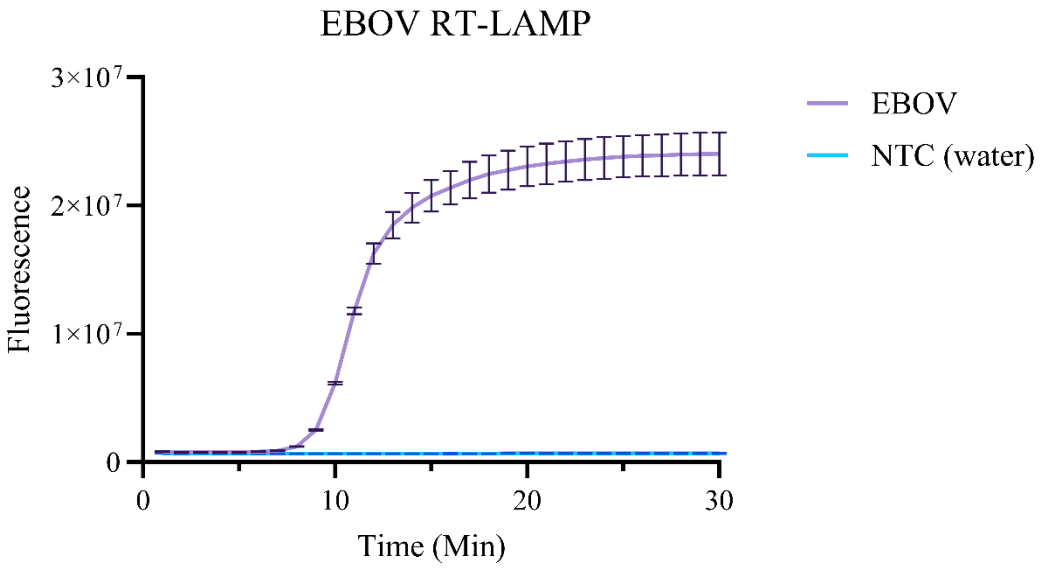

Figure 3.25 EBOV RT-LAMP assay run in triplicate. Reaction run at 65 °C on QuantStudio system.

The colorimetric assay by NEB changes the color of solution from pink to yellow in a positive reaction. This occurs as amplification creates a drop in pH, as each nucleotide addition releases a proton into the solution [144]. Six replicates of EBOV and NTC (water) were run, shown below. The EBOV replicates in the top row turned yellow, indicating amplification, while the NTC replicates in the bottom row remained pink.

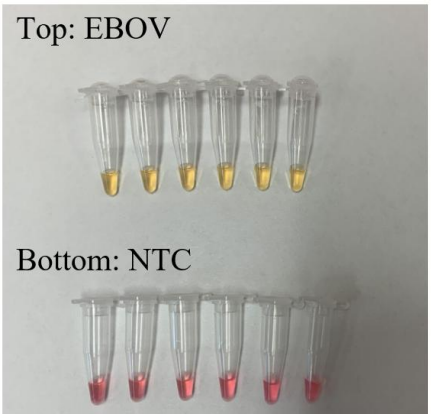

Figure 3.26 EBOV colorimetric RT-LAMP assay. Six each of EBOV (top) and NTC (bottom). Reaction run at 65 °C for 30 min.

Similarly, the successful RT-LAMP detection of EBOV is shown on the agarose gel in the figure below. In lane 2, the "ladder" banding pattern is demonstrated in the template-containing reaction indicating amplification of EBOV, while lanes 3 to 15 demonstrate no amplification of the NTC.

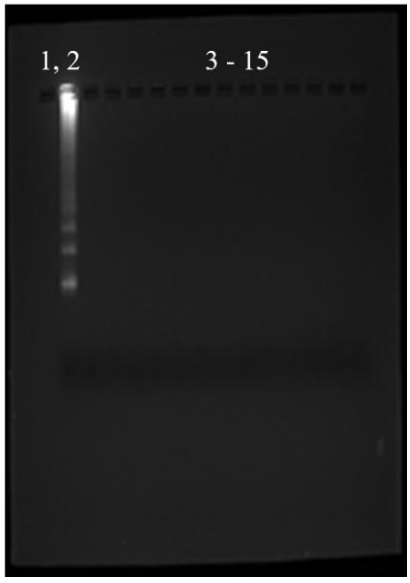

Figure 3.27 EBOV RT-LAMP gel electrophoresis. Lane 1: empty, lane 2: EBOV, lanes 3-15: NTC (water). Reaction run at 65 °C for 30 min.

3.4.4.1.1 NHP Samples

To test the RT-LAMP assay on animal samples, NHP blood samples were obtained from a previous EBOV study in the Special Pathogens laboratory. The three extracted blood RNA samples included 94 h PI, 120 h PI, and 159 h PI, with corresponding CT values of 32.9, 22.5, and 15.6, respectively. In the first run, the assay detected all samples as well as the NTC (figure 3.28). The second time, the assay did not detect the NTC, as well as the CT value of 32.9 at 96 h PI (figure 3.29).

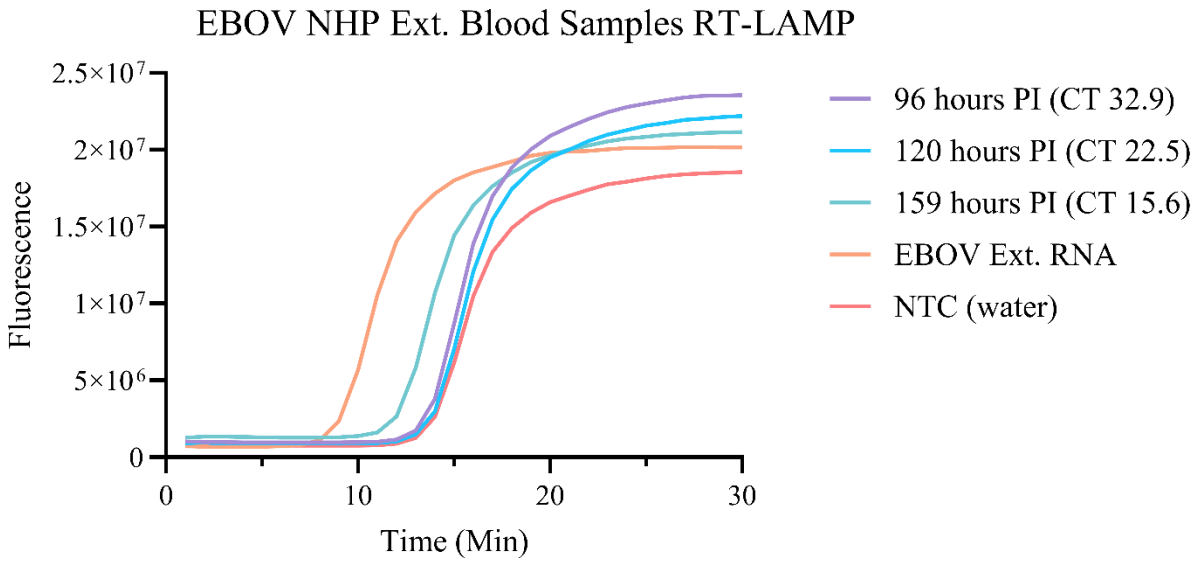

Figure 3.28 RT-LAMP of extracted EBOV blood RNA from NHP samples. Reaction run at 65 °C on QuantStudio system.

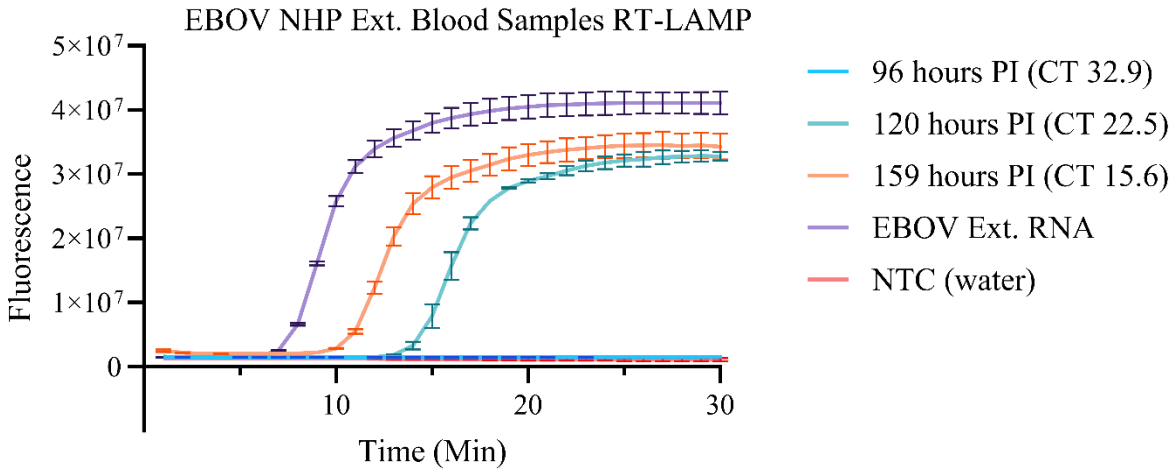

Figure 3.29 RT-LAMP of extracted EBOV blood RNA from NHP samples, run in duplicate. Reaction run at 65 °C on QuantStudio system.

3.4.4.1.2 Melting Curve Analysis

Similar to LASV, a melting curve analysis was run after the EBOV assay started producing intermittent false positive results, as a way to distinguish between RT-LAMP amplicons. The melting curve analysis below shows a melting curve for the EBOV template, but does not indicate non-specific amplification in the NTCs, which were run in triplicate, as well as another control run without LAMP primers. This indicates the possibility of the false positive results originating from the CRISPR part of the reaction instead.

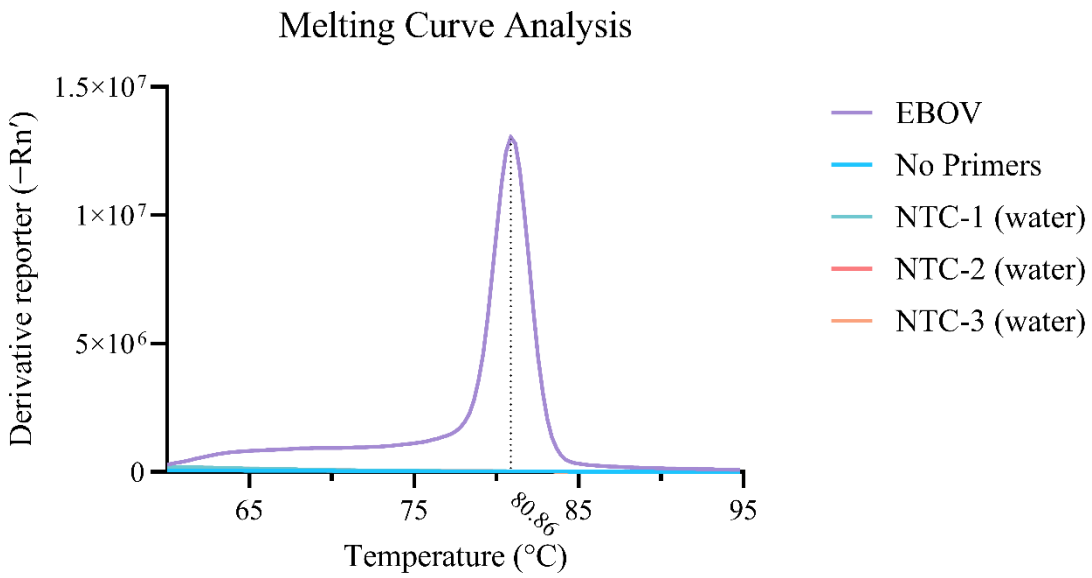

Figure 3.30 Melting curve analysis of EBOV. NTC (water) run in triplicate. Reaction run on QuantStudio system.

3.4.4.2 Two-step Reaction

A two-step reaction was run to determine if the two parts of the reaction, RT-LAMP and CRISPR-Cas12b, can work together to detect the target before combining into a one-pot reaction. In this reaction, RT-LAMP was run first, and the DNA products were then used as template for Cas12b/gRNA detection, as described in section 2.9. This is demonstrated in the figure below, where the gRNA rapidly detects the pre-amplified RT-LAMP product.

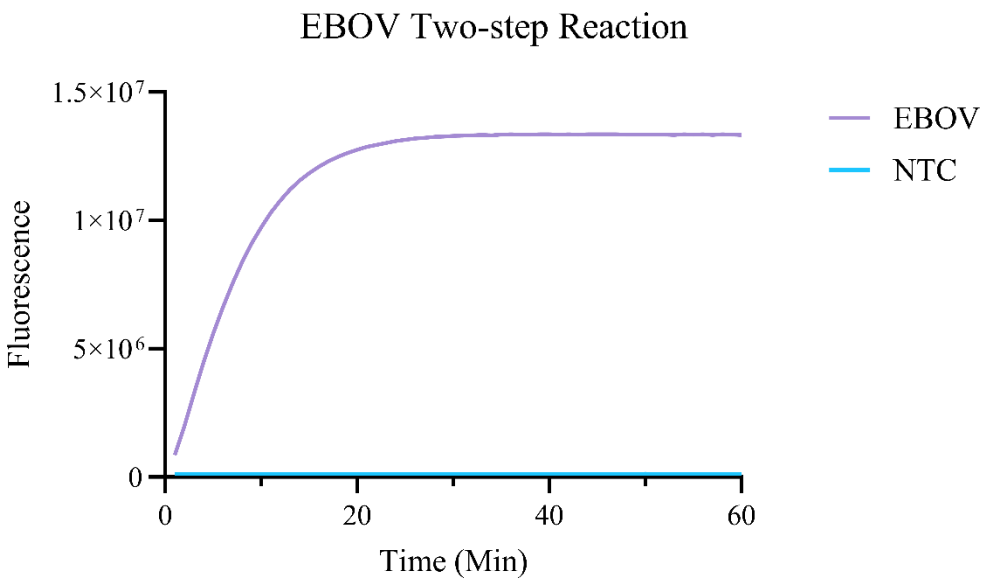

Figure 3.31 RT-LAMP and Cas12b two-step reaction detects EBOV. Reaction run on QuantStudio system.

3.4.4.3 RT-LAMP/Cas12b One-pot

In this section, the EBOV one-pot results are demonstrated across various assessments, such as testing a singular one-pot reaction in figure 3.32, testing the extracted NHP blood RNA samples in figure 3.33, assessing the LOD in figure 3.34, troubleshooting with unrelated SARS-CoV-2 RNA in figure 3.35, and assessing the variability of the one-pot reaction in figure 3.36.

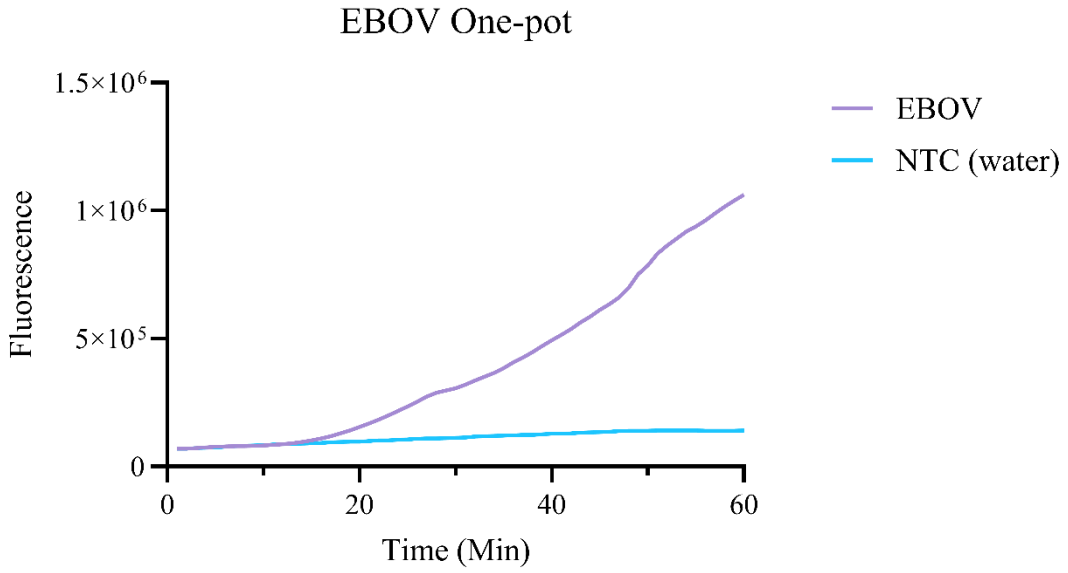

Figure 3.32 EBOV one-pot run in singlicate. Reaction run at 60 °C on QauntStudio system.

3.4.4.3.1 NHP Samples

The EBOV one-pot assay was also tested on the extracted blood RNA from the NHP samples. The findings were similar to the RT-LAMP reaction in figure 3.29, as the one-pot also did not detect the CT of 32.9 at 96 h PI.

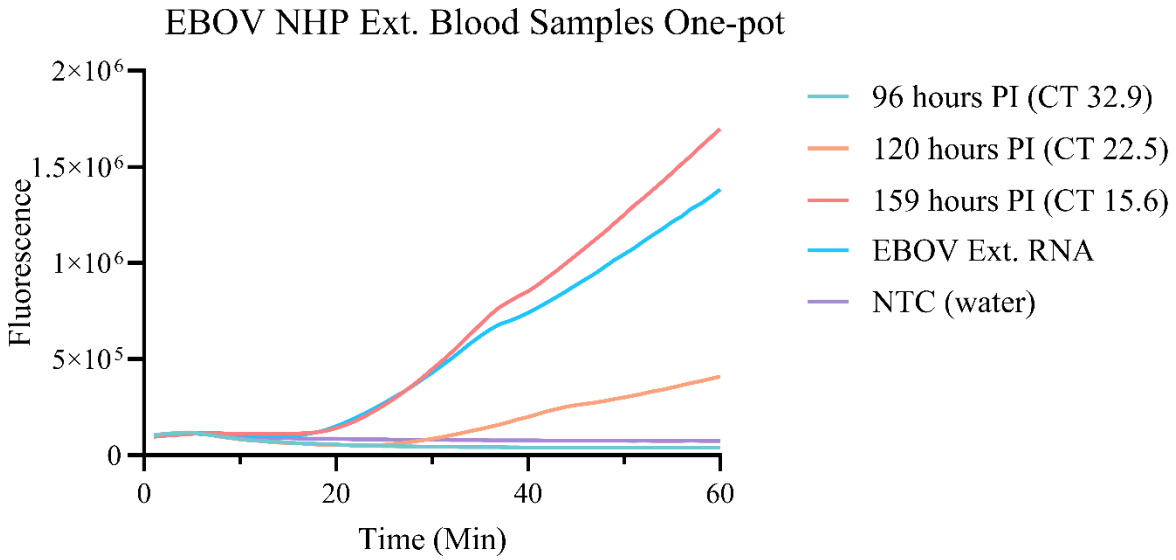

Figure 3.33 One-pot of extracted EBOV blood RNA from NHP samples. Run in triplicate, error bars not shown. Reaction run at 60 °C on QuantStudio system.

3.4.4.3.2 Limit-of-Detection

The LOD of the one-pot reaction was also assessed by serially diluting the RNA and calculating the corresponding GEQ/µL. Unfortunately, the signal from the NTC was quite high and needed to be reduced to accurately measure the LOD.

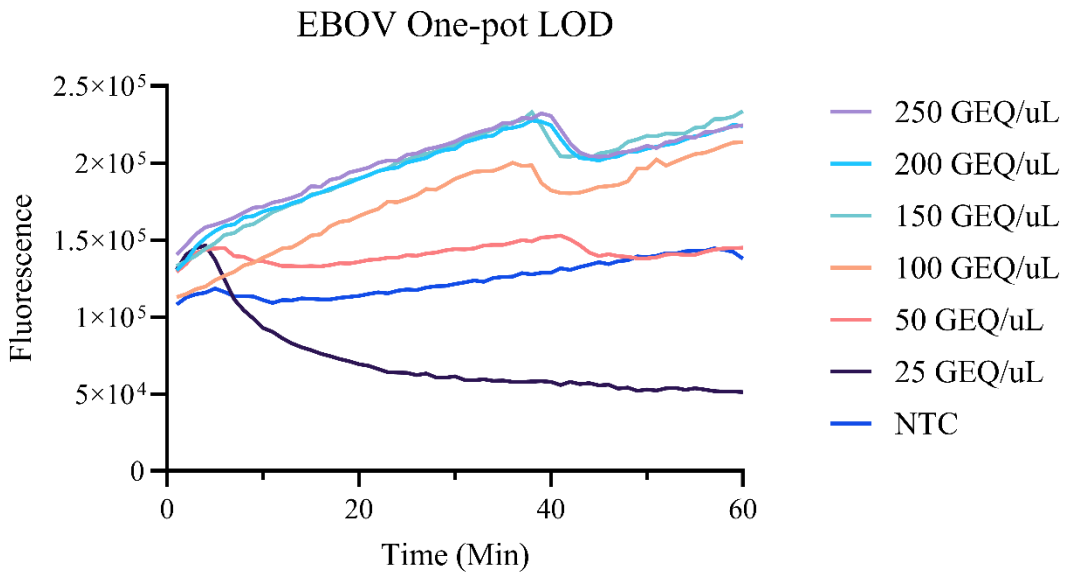

Figure 3.34 One-pot assessing range of EBOV RNA concentrations. Reaction run at 60 °C on QuantStudio system.

3.4.4.3.3 One-pot with SARS-CoV-2

It was hypothesized that running the assay with an unrelated RNA target would help reduce the background noise in the NTC. To test this, a one-pot reaction was run with extracted SARS-CoV-2 RNA in the NTC instead of water. However, this did not reduce the background signal, as shown below in figure 3.35.

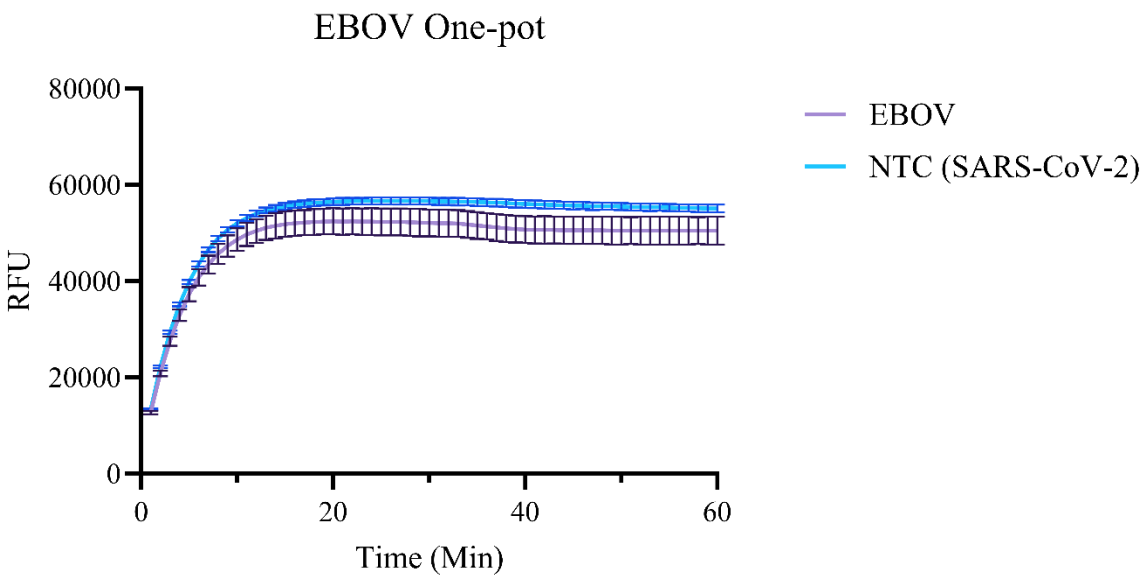

Figure 3.35 EBOV one-pot with SARS-CoV-2 RNA in the NTC. Reaction run on CFX96 system.

3.4.4.3.4 One-pot Variability

Lastly, we wanted to test the one-pot assay with respect to the number of false positive results obtained. To test this, 12 replicates containing the EBOV template and 12 NTCs containing water were run, shown in figure 3.36. Interestingly, the template-containing reactions showed more variability in their signal than the NTCs, as indicated by the large error bars.

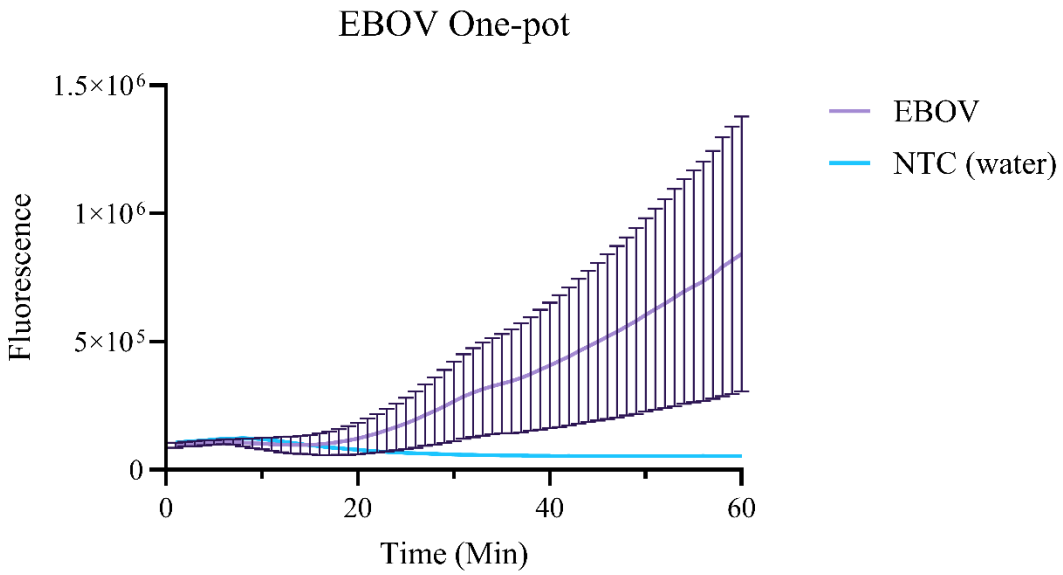

Figure 3.36 EBOV one-pot variability. Reaction run at 60 °C on QuantStudio system.

4.0 Discussion

This study was the first step in developing a CRISPR-based POCT using RT-LAMP and Cas12b. To the best of our knowledge, an RT-LAMP/Cas12b one-pot test has not yet been developed to detect LASV or EBOV. First, this study addressed the hypothesis described in section 1.8 by showing that RT-LAMP/Cas12b can detect LASV and EBOV in a one-pot format, although not as reliably as expected, as several reactions showed false positive results or large variation across replicates. Next, the objectives listed in section 1.9 were partially met. The first objective of this thesis was to optimize the STOPCovid.v2 one-pot method to detect LASV and EBOV using RT-LAMP and Cas12b. This objective was met by designing LAMP primers and gRNA to amplify and detect LASV and EBOV (listed in table 3), which were tested through running several RT-LAMP reactions, two-step and one-pot reactions, and assessing gRNA activity. Furthermore, the STOPCovid.v2 protocol was optimized by running several titrations to select the optimal concentrations of reagents in section 3.4.3.2.1, which resulted in better performance of the one-pot reaction compared to the original protocol as shown in figure 3.23. The second objective of

this project was to optimize the sensitivity of the one-pot assay by measuring the LOD and limiting the number of false positives and negatives, as well as test the assay on animal samples and spiked matrices. The LOD was assessed in figure 3.34, however high background noise and false positive results hindered this assessment. As well, extracted RNA from NHP blood samples from previous LASV and EBOV studies were tested, which showed better results for EBOV than LASV. Lastly, testing the one-pot assay on spiked matrices was not met due to many false positive results. The false positive results created a futile environment for optimizing the assay or meeting objectives, and the root cause needed to be addressed first.

It is important to note that there are many factors included in optimizing the one-pot assay for the POC. The LAMP primers and gRNA must be carefully designed to avoid non-specific amplification or detection, as reflected in figure 3.14 where the gRNA detected the BIP. As well, there are many enzymes, buffers, and temperatures that must be optimized to work together in a one-pot format. This was outlined in section 3.4.3.2.1, where selecting the most optimal concentrations of $MgSO_4$, dNTPs, LAMP primers, *Bst* 2.0 polymerase, RTx reverse transcriptase, and the reporter led to better performance of the assay, shown in figure 3.23. As well, the thermostable Cas12b was chosen for this assay as it functions at the higher temperatures that RT-LAMP runs at [76]. However, intermittent false positive results and low signals were still seen, which are discussed in further detail below.

In this study, the CT value of 32.9 in the NHP samples was not detected in either the EBOV RT-LAMP (figure 3.29) or one-pot reaction (figure 3.33). This finding is similar to another published LASV RT-LAMP assay that was only able to detect CT values less than 32 [113]. However, this finding is in contrast to an EBOV RT-LAMP assay that could detect CT values up to 37.5. Of note, they did report one negative result that corresponded with a CT value of 36.3

[112]. The differences in assay performance described here could be attributed to differences in LAMP primer design and efficiency, as this discrepancy has been seen before between RT-LAMP/CRISPR-based assays and PCR assays [59, 113].

4.1 False Positives

As seen in the LASV and EBOV assays, false positive results were frequent regardless of the actions taken to impede this, including implementing the sterile workflow outlined below in section 4.1.1, using different machines (ESEQuant TS2.4, QuantStudio 3/5 Real-Time PCR Systems, or Bio-Rad CFX96 Real-Time System), testing different RNA extraction methods, assessing the RNA quality, and assessing multiple LAMP primer sets and gRNAs for non-specific activity. Other troubleshooting techniques included the use of DMSO in RT-LAMP reactions, running melting curve analyses, running one-pot reactions without Cas12b or gRNA, assessing primer-gRNA interactions, and finally, confirmation of contamination through sequencing for the LASV assay.

As discussed in the introduction, LAMP is highly sensitive to non-specific amplification and contamination, especially due to the high stability of LAMP amplicons and the risk for carryover contamination [106]. In the assays, it was common to see the NTC fluorescence reach a higher value or fluoresce quicker than the template-containing reaction, suggesting a false positive result rather than high background noise. In other cases, false positive results showed the NTC trending upward, which could be due to non-specific amplification, contamination, or high background noise. To assess the cause of the false positive results in the LASV assay, a melting curve of the RT-LAMP reaction was run which did not address the question as the melting profiles could not be confidently identified to be the same amplicon or not (figure 3.9). Therefore, the samples were sent for Sanger sequencing which confirmed contamination, as the NTC and template-containing

reactions were a 98.3% match (data not shown). For the EBOV assay, the melting curve suggested there was no non-specific amplification occurring (figure 3.30), which is suggestive of an issue occurring in the CRISPR part of the reaction. In this case, sequencing could be done to confirm if there is contamination causing the false positive result or non-specific Cas12b activation.

One theory for the cause of the false positive results is activation of the Cas12b enzyme outside of the typical DNA-based activation. It has been shown for Cas12a, AacCas12b, and AapCas12b that both dsDNA (PAM-dependent) and ssDNA (PAM-independent) can activate the enzyme to *trans*-cleave non-specific ssDNA [76, 77, 86]. This is the basis of the CRISPR-based assay, where dsDNA amplified by RT-LAMP is cis-cleaved, followed by *trans*-cleavage of the ssDNA reporter. Aside from this, other aspects have been explored for their effect on the reaction. It has been shown for Cas12a that low ionic strength buffers and shorter targets for cleavage promote higher enzyme efficiency [145]. As well, AapCas12b maintains optimal activity between 31 °C – 59 °C, across a wide pH range from 1.0 - 8.0, and with many divalent cations, except for Zn^{2+} and Cu^{2+} [75]. However, there is no evidence in the literature to support the theory that these factors could inadvertently activate the Cas enzyme, only that these parameters are important in enzyme function.

On the same note, it was previously observed that Cas12a did not show activity towards RNA, either through enzyme activation or *trans*-cleavage [86]. In contrast, other Cas12 orthologs such as Cas12a2 display *trans*-cleavage of ssRNA, ssDNA, and dsDNA through RNA activation, while Cas12g displays similar activity except without dsDNA-cleavage [146, 147]. With respect to the enzyme used in this thesis, AapCas12b, one study reported a non-specific signal which did not resolve when steps were taken to address what was assumed to be contamination, similar to the findings in this thesis. Interestingly, it was discovered that AapCas12b also displays *trans*-cleavage

of RNA reporters [148]. Therefore, the RNA cleaving activity of Cas12b should be further explored as a potential source of false positives.

As Cas12b can become activated via ssDNA, it was hypothesized there could be activation by a LAMP primer creating template-free positive results. The LAMP primers are rather small, typically < 50 bp, although the gRNA is smaller, typically < 24 bp. A 15 bp complement is sufficient to generate cleavage, as previously demonstrated with Cas12a [86]. To explore this idea, the primers were assessed using the Multiple Primer Analyser, ThermoFisher Scientific to see if there were any primer dimers or primer-gRNA interactions that could affect the results of the one-pot assay. Several theoretical primer-primer and primer-gRNA interactions were found (data not shown). For the LASV assay, the BIP could potentially interact with two gRNAs (9 bp vs 20 bp match). The LASV assay was tested, and it was shown that the BIP could generate fluorescence with one of the gRNAs (20 bp match) (figure 3.14). Although, this was not the gRNA used in the one-pot assays and the primer concentration had to be increased by 6.25X, and therefore this result does not reflect realistically as the source of false positives. Nevertheless, strong theoretical primer-gRNA complementary in the EBOV assay could also be explored as a source of false positive results. As well, primer redesign is recommended in the case of primer-primer interactions, which can lead to non-specific amplification [106].

4.1.1 Sterile Workflow

A sterile workflow was implemented to help prevent contamination from occurring after the LASV assay was confirmed to be contaminated. A dedicated CleanSpot PCR workstation with ultraviolet (UV) light was used to prepare the master mix in a separate location away from template addition, with a separate lab coat. The CleanSpot station also contained a set of dedicated and recently cleaned pipettes with filtered tips for master mix preparation only [106] . When pipetting,

proper technique was practiced to reduce potential aerosol contamination. The CleanSpot station was cleaned with 70% ethanol and UV after use, and 1% bleach before use, as these reagents have demonstrated strong ability to remove DNA from plastic [149]. As well, dedicated pre- and post-LAMP spaces were used for when tubes must be opened after a LAMP reaction, such as when running a gel-electrophoresis [106]. All reagents were aliquoted into smaller volumes to reduce the effects of freeze-thawing and possibility of contamination. Lastly, fresh primers were ordered, and new reagents and/or lot numbers were opened frequently. Even though these steps were implemented, false positive results continued to be sporadic into the EBOV assay.

Ultimately, while this study showed that RT-LAMP and Cas12b can be paired to create a successful one-pot assay, this study also showed these methods are prone to non-specific amplification and contamination, which undermines the reliability and usefulness of the assay as a field deployable POCT.

4.2 False Negatives

False negative results were also seen, although less frequently than false positives, and occurred when template was added and fluorescence did not increase. In other cases, fluorescence was quite low overall, such as in section 3.4.3.2.1, which could have affected the ability to discern positive signals when using the cut-off values outlined in section 2.11, such as 3x the NTC signal. This could be attributed to several factors, one being inefficient LAMP primers or poorly designed gRNA, therefore several primer sets and gRNAs were designed and tested. It is also possible that other reagents such as enzymes, buffers, or salts could have been ineffective, however this is less likely as they were recently ordered, unexpired, and correctly stored. Another possibility could be the poor quality of the template RNA, of which the RIN was found to be low, or the method used to extract the RNA, which could introduce inhibitors of the downstream applications. In this case,

different RNA extraction methods were used as outlined in section 2.4. However, the different methods were not directly compared to assess their effectiveness. As well, the Cas12b enzyme activity and reporters were assessed and found to be working. Therefore, false negative results were mitigated by running RT-LAMP only reactions to ensure the primers were working and running two-step reactions shed light on whether the Cas12b enzyme and gRNA could detect the RT-LAMP amplified target.

4.3 Future Directions and Conclusion

This study was the first step in developing a CRISPR-based one-pot test using RT-LAMP and Cas12b to detect LASV and EBOV and provided many insights into the workings of RT-LAMP, Cas12b, and the optimization required to develop a one-pot POCT. There are many future directions this project could take to further develop the assay as a user-friendly and field deployable POCT including lyophilizing the formula, integrating both the HUDSON method and lateral-flow detection, further assessing the LOD for clinical sensitivity, and comparing the sensitivity of RT-LAMP to the more traditional diagnostic test, PCR. Lyophilization and lateral-flow tests have been explored for RT-LAMP and Cas12b one-pot detection prior to this study and found to be feasible [83, 135]. The use of these technologies could further develop the user-friendliness of this test at the POC, as lyophilized formulas can travel well without a cold chain, and lateral-flow strips provide an easy readout [83, 138]. As well, it would be beneficial to integrate an inactivation and extraction method such as HUDSON for a true POCT [57]. The HUDSON method was not tested as an addition to this project as it requires the use of CL4 to fully assess its suitability for the POC. However, the ability of HUDSON to inactivate nucleases could still be assessed using spiked matrices in CL2. The LOD was narrowed down for EBOV in figure 3.34, but was derailed by false positive results which made further testing of the LOD futile.

Assessing the LOD would shed light on the ability of the test to be feasible in the clinical setting during complex outbreaks of HCPs. Lastly, several studies have found LAMP to be competitive with or in agreement with PCR [11, 106, 108–119]. Therefore, future directions should include testing clinical samples across a range of CT values and comparing the RT-LAMP results to the PCR results to further elucidate the clinical usefulness of LAMP and/or CRISPR-based assays as a POCT.

Other extensions of this project could include comparing the effects of different inactivation and extraction methods on the one-pot test, as different extraction methods were employed in this thesis but not directly compared to each other. As well, the second objective could be completed by testing different spiked matrices such as urine, blood, or saliva and comparing the results to published findings, which found saliva to be a sensitive and non-invasive method to detect LASV and EBOV [59].

This study also had limitations. First, this study was limited by the lack of clinical samples. Assessing both positive and negative clinical samples through PCR and comparing the results with RT-LAMP and the CRISPR one-pot test would enhance the study by determining the realistic feasibility of the assay to perform up to standard at the POC. Second, this study was limited by the lack of proper positive (or internal) and negative controls which could further demonstrate the feasibility of the test. For example, the EBOV-tobacco mosaic virus probe, which can function alone as a positive control or be added to samples as an internal control, as well as plasmids, MS2 phage, and ribonuclease P have been developed as positive and/or internal controls for RT-LAMP and CRISPR-based tests [96, 116, 117, 148]. While water can be used as a template-free negative control, the cells from the cell line used to prepare the RNA samples could also be used a negative control [96, 148].

4.4 Conclusion

This study demonstrated that the STOPCovid.v2 method using RT-LAMP and Cas12b can be adapted to detect LASV and EBOV, helping to expand the CRISPR-based toolbox of POCTs against future outbreaks of HCPs. As well, this study shed light on the realistic feasibility of this method as a future POCT. It was determined that technical limitations of the RT-LAMP and/or CRISPR-based detection method such as non-specific amplification/activation and risk of contamination merit special considerations such as a sterile workflow including dedicated spaces, as well as primer and gRNA analysis for potential interactions. Further work into the ideas listed here as future directions or limitations of this study such as implementing lyophilization, lateral-flow strips, and the HUDSON technique, assessing clinical samples, and adjusting the controls of this project will continue to refine this method as a reliable POCT able to meet the REASSURED characteristics.

5.0 References

1. Racsa, L.D.; Kraft, C.S.; Olinger, G.G.; Hensley, L.E. Viral Hemorrhagic Fever Diagnostics. *Clin. Infect. Dis*. **2016**, *62*, 214–219. https://doi.org/10.1093/cid/civ792
2. Drosten, C.; Kümmerer, B.M.; Schmitz, H.; Günther, S. Molecular Diagnostics of Viral Hemorrhagic Fevers. *Antivir. Res*. **2003**, *57*, 61–87. https://doi.org/10.1016/S0166-3542(02)00201-2
3. Qureshi, A.I. Clinical Manifestations and Laboratory Diagnosis of Ebola Virus Infection. In: *Ebola Virus Disease*; Elsevier: Amsterdam, The Netherlands, **2016**; pp. 117–138. https://doi.org/10.1016/b978-0-12-804230-4.00009-1
4. McQuiston, J.H.; Montgomery, J.M.; Hutson, C.L. Ten Years of High-Consequence Pathogens—Research Gains, Readiness Gaps, and Future Goals. *Emerg. Infect. Dis*. **2024**, *30,* 800-802. https://doi.org/10.3201/eid3004.240160
5. Belay, E.D.; Monroe, S.S. Low-Incidence, High-Consequence Pathogens. *Emerg. Infect. Dis*. **2014**, *20*, 319–321. https://doi.org/10.3201/eid2002.131748

6. Chan, J.; Levine, C.B.; Herstein, J.J.; Cloutier, N.; Sauer, L.; Mehta, A.K.; Evans, J. Preparedness and Response Considerations for High-Consequence Infectious Disease. *Emerg. Infect. Dis*. **2025**, *31*, 1507–1155. https://doi.org/10.3201/eid3108.250313
7. Centers for Disease Control and Prevention. Ebola Outbreak History. Available online: https://www.cdc.gov/ebola/outbreaks/ (Accessed on 12 March 2026).
8. World Health Organization. Dengue and Severe Dengue. Available online: https://www.who.int/news-room/fact-sheets/detail/dengue-and-severe-dengue (Accessed on 12 March 2026).
9. Marty, A.M.; Jahrling, P.B.; Geisbert, T.W. Viral Hemorrhagic Fevers. *Clin. Lab. Med*. **2006**, *26*, 345–386. https://doi.org/10.1016/j.cll.2006.05.001
10. Simons, D. Lassa Fever Cases Suffer from Severe Underreporting Based On Reported Fatalities. *Int. Health* **2023**, *15*, 608–610. https://doi.org/10.1093/inthealth/ihac076
11. Fukuma, A.; Kurosaki, Y.; Morikawa, Y.; Grolla, A.; Feldmann, H.; Yasuda, J. Rapid Detection of Lassa Virus by Reverse Transcription-Loop-Mediated Isothermal Amplification. *Microbiol. Immunol*. **2011**, *55*, 44–50. https://doi.org/10.1111/j.1348-0421.2010.00286.x
12. Li, H.; Bello, A.; Smith, G.; Kielich, D.M.S.; Strong, J.E.; Pickering, B.S. Degenerate Sequence-Based CRISPR Diagnostic for Crimean–Congo Hemorrhagic Fever Virus. *PLoS Negl. Trop. Dis*. **2022**, *16*, e0010285. https://doi.org/10.1371/journal.pntd.0010285
13. Haider, N.; Hasan, M.N.; Onyango, J.; Billah, M.; Khan, S.; Papakonstantinou, D.; Paudyal, P.; Asaduzzaman, M. Global dengue epidemic worsens with record 14 million cases and 9000 deaths reported in 2024. *Int. J. Infect. Dis*. **2025**, *158*, 107940. https://doi.org/10.1016/j.ijid.2025.107940
14. World Health Organization. Lassa fever. Available online: https://www.who.int/news-room/fact-sheets/detail/lassa-fever (Accessed on 12 March 2026).
15. World Health Organization. Ebola disease. Available online: https://www.who.int/news-room/fact-sheets/detail/ebola-virus-disease (Accessed on 12 March 2026).
16. World Health Organization. Crimean-Congo haemorrhagic fever. Available online: https://www.who.int/news-room/fact-sheets/detail/crimean-congo-haemorrhagic-fever (Accessed on 12 March 2026).

17. Goldstein, T.; Anthony, S.J.; Gbakima, A.; Bird, B.H.; Bangura, J.; Tremeau-Bravard, A.; Belaganahalli, M.N.; Wells, H.L.; Dhanota, J.K.; Liang, E.; et al. The discovery of Bombali virus adds further support for bats as hosts of ebolaviruses. *Nat. Microbiol*. **2018**, *3*, 1084–1089. https://doi.org/10.1038/s41564-018-0227-2

18. de La Vega, M.A.; Stein, D.; Kobinger, G.P. Ebolavirus Evolution: Past and Present. *PLoS Pathog*. **2015**, *11*, e1005221. https://doi.org/10.1371/journal.ppat.1005221

19. Cantoni, D.; Hamlet, A.; Michaelis, M.; Wass, M.N.; Rossman, J.S. Risks Posed by Reston, the Forgotten Ebolavirus. *mSphere*. **2016**, *1*, e00322-16. https://doi.org/10.1128/msphere.00322-16

20. Le Guenno, B.; Formenty, P.; Wyers, M.; Gounon, P.; Walker, F.; Boesch, C. Isolation and partial characterisation of a new strain of Ebola virus. *Lancet* **1995**, *345*, 1271–1274. https://doi.org/10.1016/S0140-6736(95)90925-7

21. Towner, J.S.; Sealy, T.K.; Khristova, M.L.; Albariño, C.G.; Conlan, S.; Reeder, S.A.; Quan, P.L.; Lipkin, W.I., Downing, R.; Tappero, J.W.; et al. Newly Discovered Ebola Virus Associated with Hemorrhagic Fever Outbreak in Uganda. *PLoS Pathog*. **2008**, *4*, e1000212. https://doi.org/10.1371/journal.ppat.1000212

22. Yamaoka, S.; Ebihara, H. Pathogenicity and Virulence of Ebolaviruses with Species- and Variant-specificity. *Virulence* **2021**, *12*, 885–901. https://doi.org/10.1080/21505594.2021.1898169

23. Sundaram, M.; Gottdenker, N.L.; Stephens, P.R. Where is the elusive primary *ebolavirus* reservoir and how do we find It? *BioScience* **2025**, *0*, 1-9. https://doi.org/10.1093/biosci/biaf050

24. Leroy, E.M.; Kumulungui, B.; Pourrut, X.; Rouquet, P.; Hassanin, A.; Yaba, P.; Délicat, A.; Paweska, J.T.; Gonzalez, J.P; Swanepoel, R. Fruit bats as reservoirs of Ebola virus. *Nature* **2005**, *438*, 575–576. https://doi.org/10.1038/438575a

25. Oloniniyi, O.K.; Unigwe, U.S.; Okada, S.; Kimura, M.; Koyano, S.; Miyazaki, Y.; Iroezindu, M.O.; Ajayi, N.A.; Chukwubike, C.M.; Chika-Igwenyi, N.M.; et al. Genetic characterization of Lassa virus strains isolated from 2012 to 2016 in southeastern Nigeria. *PLoS Negl. Trop. Dis*. **2018**, *12*, e0006971. https://doi.org/10.1371/journal.pntd.0006971

26. Garry, R.F. Lassa fever — the road ahead. *Nat. Rev. Microbiol*. **2023**, *21*, 87–96. https://doi.org/10.1038/s41579-022-00789-8

27. Bowen, M.D.; Rollin, P.E.; Ksiazek, T.G.; Hustad, H.L.; Bausch, D.G.; Demby, A.H.; Bajani, M.D.; Peters, C.J.; Nichol, S.T. Genetic Diversity among Lassa Virus Strains. *J. Virol*. **2000**, *74,* 6992–7004. https://doi.org/10.1128/JVI.74.15.6992-7004.2000
28. Ibukun, F.I. Inter-lineage Variation of Lassa Virus Glycoprotein Epitopes: A Challenge to Lassa Virus Vaccine Development. *Viruses* **2020**, *12*, 386. https://doi.org/10.3390/v12040386
29. Wiley, M.R.; Fakoli, L.; Letizia, A.G.; Welch, S.R.; Ladner, J.T.; Prieto, K.; Reyes, D.; Epsy, N.; Chitty, J.A.; Pratt,C.B.; et al. Lassa virus circulating in Liberia: a retrospective genomic characterisation. *Lancet Infect. Dis*. **2019**, *19*, 1371–1378. https://doi.org/10.1016/S1473-3099(19)30486-4
30. Olayemi, A.; Cadar, D.; Magassouba, N.; Obadare, A.; Kourouma, F.; Oyeyiola, A.; Fasogbon, S.; Igbokwe, J.; Rieger, T. Bockholt, S.; et al. New Hosts of The Lassa Virus. *Sci. Rep*. **2016**, *6*, 25280. https://doi.org/10.1038/srep25280
31. Whitmer, S.L.M.; Strecker, T.; Cadar, D.; Dienes, H.P.; Faber, K.; Patel, K.; Brown, S.M.; Davis, W.G.; Klena, J.D.; Rollin, P.E.; et al. New lineage of Lassa virus, Togo, 2016. *Emerg. Infect. Dis*. **2018**, *24*, 599–602. https://doi.org/10.3201/eid2403.171905
32. Manning, J.T.; Forrester, N.; Paessler, S. Lassa virus isolates from Mali and the Ivory Coast represent an emerging fifth lineage. *Front. Microbiol*. **2015**, *6*, 1037. https://doi.org/10.3389/fmicb.2015.01037
33. Monath, T.P.; Newhouse, V.F.; Kemp, G.E.; Setzer, H.W.; Cacciapuoti, A. Lassa Virus Isolation from Mastomys natalensis Rodents during an Epidemic in Sierra Leone. *Science* **1974**, *185*, 263–265. https://doi.org/10.1126/science.185.4147.263
34. Andersen, K.G.; Shapiro, B.J.; Matranga, C.B.; Sealfon, R.; Lin, A.E.; Moses, L.M.; Folarin, O.A.; Goba, A.; Odia, I.; Ehiane, P.; et al. Clinical Sequencing Uncovers Origins and Evolution of Lassa Virus. *Cell* **2015**, *162*, 738–750. https://doi.org/10.1016/j.cell.2015.07.020
35. Rugarabamu, S.; Rumisha, S.F.; Mwanyika, G.O.; Sindato, C.; Lim, H.Y.; Misinzo, G.; Mboera, L.E.G. Viral Haemorrhagic Fevers and Malaria Co-infections among Febrile Patients Seeking Health Care in Tanzania. *Infect. Dis. Poverty* **2022**, *11*, 33. https://doi.org/10.1186/s40249-022-00959-z

36. McCormick, J.B.; King, I.J.; Webb, P.A.; Johnson, K.M.; O'Sullivan, R.; Smith, E.S.; Trippel, S.; Tong, T.C. A Case-Control Study of the Clinical Diagnosis and Course of Lassa Fever. *J. Infect. Dis*. **1987**, *155*, 445–455. https://doi.org/10.1093/infdis/155.3.445

37. McCormick, J.B.; King, I.J.; Webb, P.A.; Scribner, C.L.; Craven, R.B.; Johnson, K.M.; Elliott, L.H.; Belmont-Williams, R. Lassa Fever. *N. Engl. J. Med*. **1986**, *314*, 20–26. https://doi.org/10.1056/NEJM198601023140104

38. Bausch, D.G.; Rollin, P.E.; Demby, A.H.; Coulibaly, M.; Kanu, J.; Conteh, A.S.; Wagoner, K.D.; Mcmullan, L.K.; Bowen, M.D.; Peters, C.J.; et al. Diagnosis and Clinical Virology of Lassa Fever as Evaluated by Enzyme-Linked Immunosorbent Assay, Indirect Fluorescent-Antibody Test, and Virus Isolation. *J. Clin. Microbiol.* **2000**, *38*, 2670–2677. https://doi.org/10.1128/JCM.38.7.2670-2677.2000

39. Land, K.J.; Boeras, D.I.; Chen, X.S.; Ramsay, A.R.; Peeling, R.W. REASSURED Diagnostics to Inform Disease Control Strategies, Strengthen Health Systems and Improve Patient Outcomes. *Nat. Microbiol.* **2019**, *4*, 46–54. https://doi.org/10.1038/s41564-018-0295-3

40. García-Bernalt Diego, J.; Fernández-Soto, P.; Muro, A. Lamp in Neglected Tropical Diseases: A Focus on Parasites. *Diagnostics* **2021**, *11*, 521. https://doi.org/10.3390/diagnostics11030521

41. Tricou, V.; Vu, H.T.T.; Quynh, N.V.N.; Nguyen, C.V.V.; Tran, H.T.; Farrar, J.; Wills, B.; Simmons, C.P. Comparison of two dengue NS1 rapid tests for sensitivity, specificity and relationship to viraemia and antibody responses. *BMC Infect. Dis*. **2010**, *10*, 142. https://doi.org/10.1186/1471-2334-10-142

42. Brangel, P.; Sobarzo, A.; Parolo, C.; Miller, B.S.; Howes, P.D.; Gelkop, S.; Lutwama, J.J.; Dye, J.M.; McKendry, R.A.; Lobel, L.; et al. A Serological Point-of-Care Test for the Detection of IgG Antibodies against Ebola Virus in Human Survivors. *ACS Nano* **2018**, *12*, 63–73. https://doi.org/10.1021/acsnano.7b07021

43. Wulff, H.; Johnson, K.M. Immunoglobulin M and G responses measured by immunofluorescence in patients with Lassa or Marburg virus infections. *Bull. World Health Organ*. **1979**, *57*, 631–635.

44. Ksiazek, T.G.; Rollin, P.E.; Williams, A.J.; Bressler, D.S.; Martin, M.L.; Swanepoel, R.; Burt, F.J.; Leman, P.A.; Khan, A.S.; Rowe, A.K.; et al. Clinical Virology of Ebola

Hemorrhagic Fever (EHF): Virus, Virus Antigen, and IgG and IgM Antibody Findings among EHF Patients in Kikwit, Democratic Republic of the Congo, 1995. *J. Infect. Dis.* **1999**, *179*, S177–S187. https://doi.org/10.1086/514321

45. Liu, G.; Rusling, J.F. COVID-19 Antibody Tests and Their Limitations. *ACS Sens*. **2021**, *6*, 593–612. https://doi.org/10.1021/acssensors.0c02621
46. Robosa, R.S.; Sandaradura, I.; Dwyer, D.E.; O'Sullivan, M.V.N. Clinical evaluation of SARS-CoV-2 point-of-care antibody tests. *Pathology* **2020**, *52*, 783–789. https://doi.org/10.1016/j.pathol.2020.09.002
47. Atçeken, N.; Yigci, D.; Ozdalgic, B.; Tasoglu, S. CRISPR-Cas-Integrated LAMP. *Biosensors* **2022**, *12*, 1035. https://doi.org/10.3390/bios12111035
48. Ghouneimy, A.; Mahas, A.; Marsic, T.; Aman, R.; Mahfouz, M. CRISPR-Based Diagnostics: Challenges and Potential Solutions toward Point-of-Care Applications. *ACS Synth. Biol*. **2023**, *12*, 1–16. https://doi.org/10.1021/acssynbio.2c00496
49. Oliveira, B.B.; Veigas, B.; Baptista, P.V. Isothermal Amplification of Nucleic Acids: The Race for the Next "Gold Standard." *Front. Sens*. **2021**, *2*, 752600. https://doi.org/10.3389/fsens.2021.752600
50. Kubista, M.; Andrade, J.M.; Bengtsson, M.; Forootan, A.; Jonák, J.; Lind, K.; Sindelka, R.; Sjöback, R.; Sjögreen, B.; Strömbom, L.; et al. The real-time polymerase chain reaction. *Mol. Asp. Med.* **2006**, *27*, 95–125. https://doi.org/10.1016/j.mam.2005.12.007
51. Ulinici, M.; Covantev, S.; Wingfield-Digby, J.; Beloukas, A.; Mathioudakis, A.G.; Corlateanu, A. Screening, Diagnostic and Prognostic Tests for COVID-19: A Comprehensive Review. *Life* **2021**, *11*, 561. https://doi.org/10.3390/life11060561
52. Javalkote, V.S.; Kancharla, N.; Bhadra, B.; Shukla, M.; Soni, B.; Sapre, A.; Goodin, M.; Bandyopadhyay, A.; Dasgupta, S. CRISPR-based assays for rapid detection of SARS-CoV-2. *Methods* **2022**, *203*, 594–603. https://doi.org/10.1016/j.ymeth.2020.10.003
53. Broadhurst, M.J.; Kelly, J.D.; Miller, A.; Semper, A.; Bailey, D.; Groppelli, E.; Simpson, A.; Brooks, T.; Hula, S.; Nyoni, W.; et al. ReEBOV Antigen Rapid Test kit for point-of-care and laboratory-based testing for Ebola virus disease: a field validation study. *Lancet* **2015**, *386*, 867–874. https://doi.org/10.1016/S0140-6736(15)61042-X

54. Kaushik, A.; Tiwari, S.; Dev Jayant, R.; Marty, A.; Nair, M. Towards detection and diagnosis of Ebola virus disease at point-of-care. *Biosens. Bioelectron*. **2016**, *75*, 254–272. https://doi.org/10.1016/j.bios.2015.08.040

55. Yang, S.; Rothman, R.E. PCR-based diagnostics for infectious diseases: Uses, limitations, and future applications in acute-care settings. *Lancet Infect. Dis*. **2004**, *4*, 337–348. https://doi.org/10.1016/S1473-3099(04)01044-8

56. Boisen, M.L.; Uyigue, E.; Aiyepada, J.; Siddle, K.J.; Oestereich, L.; Nelson, D.K.S.; Bush, D.J.; Rowland, M.M.; Heinrich, M.L.; Eromon, P.; et al. Field evaluation of a Pan-Lassa rapid diagnostic test during the 2018 Nigerian Lassa fever outbreak. *Sci. Rep*. **2020**, *10*, 8724. https://doi.org/10.1038/s41598-020-65736-0

57. Myhrvold, C.; Freije, C.A.; Gootenberg, J.S.; Abudayyeh, O.O.; Metsky, H.C.; Durbin, A.F.; Kellner, M.J.; Tan, A.L.; Paul, L.M.; Parham, L.A.; et al. Field-deployable viral diagnostics using CRISPR-Cas13. *Science* **2018**, *360*, 444–448. https://doi.org/10.1126/science.aas8836

58. Pilarowski, G.; Lebel, P.; Sunshine, S.; Liu, J.; Crawford, E.; Marquez, C.; Rubio, L.; Chamie, G.; Martinez, J.; Peng, J.; et al. Performance Characteristics of a Rapid Severe Acute Respiratory Syndrome Coronavirus 2 Antigen Detection Assay at a Public Plaza Testing Site in San Francisco. *J. Infect. Dis*. **2021**, *223*, 1139–1144. https://doi.org/10.1093/infdis/jiaa802

59. Barnes, K.G.; Lachenauer, A.E.; Nitido, A.; Siddiqui, S.; Gross, R.; Beitzel, B.; Siddle, K.J.; Freije, C.A.; Dighero-Kemp, B.; Mehta, S.B.; et al. Deployable CRISPR-Cas13a diagnostic tools to detect and report Ebola and Lassa virus cases in real-time. *Nat. Commun*. **2020**, *11*, 4131. https://doi.org/10.1038/s41467-020-17994-9

60. Ishino, Y.; Shinagawa, H.; Makino, K.; Amemura, M.; Nakata, A. Nucleotide Sequence of the *Iap* Gene, Responsible for Alkaline Phosphatase Isozyme Conversion in *Escherichia Coli*, and Identification of the Gene Product. *J. Bacteriol*. **1987**, *169*, 5429–5433. https://doi.org/10.1128/jb.169.12.5429-5433.1987

61. Tao, S.; Chen, H.; Li, N.; Liang, W. The Application of the CRISPR-Cas System in Antibiotic Resistance. *Infect. Drug Resist*. **2022**, *15*, 4155–4168. https://doi.org/10.2147/idr.s370869

62. Xu, Y.; Li, Z. CRISPR-Cas systems: Overview, innovations and applications in human disease research and gene therapy. *Comput. Struct. Biotechnol. J.* **2020**, *18*, 2401–2415. https://doi.org/10.1016/j.csbj.2020.08.031

63. Ricroch, A.; Clairand, P.; Harwood, W. Use of CRISPR systems in plant genome editing: toward new opportunities in agriculture. *Emerg. Top. Life Sci.* **2017**, *1*, 169–182. https://doi.org/10.1042/ETLS20170085

64. Frangoul, H.; Locatelli, F.; Sharma, A.; Bhatia, M.; Mapara, M.; Molinari, L.; Wall, D.; Liem, R.I.; Telfer, P.; Shah, A.J.; et al. Exagamglogene Autotemcel for Severe Sickle Cell Disease. *N. Engl. J. Med.* **2024**, *390*, 1649–1662. https://doi.org/10.1056/nejmoa2309676

65. Brogan, D.J.; Akbari, O.S. CRISPR Diagnostics: Advances toward the Point of Care. *Biochemistry* **2022**, *62*, 3488-3492. https://doi.org/10.1021/acs.biochem.2c00051

66. Deltcheva, E.; Chylinski, K.; Sharma, C.M.; Gonzales, K.; Chao, Y.; Pirzada, Z.A.; Eckert, M.R.; Vogel, J.; Charpentier, E. CRISPR RNA maturation by *trans*-encoded small RNA and host factor RNase III. *Nature* **2011**, *471*, 602–607. https://doi.org/10.1038/nature09886

67. Li, X.; Zhong, J.; Li, H.; Qiao, Y.; Mao, X.; Fan, H.; Zhong, Y.; Imani, S.; Zheng, S.; Li, J. Advances in the application of CRISPR-Cas technology in rapid detection of pathogen nucleic acid. *Front. Mol. Biosci*. **2023**, *10*, 1260883. https://doi.org/10.3389/fmolb.2023.1260883

68. Yoshimi, K.; Mashimo, T. Genome editing technology and applications with the type I CRISPR system. *Gene Genome Ed*. **2022**, *3–4*, 100013. https://doi.org/10.1016/j.ggedit.2022.100013

69. Irkham, I.; Ibrahim, A.U.; Pwavodi, P.C.; Nwekwo, C.W.; Hartati, Y.W. CRISPR-based biosensor for the detection of Marburg and Ebola virus. *Sens. Biosensing Res*. **2024**, *43*, 100601. https://doi.org/10.1016/j.sbsr.2023.100601

70. Karlikow, M.; Amalfitano, E.; Yang, X.; Doucet, J.; Chapman, A.; Mousavi, P.S.; Homme, P.; Sutyrina, P.; Chan, W.; Lemak, S.; et al. CRISPR-induced DNA reorganization for multiplexed nucleic acid detection. *Nat. Commun*. **2023**, *14*, 1505. https://doi.org/10.1038/s41467-023-36874-6

71. Okafor, I.C.; Choi, J.; Ha, T. Single molecule methods for studying CRISPR Cas9-induced DNA unwinding. *Methods* **2022**, *204*, 319–326. https://doi.org/10.1016/j.ymeth.2021.11.003

72. Makarova, K.S.; Wolf, Y.I.; Alkhnbashi, O.S.; Costa, F.; Shah, S.A.; Saunders, S.J.; Barrangou, R.; Brouns, S.J.J.; Charpentier, E.; Haft, D.H.; et al. An updated evolutionary classification of CRISPR–Cas systems. *Nat. Rev. Microbiol*. **2015**, *13*, 722–736. https://doi.org/10.1038/nrmicro3569

73. Bhardwaj, P.; Kant, R.; Behera, S.P.; Dwivedi, G.R.; Singh, R. Next-Generation Diagnostic with CRISPR/Cas: Beyond Nucleic Acid Detection. *Int. J. Mol. Sci*. **2022**, *23*, 6052. https://doi.org/10.3390/ijms23116052

74. Shmakov, S.; Abudayyeh, O.O.; Makarova, K.S.; Wolf, Y.I.; Gootenberg, J.S.; Semenova, E.; Minakhin, L.; Joung, J.; Konermann, S.; Severinov, K.; et al. Discovery and Functional Characterization of Diverse Class 2 CRISPR-Cas Systems. *Mol. Cell*. **2015**, *60*, 385–397. https://doi.org/10.1016/j.molcel.2015.10.008

75. Teng, F.; Cui, T.; Feng, G.; Guo, L.; Xu, K.; Gao, Q.; Li, T.; Jing, L.; Zhou, Q.; Wei, L. Repurposing CRISPR-Cas12b for mammalian genome engineering. *Cell Discov*. **2018**, *4*, 63. https://doi.org/10.1038/s41421-018-0069-3

76. Li, L.; Li, S.; Wu, N.; Wu, J.; Wang, G.; Zhao, G.; Wang, J. HOLMESv2: A CRISPR-Cas12b-Assisted Platform for Nucleic Acid Detection and DNA Methylation Quantitation. *ACS Synth. Biol*. **2019**, *8*, 2228–2237. https://doi.org/10.1021/acssynbio.9b00209

77. Teng, F.; Guo, L.; Cui, T.; Wang, X.G.; Xu, K.; Gao, Q.; Zhou, Q.; Li, W. CDetection: CRISPR-Cas12b-based DNA detection with sub-attomolar sensitivity and single-base specificity. *Genome Biol*. **2019**, *20*, 132. https://doi.org/10.1186/s13059-019-1742-z

78. Piepenburg, O.; Williams, C.H.; Stemple, D.L.; Armes, N.A. DNA Detection Using Recombination Proteins. *PLoS Biol*. **2006**, *4*, 1115–1121. https://doi.org/10.1371/journal.pbio.0040204

79. Hang, X.M.; Wang, H.Y.; Liu, P.F.; Zhao, K.R.; Wang, L. Cas12a-assisted RTF-EXPAR for accurate, rapid and simple detection of SARS-CoV-2 RNA. *Biosens. Bioelectron*. **2022**, *216*, 114683. https://doi.org/10.1016/j.bios.2022.114683

80. Cao, Y.; Lu, X.; Lin, H.; Serrano, A.F.R.; Lui, G.C.Y.; Hsing, I.M. CoLAMP: CRISPR-based one-pot loop-mediated isothermal amplification enables at-home diagnosis of

SARS-CoV-2 RNA with nearly eliminated contamination utilizing amplicons depletion strategy. *Biosens. Bioelectron*. **2023**, *236*, 115402. https://doi.org/10.1016/j.bios.2023.115402

81. Pang, B.; Xu, J.; Liu, Y.; Peng, H.; Feng, W.; Cao, Y.; Wu, J.; Xiao, H.; Pabbaraju, K.; Tipples, G.; et al. Isothermal Amplification and Ambient Visualization in a Single Tube for the Detection of SARS-CoV-2 Using Loop-Mediated Amplification and CRISPR Technology. *Anal. Chem*. **2020**, *92*, 16204–16212. https://doi.org/10.1021/acs.analchem.0c04047
82. Wang, R.; Mao, X.; Xu, J.; Yao, P.; Jiang, J.; Li, Q.; Wang, F. Engineering of the LAMP-CRISPR/Cas12b platform for *Chlamydia psittaci* detection. *J. Med. Microbiol*. **2023**, *72*, 001781. https://doi.org/10.1099/jmm.0.001781
83. Nguyen, L.T.; Macaluso, N.C.; Pizzano, B.L.M.; Cash, M.N.; Spacek, J.; Karasek, J.; Miller, M.R.; Lednicky, J.A.; Dinglasan, R.R.; Salemi, M.; et al. A thermostable Cas12b from *Brevibacillus* leverages one-pot discrimination of SARS-CoV-2 variants of concern. *EBioMedicine* **2022**, *77*, 103926. https://doi.org/10.1016/j.ebiom.2022.103926
84. Wang, Y.; Li, J.; Li, S.; Zhu, X.; Wang, X.; Huang, J.; Yang, X.; Tai, J. LAMP-CRISPR-Cas12-based diagnostic platform for detection of *Mycobacterium tuberculosis* complex using real-time fluorescence or lateral flow test. *Microchim. Acta* **2021**, *188*, 347. https://doi.org/10.1007/s00604-021-04985-w
85. Sam, I.K.; Chen, Y.Y.; Ma, J.; Li, S.Y.; Ying, R.Y.; Li, L.X.; Ji, P.; Wang, S.J.; Xu, J.; Bao, Y.J.; et al. TB-QUICK: CRISPR-Cas12b-assisted rapid and sensitive detection of *Mycobacterium tuberculosis*. *J. Infect*. **2021**, *83*, 54–60. https://doi.org/10.1016/j.jinf.2021.04.032
86. Chen, J.S.; Ma, E.; Harrington, L.B.; Da Costa, M.; Tian, X.; Palefsky, J.M.; Doudna, J.A. CRISPR-Cas12a target binding unleashes indiscriminate single-stranded DNase activity. *Science* **2018**, *360*, 436–439. https://doi.org/10.1126/science.aar6245
87. Gootenberg, J.S.; Abudayyeh, O.O.; Kellner, M.J.; Joung, J.; Collins, J.J.; Zhang, F. Multiplexed and portable nucleic acid detection platform with Cas13, Cas12a, and Csm6. *Science* **2018,** *360*, 439–444. https://doi.org/10.1126/science.aaq0179

88. Mao, Z.; Lei, H.; Chen, R.; Ren, S.; Liu, B.; Gao, Z. CRISPR/Cas13a analysis based on NASBA amplification for norovirus detection. *Talanta* **2024**, *280*, 126725. https://doi.org/10.1016/j.talanta.2024.126725

89. Pardee, K.; Green, A.A.; Takahashi, M.K.; Braff, D.; Lambert, G.; Lee, J.W.; Ferrante, T.; Ma, D.; Donghia, N.; Fan, M.; et al. Rapid, Low-Cost Detection of Zika Virus Using Programmable Biomolecular Components. *Cell* **2016**, *165*, 1255–1266. https://doi.org/10.1016/j.cell.2016.04.059

90. Zhou, W.; Hu, L.; Ying, L.; Zhao, Z.; Chu, P.K.; Yu, X.F. A CRISPR–Cas9-triggered strand displacement amplification method for ultrasensitive DNA detection. *Nat. Commun*. **2018**, *9*, 5012. https://doi.org/10.1038/s41467-018-07324-5

91. Li, T.; Wang, J.; Fang, J.; Chen, F.; Wu, X.; Wang, L.; Gao, M.; Zhang, L.; Li, S. A universal nucleic acid detection platform combing CRISPR/Cas12a and strand displacement amplification with multiple signal readout. *Talanta* **2024**, *273*, 125922. https://doi.org/10.1016/j.talanta.2024.125922

92. Wang, C.; Ye, Q.; Chen, M.; Wang, J.; Ding, Y.; Wu, Q. The Crispr/Cas12a system combined with Helicase-Dependent Amplification (Hda) technology to rapidly identify monovalent serogroup e strains of water-borne *Pseudomonas aeruginosa*. Available online: https://doi.org/10.2139/ssrn.4415992 (accessed on 29 November 2024).

93. Miao, J.; Zuo, L.; He, D.; Fang, Z.; Berthet, N.; Yu, C.; Wong, G. Rapid detection of Nipah virus using the one-pot RPA-CRISPR/Cas13a assay. *Virus Res*. **2023**, *332,* 199130. https://doi.org/10.1016/j.virusres.2023.199130

94. Gootenberg, J.S.; Abudayyeh, O.O.; Lee, J.W.; Essletzbichler, P.; Dy, A.J.; Joung, J.; Verdine, V.; Donghia, N.; Daringer, N.M.; Freije, C.A.; et al. Nucleic acid detection with CRISPR-Cas13a/C2c2. *Science* **2017**, *356*, 438–442. https://doi.org/10.1126/science.aam9321

95. Wei, T.; Yan, Y.; Niu, M.; Dong, X.; Li, H.; Sun, Y.; Fa, Y. A rapid LASV detection method based on CRISPR-Cas13a and recombinase aided amplification with special lateral-flow test strips. *Sci. Rep.* **2025**, *15*, 20640. https://doi.org/10.1038/s41598-025-07071-w

96. Huang, Z.; Huang, P.; Cao, Z.; Zhang, T.; Jin, K.; Liu, M.; Bai, Y.; Gong, Z.; Li, X.; Li, Y.; et al. Specific and visual detection of EBOV based on a one-pot RT-RAA-

CRISPR/Cas12a assay. *Virol. Sin*. **2025**, *40*, 1054–1057. https://doi.org/10.1016/j.virs.2025.11.011

97. Zhong, J.; Li, J.; Chen, S.; Xu, Y.; Mao, X.; Xu, M.; Luo, S.; Yang, Y.; Zhou, J.; Yuan, J.; et al. Rapid and efficient CRISPR-based detection of dengue virus in a single-tube. *J. Appl. Microbiol*. **2025**, *136,* lxaf070. https://doi.org/10.1093/jambio/lxaf070
98. Shu, T.; Yin, X.; Xiong, Q.; Hua, C.; Bu, J.; Yang, K.; Zhao, J.; Liu, Y.; Zhu, L.; Zhu, C. Lift-CM: An integrated lift-heater centrifugal microfluidic platform for point-of-care pathogen nucleic acid detection using isothermal amplification and CRISPR/Cas12a. *Biosens. Bioelectron*. **2025**, *274*, 117178. https://doi.org/10.1016/j.bios.2025.117178
99. Kersting, S.; Rausch, V.; Bier, F.F.; von Nickisch-Rosenegk, M. Rapid detection of *Plasmodium falciparum* with isothermal recombinase polymerase amplification and lateral flow analysis. *Malar. J.* **2014**, *13*, 99. https://doi.org/10.1186/1475-2875-13-99
100. Qin, P.; Park, M.; Alfson, K.J.; Tamhankar, M.; Carrion, R.; Patterson, J.L.; Griffiths, A.; He, Q.; Yildiz, A.; Mathies, R.; et al. Rapid and Fully Microfluidic Ebola Virus Detection with CRISPR-Cas13a. *ACS Sens*. **2019**, *4*, 1048–1054. https://doi.org/10.1021/acssensors.9b00239
101. Zhang, Y.; Xiang, Y.; Hou, D.; Fang, L.; Cai, S.; Zhang, J.; Wang, Y.; Jiang, Y.; Liu, B.; Bai, J.; et al. A one-pot method for universal Dengue virus detection by combining RT-RPA amplification and CRISPR/Cas12a assay. *BMC Microbiol.* **2025**, *25*, 163. https://doi.org/10.1186/s12866-025-03882-z
102. Xie, M.; Ma, J.; Zhou, X.; Wei, Y.; Zhao, Y.; Ye, C.; Liu, X.; Qing, J.; Chen, Z. Recombinase-aided amplification technology: A comprehensive review of innovations and multi-technology integration for rapid infectious disease diagnosis. *Anal. Chim. Acta* **2026**, *1387*, 344932. https://doi.org/10.1016/j.aca.2025.344932
103. Li, Z.; Dai, J.; Yang, Z.; Zhang, M.; Wang, X.; Ge, C.; Lu, Y.; Feng, W.; Song, S.; Zhang, C.; et al. A Rapid RT-RAA Assay for Visual Detection of Ebola Virus: Advancing Early Diagnosis in Resource-Limited Settings. *Pathogens* **2025**, *14*, 1266. https://doi.org/10.3390/pathogens14121266
104. Notomi, T.; Okayama, H.; Masubuchi, H.; Yonekawa, T.; Watanabe, K.; Amino, N.; Hase, T. Loop-mediated isothermal amplification of DNA. *Nucleic Acids Res*. **2000**, *28*, 63e. https://doi.org/10.1093/nar/28.12.e63

105. Nagamine, K.; Hase, T.; Notomi, T. Accelerated reaction by loop-mediated isothermal amplification using loop primers. *Mol. Cell. Probes* **2002**, *16*, 223–229. https://doi.org/10.1006/mcpr.2002.0415

106. Wong, Y.P.; Othman, S.; Lau, Y.L.; Radu, S.; Chee, H.Y. Loop-mediated isothermal amplification (LAMP): a versatile technique for detection of micro-organisms. *J. Appl. Microbiol*. **2018**, *124*, 626–643. https://doi.org/10.1111/jam.13647

107. Crego-Vicente, B.; del Olmo M.D.; Muro, A.; Fernández-Soto, P. Multiplexing LAMP Assays: A Methodological Review and Diagnostic Application. *Int. J. Mol. Sci.* **2024**, *25*, 6374. https://doi.org/10.3390/ijms25126374

108. Oloniniyi, O.K.; Kurosaki, Y.; Miyamoto, H.; Takada, A.; Yasuda, J. Rapid detection of all known ebolavirus species by reverse transcription-loop-mediated isothermal amplification (RT-LAMP). *J. Virol. Methods* **2017**, *246*, 8-14. https://doi.org/10.1016/j.jviromet.2017.03.011

109. Soroka, M.; Wasowicz, B.; Rymaszewska, A. Loop-Mediated Isothermal Amplification (Lamp): The Better Sibling of PCR? *Cells* **2021**, *10*, 1931. https://doi.org/10.3390/cells10081931

110. Siddique, M.P.; Jang, W.J.; Lee, J.M.; Ahn, S.H.; Suraiya, S.; Kim, C.H.; Kong, I.S. *groEL* is a suitable genetic marker for detecting *Vibrio parahaemolyticus* by loop-mediated isothermal amplification assay. *Lett. Appl. Microbiol*. **2017**, *65*, 106–113. https://doi.org/10.1111/lam.12760

111. Peyrefitte, C.N.; Boubis, L.; Coudrier, D.; Bouloy, M.; Grandadam, M.; Tolou, H.J.; Plumet, S. Real-Time Reverse-Transcription Loop-Mediated Isothermal Amplification for Rapid Detection of Rift Valley Fever Virus. *J. Clin. Microbiol*. **2008**, *46*, 3653–3659. https://doi.org/10.1128/JCM.01188-08

112. Kurosaki, Y.; Magassouba, N.; Oloniniyi, O.K.; Cherif, M.S.; Sakabe, S.; Takada, A.; Hirayama, K.; Yasuda, J. Development and Evaluation of Reverse Transcription-Loop-Mediated Isothermal Amplification (RT-LAMP) Assay Coupled with a Portable Device for Rapid Diagnosis of Ebola Virus Disease in Guinea. *PLoS Negl. Trop. Dis*. **2016**, *10*, e0004472. https://doi.org/10.1371/journal.pntd.0004472

113. Pemba, C.M.; Kurosaki, Y.; Yoshikawa, R.; Oloniniyi, O.K.; Urata, S.; Sueyoshi, M.; Zadeh, V.R.; Nwafor, I.; Iroezindu, M.O.; Ajayi, N.A.; et al. Development of an RT-LAMP

assay for the detection of Lassa viruses in southeast and south-central Nigeria. *J. Virol. Methods* **2019**, *269*, 30–37. https://doi.org/10.1016/j.jviromet.2019.04.010

114. Kumar, J.S.; Dash, P.K.; Srivastava, A.; Sharma, S.; Tandel, K.; Parida, M. One-step single-tube accelerated quantitative nucleoprotein gene-specific reverse transcription loop-mediated isothermal gene amplification (RT-LAMP) assay for rapid, real-time & reliable clinical detection of Ebola virus. *Indian J. Med. Res*. **2021**, *154*, 598–606. https://doi.org/10.4103/ijmr.IJMR_864_19

115. Li, H.; Nie, Y.; Wu, Y.; Cao, Y.; Liu, W.; Zhao, R.; Feng, X.; Hao, R. Portable microfluidic-LAMP assay for rapid on-site detection of eight highly pathogenic viruses. *Anal. Chim. Acta* **2025**, *1365*, 344236. https://doi.org/10.1016/j.aca.2025.344236

116. Lam, P.; Keri, R.A.; Steinmetz, N.F. A Bioengineered Positive Control for Rapid Detection of the Ebola Virus by Reverse Transcription Loop-Mediated Isothermal Amplification (RT-LAMP). *ACS Biomater. Sci. Eng*. **2017**, *3*, 452–459. https://doi.org/10.1021/acsbiomaterials.6b00769

117. Benzine, J.W.; Brown, K.M.; Agans, K.N.; Godiska, R.; Mire, C.E.; Gowda, K.; Converse, B.; Geisbert, T.W.; Mead, D.A.; Chander, Y. Molecular Diagnostic Field Test for Point-of-Care Detection of Ebola Virus Directly from Blood. *J. Infect. Dis.* **2016**, *214*, S234–S242. https://doi.org/10.1093/infdis/jiw330

118. Li, H.; Wang, X.; Liu, W.; Wei, X.; Lin, W.; Li, E.; Li, P.; Dong, D.; Cui, L.; Hu, X.; et al. Survey and Visual Detection of *Zaire Ebolavirus* in Clinical Samples Targeting the Nucleoprotein Gene in Sierra Leone. *Front. Microbiol*. **2015**, *6*, 1332. https://doi.org/10.3389/fmicb.2015.01332

119. Kurosaki, Y.; Grolla, A.; Fukuma, A.; Feldmann, H.; Yasuda, J. Development and Evaluation of a Simple Assay for Marburg Virus Detection Using a Reverse Transcription-Loop-Mediated Isothermal Amplification Method. *J. Clin. Microbiol*. **2010**, *48*, 2330–2336. https://doi.org/10.1128/JCM.01224-09

120. Nwe, M.K.; Jangpromma, N.; Taemaitree, L. Evaluation of molecular inhibitors of loop-mediated isothermal amplification (LAMP). *Sci. Rep*. **2024**, *14*, 5916. https://doi.org/10.1038/s41598-024-55241-z

121. PrimerExplorerV5. Available online: https://primerexplorer.eiken.co.jp/lampv5e/index.html (Accessed on 14 March 2026).

122. New England Biolabs. NEB LAMP Primer Design Tool. Available online: https://lamp.neb.com/#!/ (Accessed on 14 March 2026).
123. Bonney, L.C.; Watson, R.J.; Slack, G.S.; Bosworth, A.; Vasileva Wand, N.I.; Hewson, R. A flexible format LAMP assay for rapid detection of Ebola virus. *PLoS Negl. Trop. Dis*. **2020**, *14*, 1–22. https://doi.org/10.1371/journal.pntd.0008496
124. Lin, X.; Jin, X.; Xu, B.; Wang, R.; Fu, R.; Su, Y.; Jiang, K.; Yang, H.; Lu, Y.; Guo, Y.; et al. Fast and Parallel Detection of Four Ebola Virus Species on a Microfluidic-Chip-Based Portable Reverse Transcription Loop-Mediated Isothermal Amplification System. *Micromachines* **2019**, *10*, 777. https://doi.org/10.3390/mi10110777
125. Xu, C.; Wang, H.; Jin, H.; Feng, N.; Zheng, X.; Cao, Z.; Li, L.; Wang, J.; Yan, F.; Wang, L.; et al. Visual detection of Ebola virus using reverse transcription loop-mediated isothermal amplification combined with nucleic acid strip detection. *Arch. Virol*. **2016**, *161*, 1125–1133. https://doi.org/10.1007/s00705-016-2763-5
126. Kurosaki, Y.; Takada, A.; Ebihara, H.; Grolla, A.; Kamo, N.; Feldmann, H.; Kawaoka, Y.; Yasuda, J. Rapid and simple detection of Ebola virus by reverse transcription-loop-mediated isothermal amplification. *J. Virol. Methods* **2007**, *141*, 78–83. https://doi.org/10.1016/j.jviromet.2006.11.031
127. Malkin, E.; Zaric, M.; Kieh, M.; Baden, L.R.; Fitz-Patrick, D.; Marini, A.; Yun, H.; Hayes, P.; Bromell, R.; Ayorinde, M.; et al. Safety and Immunogenicity of an rVSV Lassa Fever Vaccine Candidate. *N. Engl. J. Med*. **2025**, *393*, 1807–1818. https://doi.org/10.1056/nejmoa2501073
128. Chen, Y.; Ma, X.; Pan, L.; Yang, S.; Chen, X.; Wang, F.; Yang, D.; Li, M.; Wang, P. A CRISPR-Cas12a-based assay for one-step preamplification-free detection of viral DNA. *Sens. Actuators B Chem*. **2024**, *399*, 134813. https://doi.org/10.1016/j.snb.2023.134813
129. Fozouni, P.; Son, S.; Díaz de León Derby, M.; Knott, G.J.; Gray, C.N.; D'Ambrosio, M.V.; Zhao, C.; Switz, N.A.; Kumar, G.R.; Stephens, S.I.; et al. Amplification-free detection of SARS-CoV-2 with CRISPR-Cas13a and mobile phone microscopy. *Cell* **2021**, *184*, 323-333.e9. https://doi.org/10.1016/j.cell.2020.12.001
130. Shinoda, H.; Taguchi, Y.; Nakagawa, R.; Makino, A.; Okazaki, S.; Nakano, M.; Muramoto, Y.; Takahashi, C.; Takahashi, I.; Ando, J.; et al. Amplification-free RNA detection with

CRISPR–Cas13. *Commun. Biol.* **2021**, *4*, 476. https://doi.org/10.1038/s42003-021-02001-8

131. Yang, J.; Song, Y.; Deng, X.; Vanegas, J.A.; You, Z.; Zhang, Y.; Weng, Z.; Avery, L.; Dieckhaus, K.D.; Peddi, A.; et al. Engineered LwaCas13a with enhanced collateral activity for nucleic acid detection. *Nat. Chem. Biol*. **2023**, *19*, 45–54. https://doi.org/10.1038/s41589-022-01135-y

132. Liu, T.Y.; Knott, G.J.; Smock, D.C.J.; Desmarais, J.J.; Son, S.; Bhuiya, A.; Jakhanwal, S.; Prywes, N.; Agrawal, S.; de León Derby, M.D.; et al. Accelerated RNA detection using tandem CRISPR nucleases. *Nat. Chem. Biol*. **2021**, *17*, 982–988. https://doi.org/10.1038/s41589-021-00842-2

133. Tian, G.; Tan, J.; Liu, B.; Xiao, M.; Xia, Q. Field-deployable viral diagnostic tools for dengue virus based on Cas13a and Cas12a. *Anal. Chim. Acta* **2024**, *1316*, 342838. https://doi.org/10.1016/j.aca.2024.342838

134. Li, S.Y.; Cheng, Q.X.; Li, X.Y.; Zhang, Z.L.; Gao, S.; Cao, R.B.; Zhao, G.P.; Wang, J.; Wang, J.M. CRISPR-Cas12a-assisted nucleic acid detection. *Cell Discov*. **2018**, *4,* 20. https://doi.org/10.1038/s41421-018-0028-z

135. Joung, J.; Ladha, A.; Saito, M.; Kim, N.G.; Woolley, A.E.; Segel, M.; Barretto, R.P.J.; Ranu, A.M.; Macrae, R.K.; Faure, G.; et al. Detection of SARS-CoV-2 with SHERLOCK One-Pot Testing. *N. Engl. J. Med*. **2020**, *383*, 1492–1494. https://doi.org/10.1056/NEJMc2026172

136. Jeremiah Matson, M.; Ricotta, E.; Feldmann, F.; Massaquoi, M.; Sprecher, A.; Giuliani, R.; Edwards, J.K.; Rosenke, K.; de Wit, E.; Feldmann, H.; et al. Evaluation of viral load in patients with Ebola virus disease in Liberia: a retrospective observational study. *Lancet Microbe* **2022**, *3*, e533–e542. https://doi.org/10.1016/S2666-5247(22)00065-9

137. Sweileh, W.M. Global research trends of World Health Organization's top eight emerging pathogens. *Glob. Health* **2017**, *13*, 9. https://doi.org/10.1186/s12992-017-0233-9

138. Broughton, J.P.; Deng, X.; Yu, G.; Fasching, C.L.; Servellita, V.; Singh, J.; Miao, X.; Streithorst, J.A.; Granados, A.; Sotomayor-Gonzalez, A.; et al. CRISPR–Cas12-based detection of SARS-CoV-2. *Nat. Biotechnol*. **2020**, *38*, 870–874. https://doi.org/10.1038/s41587-020-0513-4

139. Kellner, M.J.; Koob, J.G.; Gootenberg, J.S.; Abudayyeh, O.O.; Zhang, F. SHERLOCK: nucleic acid detection with CRISPR nucleases. *Nat. Protoc.* **2019**, *14*, 2986–3012. https://doi.org/10.1038/s41596-019-0210-2

140. LucigenVideo. Loop-Mediated Isothermal Amplification (LAMP): Primer Design and Assay Optimization [video]. YouTube. Available online: https://www.youtube.com/watch?v=GJkvQqDufh0 (Accessed on 4 December 2025)

141. Eiken. Design of primers. Available online: https://loopamp.eiken.co.jp/en/lamp/0202.html (Accessed on 4 December 2025)

142. Schroeder, A.; Mueller, O.; Stocker, S.; Salowsky, R.; Leiber, M.; Gassmann, M.; Lightfoot, S.; Menzel, W.; Granzow, M.; Ragg, T. The RIN: an RNA integrity number for assigning integrity values to RNA measurements. *BMC Mol. Biol*. **2006**, *7,* 3. https://doi.org/10.1186/1471-2199-7-3

143. Wang, D.G.; Brewster, J.D.; Paul, M.; Tomasula, P.M. Two Methods for Increased Specificity and Sensitivity in Loop-Mediated Isothermal Amplification. *Molecules* **2015**, *20*, 6048–6059. https://doi.org/10.3390/molecules20046048

144. Calvert, A.E.; Biggerstaff, B.J.; Tanner, N.A.; Lauterbach, M.; Lanciotti, R.S. Rapid colorimetric detection of Zika virus from serum and urine specimens by reverse transcription loop-mediated isothermal amplification (RT-LAMP). *PLoS One* **2017**, *12,* e0185340. https://doi.org/10.1371/journal.pone.0185340

145. Nalefski, E.A.; Hedley, S.; Rajaraman, K.; Kooistra, R.M.; Parikh, I.; Sinan, S.; Finkelstein, I.J.; Madan, D. Unleashing high *trans*-substrate cleavage kinetics of Cas12a for nucleic acid diagnostics. *Nucleic Acids Res*. **2025**, *53,* gkaf712. https://doi.org/10.1093/nar/gkaf712

146. Dmytrenko, O.; Neumann, G.C.; Hallmark, T.; Keiser, D.J.; Crowley, V.M.; Vialetto, E.; Mougiakos, I.; Wandera, K.G.; Domgaard, H.; Weber, J.; et al. Cas12a2 elicits abortive infection through RNA-triggered destruction of dsDNA. *Nature* **2023**, *613*, 588–594. https://doi.org/10.1038/s41586-022-05559-3

147. Yan, W.X.; Hunnewell, P.; Alfonse, L.E.; Carte, J.M.; Keston-Smith, E.; Sothiselvam, S.; Garrity, A.J.; Chong, S.; Makarova, K.S.; Koonin, E.V.; et al. Functionally diverse type V CRISPR-Cas systems. *Science* **2019**, *363*, 88–91. https://doi.org/10.1126/science.aav7271

148. Ghouneimy, A.; Ali, Z.; Aman, R.; Jiang, W.; Aouida, M.; Mahfouz, M. CRISPR-Based Multiplex Detection of Human Papillomaviruses for One-Pot Point-of-Care Diagnostics. *ACS Synth. Biol*. **2024**, *13*, 837–850. https://doi.org/10.1021/acssynbio.3c00655

149. Nilsson, M.; De Maeyer, H.; Allen, M. Evaluation of Different Cleaning Strategies for Removal of Contaminating DNA Molecules. *Genes* **2022**, *13,* 162. https://doi.org/10.3390/genes13010162